MICROFACIES ANALYSIS, DEPOSITIONAL ENVIRONMENTS AND SEQUENCE STRATIGRAPHY OF THE LATE CRETACEOUS KARABABA AND DERDERE FORMATIONS IN THE CEMBERLITAS OIL FIELD, ADIYAMAN, SOUTHEASTERN TURKEY

by

OĞUZ MÜLAYİM

IBRAHİM ÇEMEN, COMMITTEE CHAIR

ERNEST A. MANCINI
ALBERTO P. HUERTA
JACK C. PASHIN

A THESIS

Submitted in partial fulfillment of the requirements for the degree of
Master of Science in the Department of Geological Sciences
in the Graduate School of The University of Alabama

TUSCALOOSA, ALABAMA

2013

ABSTRACT

The frontal belt of the southeastern Anatolia fold-thrust belt in Turkey contains several small to mid-size oil fields, producing from Cretaceous carbonate of the Mardin Group. Many oil fields are located narrow, asymmetrical anticlinal structures, which are associated with contractional faulting. The Cemberlitas oil field (COF) in Adiyaman, Southeastern Turkey is one of the most important oil fields in the region. The Upper Cretaceous Derdere and Karababa formations of the Mardin Group contain the main reservoir and source rocks in the oil field. We have conducted a detailed study of microfacies, depositional environments and sequence stratigraphy of the Derdere (Mid-Cenomanian-Turonian) and Karababa (Coniacian-Lower Campanian) formations in the oil field. We have recognized 8 microfacies in the Derdere and Karababa Formations in the study area; (1) fine crystalline dolomite, (2) medium-coarse crystalline dolomite, (3) bioclastic wackestone/packstone, (4) lime mudstone (5) phosphatic-glauconitic planktonic wackestone, 6) planktonic foraminiferous wackestone/packstone, (7) dolomitic planktonic wackestone, and (8) mollusk-echinoid wackestone/packstone. These microfacies suggest that the Derdere Formation was deposited in lagoonal to shelf depositional environments. The microfacies also suggest that Karababa Formation was deposited in a deep to shallow marine intra shelf basin. We have identified two-third-order sequence boundaries in the reservoir. These boundaries are of late Turonian and early Campanian age. Each sequence contains transgressive and highstand systems tracts. These sequences are compared with those in other regions to differentiate the local, regional and global factors that controlled sedimentation within the study area.

DEDICATION

Research is to see what everybody else has seen, and to think what nobody else has thought. Albert Szent-Gyorgi

This thesis is dedicated to my family and fiancée. Without them I would not be where I am today. They have supported me throughout my life and I am ever grateful to them for their graciousness.

LIST OF ABBREVIATIONS AND SYMBOLS

BOPD Barrels of oil per day

MMBLS Millions of barrels

NAF North Anatolian Fault

EAF East Anatolian Fault

DSF Dead Sea Fault

COF Cemberlitas Oil Field

CS Condensed Section

m meter

MF-1 Microfacies

TPAO Turkish Petroleum Corporation

CEM-1 Cemberlitas well

PPL Plane-polarized light

XPL Cross-polarized light

ACKNOWLEDGMENTS

I am pleased to have this opportunity to thank the many colleagues, friends, and faculty members who have helped me with this research project. I am most indebted to Ibrahim Cemen the chairman of this thesis, for sharing his research expertise. I would also like to thank all of my committee members, Ernest Mancini, Jack Pashin, and Alberto Perez Huerta for their invaluable input, inspiring questions, and support of both the thesis and my academic progress. I would likely to solely acknowledge Remzi Aksu for sharing his expertise on all things southeast Turkey. I would like to thank Zeynep Oner for helping me and taking the time to explain them thoroughly.

This research would not have been possible without the support of my friends and fellow graduate students and of course my family who never stopped encouraging me to persist. I would also like to acknowledge my fiancée Gulden Cinar, who has always been by my side and knew just what to say to motivate me to finish this thesis.

This project was supported through Turkish Petroleum Corporation issued by the Department of Adıyaman Exploration. I also acknowledge generous support through The University of Alabama Department of Geological Sciences. The Turkish Petroleum Exploration and Research departments are thanked for providing unlimited access to core facilities and resources. Also, a great thanks to the staff at the AGS library for helping with the collection of resources.

CONTENTS

LIST OF TABLES

LIST OF FIGURES

1. INTRODUCTION

Purpose and Scope

The Adiyaman region of Turkey is located within the southeast Anatolian fold and thrust belt (Figure 1). The region underwent late Cretaceous and late Miocene compressional tectonics and Pliocene-Quaternary transtensional tectonics. The region contains several active oil fields. The Cemberlitas oil field produces from the Cretaceous Mardin Group.

This investigation is aimed at a detailed study of the depositional characteristics of the Karababa and Derdere formations of the Mardin Group which contains the principal reservoir and source rocks in the Cemberlitas oil field. These two formations are penetrated by all of the wells in the field (Figure 2). This investigation will attempt to resolve the following research questions:

1) What are the depositional environments represented by the Karababa and Derdere formations in the Cemberlitas oil field?
2) What is the sequence stratigraphic framework of the Karababa and Derdere formations in the Cemberlitas oil field?
3) What is the role of structure control on deposition of the Karababa and Derdere formations in the Cemberlitas oil field?

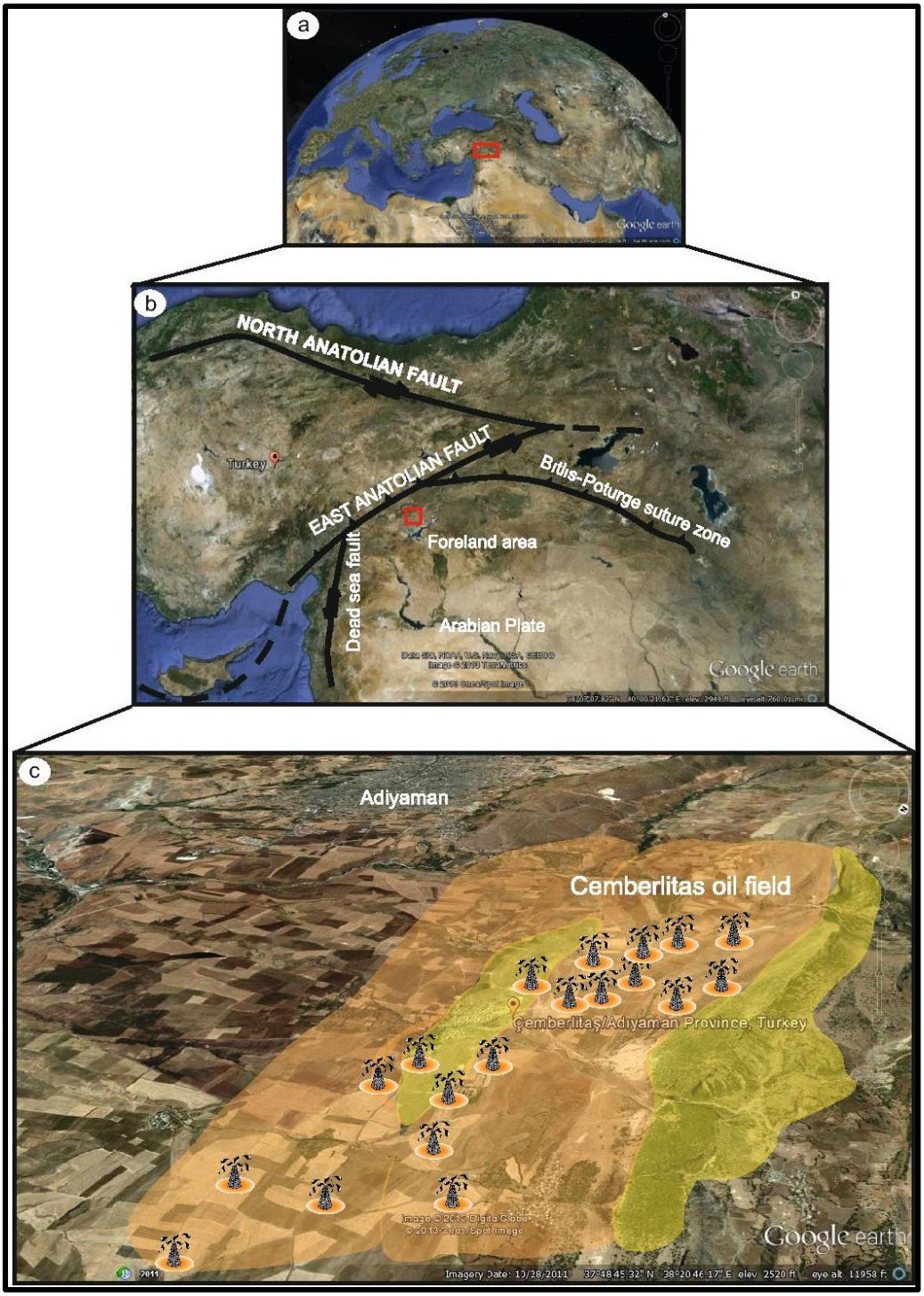

Figure 1: (a) Location of Cemberlitas oil field, (b) major tectonic units, (c) active oil production wells in the Anatolian fold-thrust belt of Turkey.(orange; yellow areas: Selmo and Hoya Fm.)

Location and Field History

The Cemberlitas oil field is located, 10 km northeast of Adiyaman and 164 km southwest of Gaziantep (Figure 2). It contains a NE-SW trending anticline. The middle to upper Eocene Hoya Formation is the oldest unit exposed along the crest of the anticline. The Pliocene Lahti and upper Miocene Şelmo formations crop out along the flanks of the anticline. The northern section of the field contains Gebeli syncline and the Cemberlitas thrust fault system. The southern part of the field includes the Adiyaman anticline and the Kinik syncline. The anticlines are NE-SW asymmetric folds with layers dipping to the east and southwest on their limbs. A syncline with a fold axis parallels to the Adiyaman anticline is also present to the north of the thrust fault (Figure 3).

The first well in the Cemberlitas oil field, Cemberlitas-1 was spudded in 1982 and abandoned as a dry hole without being properly tested because of drilling problems. In 1983, the Cemberlitas- 5 well was drilled and characterized as a discovery well. Since 1983, the Turkish Petroleum Corporation has drilled a total of 54 wells. However, only 28 of 54 wells produced oil. Presently, the number of those promising wells decreased to 14 wells because of water and oil mixing and intense fracture system in the Mardin group reservoir rocks and the remaining mixed wells have been abandoned for technical problems. In the last 30 years, production rate of the yield wells decreased, whereas the percentage of water in the wells increased.

Previous Works

The following is a brief summary of the important previous studies in the Cemberlitas and oil field and surrounding region:

Rigo de Righi and Cortesini, (1964) established the stratigraphy and structural setting of Southeastern Turkey. Cordey and Demirmen (1971) determined the stratigraphical position of the Mardin Group Carbonates. Sungurlu (1974) produced the first comprehensive geological map of SE Anatolia. Wagner et al. (1986) concluded that the Karababa-A Member of the Karababa Formation and the Karabogaz Formation have source rock potential\ and that the Karababa-C Member and the Derdere formations are the main reservoirs.

Gorur et al. (1987) identified cyclicity in the Mardin Group carbonates, with each regressive cycles being capped by an unconformity. Gorur et al. (1991) suggested that sedimentary environment (deep subtidal) of Karababa-A Member of the Mardin Group is suitable for oil generation. They determined that a) the Karababa-B Member of the Mardin Group contains phosphatic nodules; and b) the Karababa-C Member is a lagoonal facies having benthic foraminifers and fossils indicating a subtidal environment.

Duran and Alaygut (1992) determined that the Karababa-C Member is one of the main reservoir units in Southeastern Turkey. They produced facies and isopach maps of the Karababa and Karabogaz formations and mapped the porosity and porous zone thicknesses of the Karababa-C Member reservoir facies.

.

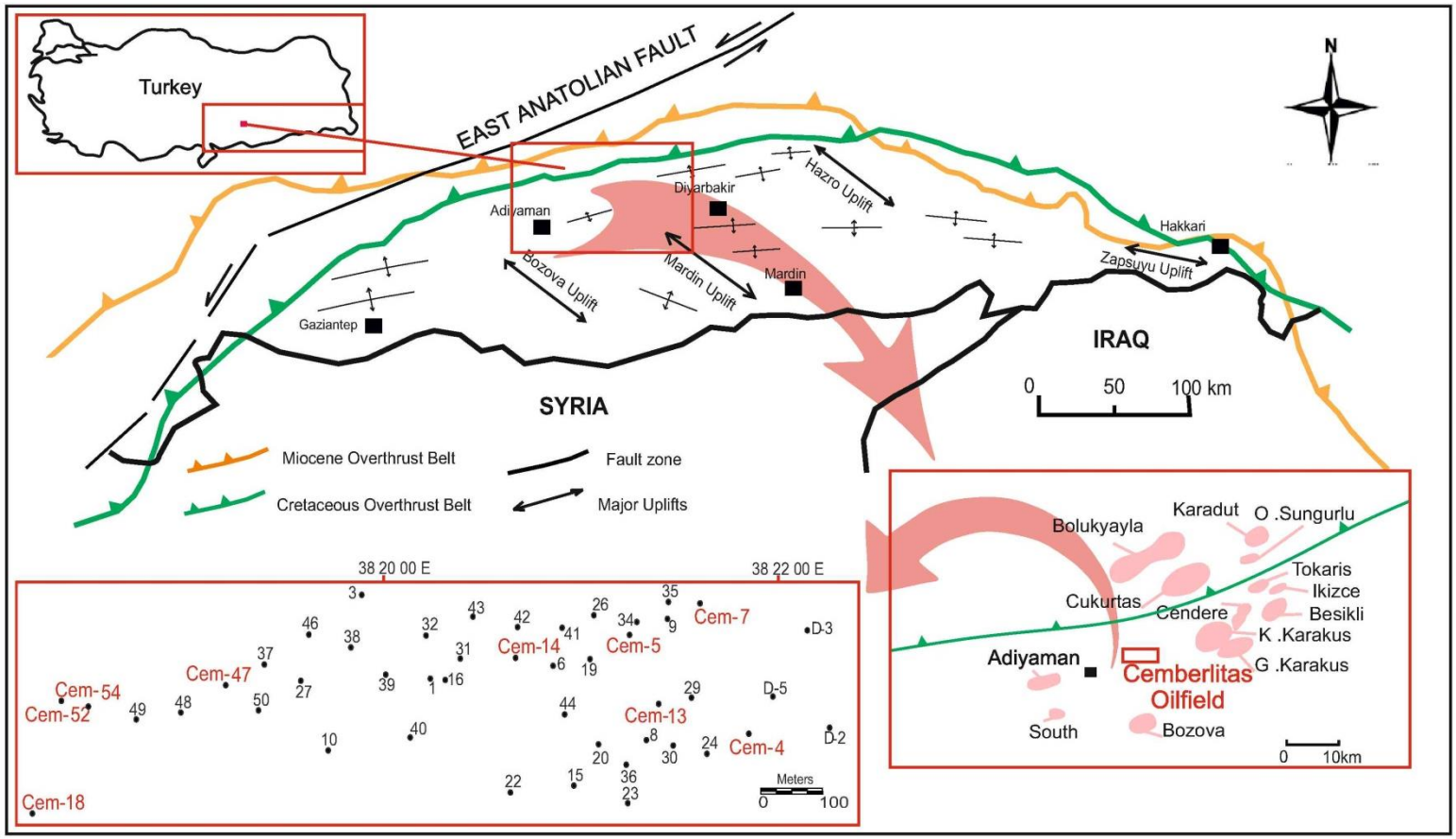

Figure 2: Tectonic units in SE of Anatolia; The Cemberlitas and surrounding oil fields; and well locations in study area (modified from Perincek, 1987 and Yıldızel, 2008).

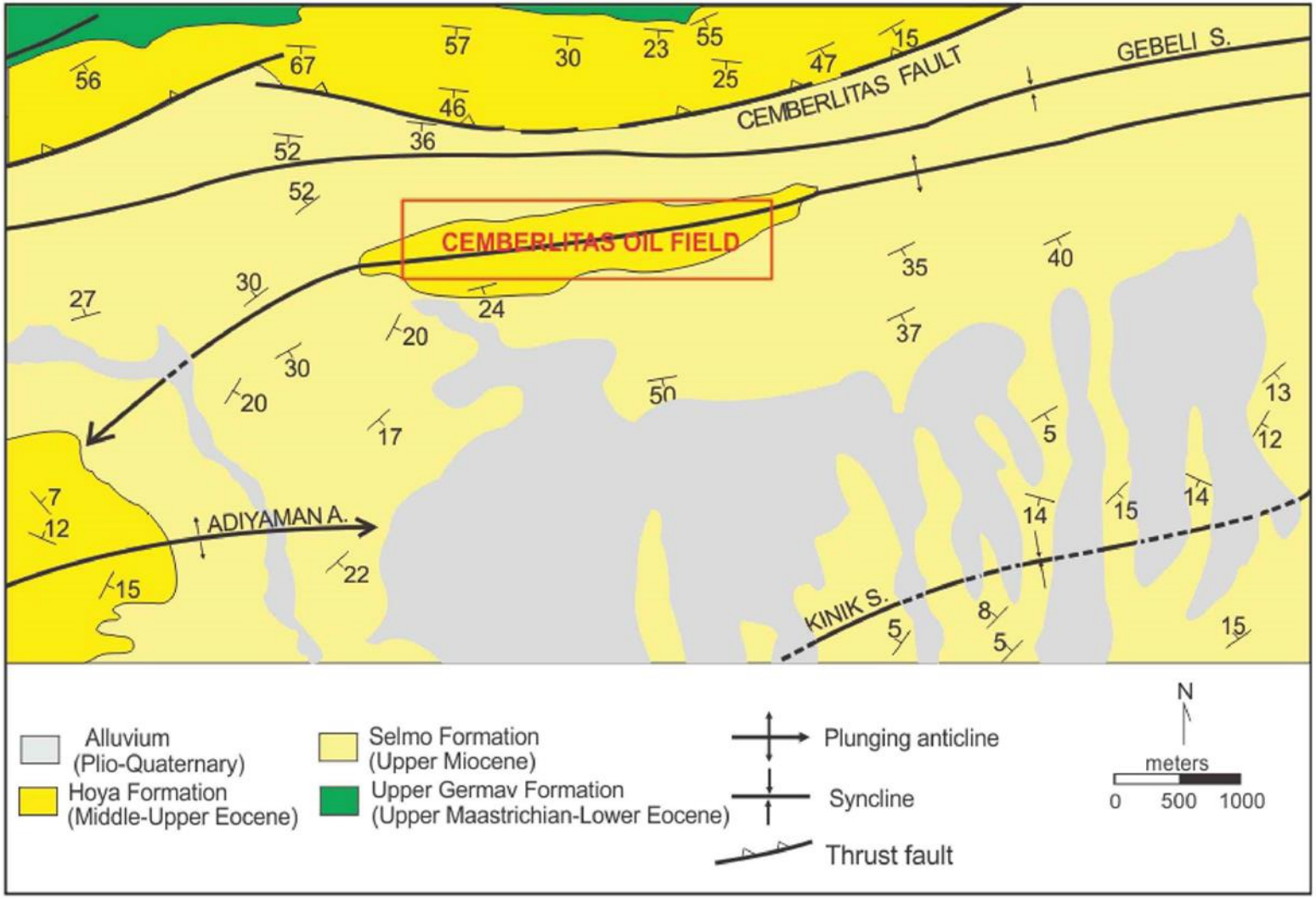

Figure 3: Geologic map of the Cemberlitas oil field and surrounding area (modified from Guven et. al., 1991)

2. GEOLOGICAL SETTING

2.1 Mesozoic stratigraphy of Southeastern Turkey

Subsurface Stratigraphy

Mardin Group

The Mardin Group is composed of the Areban, Sabunsuyu, Derdere and Karababa formations. This thesis focuses on the two formations that constitute the upper part of the Mardin Group, the Karababa and Derdere formations (Figure 4). The Karababa Formation unconformably overlies the Derdere Formation and is unconformably overlain by the Karabogaz Formation.

The Karababa Formation is divided into three members; Karababa-A, Karababa-B, Karababa-C (Tuna, 1973). The Karababa-A is composed mainly of limestone containing planktonic foraminifera. It contains dark yellowish, brown, blackish grey, dark to light grey, phosphatic-glauconitic limestone including mollusks, spheroidal planktonic foraminiferous, narrow calcite filled fractures and abundant organic matter.

Karababa-B contains some distinctive features such as dolomitic carbonate. It is mostly composed of grey, greyish brown, brown, organic rich chert interbedded with spheroidal planktonic foraminiferous limestone. Karababa-B contains micritic matrix, but some samples have neomorphic characteristics due to dedolomitization and recrystallization.

Karababa-C characterized by mollusk and echinoid microfacies. It consists of yellowish, greyish yellow light-white grey, tight and hard, medium- thick bedded, cherty limestone. It contains calcite veinlet, echinoid, and gastropod. In most Cemberlitas wells, it is found around 77-133 m. Coruh et al. (1997) determined that the Karababa-C and Karababa -B Members are Santonian-lower Campanian in age and Karababa-A Member is Coniacian- early Santonian in age (Figure 4).

The Derdere Formation is composed of limestone and dolomite. Dolomite constitutes the lower part of the Derdere Formation and ranges in thickness from 5-84 m in study area. The most abundant lithologic type in the Derdere Formation is greyish yellow, light grey to moderate grey brown, white- grey, hard to very hard to extremely hard, partly fractured, massive, blocky, coarse to fine crystalline ,locally sucrosic dolomite with characteristic vugs identified found in the cores of the wells in the study area.

Coarse, medium and fine crystalline dolomite mosaic represent the high degree of dolomitization and effect of other diagenesis processes like dissolution, cementation and dedolomitization. The dolomite contains well-developed. Intercrystalline, moldic, are vug porosity common types of porosity of dolomite unit. The unit also contains stylolites that are filled by oil “dead oil staining" and fractures are occasionally stained by oil stain or filled by cement.

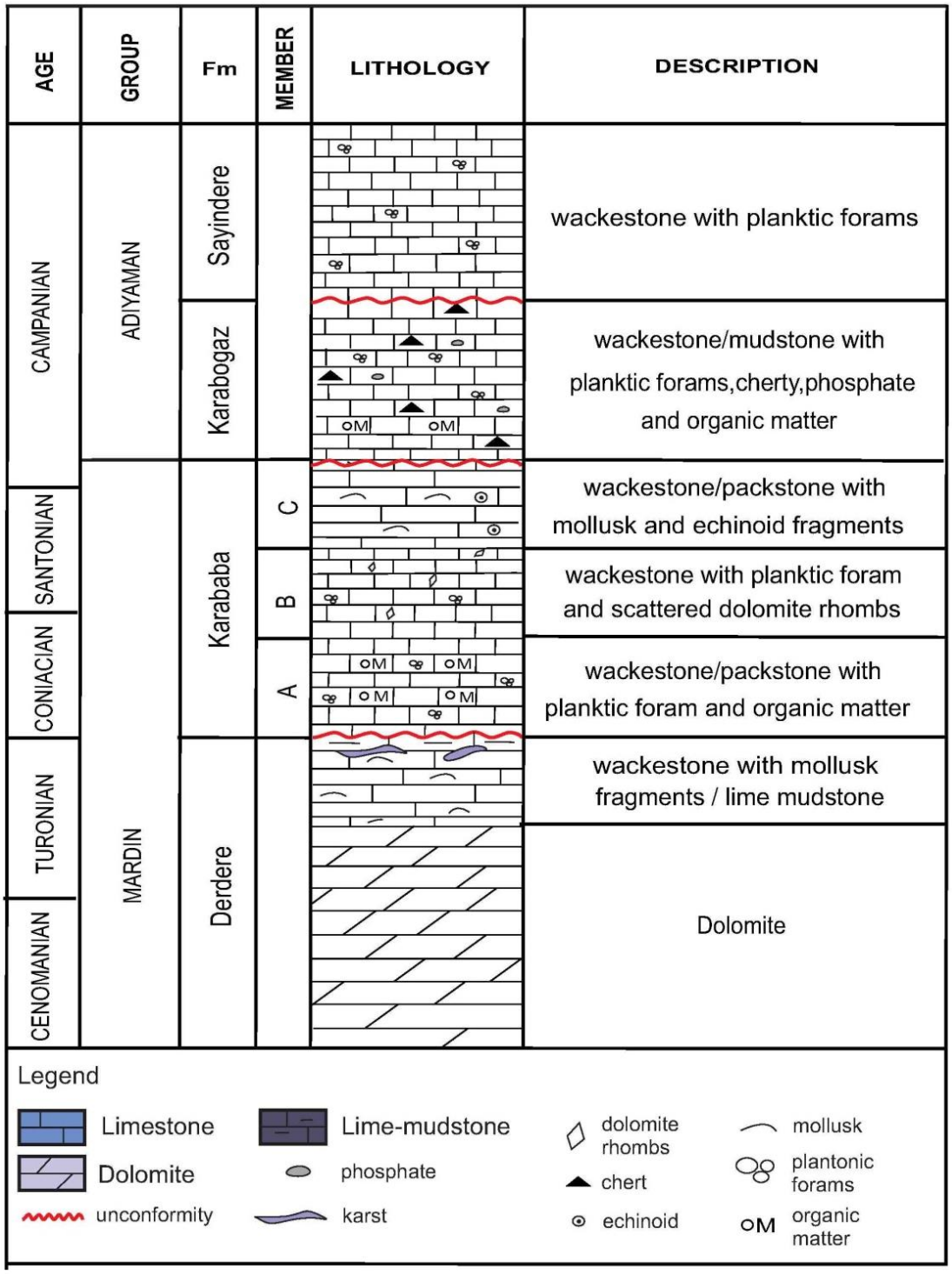

Figure 4: Generalized columnar section of the Cemberlitas oil field, Cem-18. No vertical scale implied.

Limestone unit is the upper part of the formation with sedimentary thickness ranging from 8-32 m in Cemberlitas oil field and represents the undolomitized part of the original carbonate facies of the formation. It alternates with thin dolomitic limestone horizons. This unit consists of lime mudstone and bioclastic wackestone/packestone with abundant bioclasts such as shell fragments. These rocks are observed as light grey, greyish brown, hard, blocky, crispy and intensely fractured. The most common allochems are bivalves (Figure 4). These shells are commonly replaced or filled by cement. Perincek, (1991) reported that the Derdere Formation is deposited in restricted shallow marine depositional environment and is late Cenomanian in age.

The Derdere Formation has displayed a range of features indicative of strong karstic alteration. Consequently, the Derdere is considered to be a genuine paleokarst (Wagner and Pehlivanli, 1985). The brecciation observed in subsurface sections of the Derdere Formation (Wagner and Pehlivanli, 1985) and core samples from Cemberlitas oil field indicate subaerial exposure and karst development. Karst breccias were found in the cores of the Derdere Formation in the Cemberlitas wells. Breccia fragments are angular to sub-angular varying in size from 2 mm to tens of centimeters. This breccia is interpreted to have resulted from subaerial exposures of carbonates where dissolution widening associated with karstification and collapse of the overlying beds. Evidence for subaerial exposure in the Derdere Formation in Cemberlitas oil field core section includes; solution widened fissures, collapse breccia, vugs and cave floor deposits (Wagner and Pehlivanli, 1985).

Adıyaman Group

The Adiyaman Group overlies the Karababa Formation and contains the Sayindere and Karabogaz formations.

The Sayındere Formation is composed of pelagic clayey limestones (Aydemir et al., 2006) (Figure 4). It consists of white, light gray, cream, beige, light brown, grayish beige colored, generally crypto- occasionally microcrystalline, argillaceous, and rarely stylolitic, occasionally chalky, fossiliferous, limestones beds. The formation includes pyrite crystals and micro-fractures filled with calcite crystals. It is late Campanian in age (Dincer 1991).

The Karabogaz Formation consists of dark colored, clayey, generally cryptocrystalline, occasionally earthy textured, fossiliferous, occasionally clayey, rarely chalky, rarely micro-fractured limestones beds. It contains brown or black, very hard, chert interbeds and nodules. Sarı & Bahtiyar (1999) stated that phosphate, glauconite and organic matter are abundant in Karabogaz Formation. The boundary between the Karabogaz and Sayındere formations is gradational (Dincer, 1991). Age of the formation is Middle Campanian (Figure 4).

2.2 Mesozoic tectonic of Southeastern Turkey

Southeast Anatolia constitutes the northernmost part of the Arabian Platform that formed a part of the north facing, passive Gondwanaian margin of the southern branch of the Neo-Tethys Ocean during Cretaceous (Sengör & Yılmaz, 1981). Before deposition of the Mardin Carbonates, the Arabian Platform experienced an extensional tectonics which was initiated in Jurassic and continued until early Cretaceous (Ala & Moss 1979) (Figure 5). During late Jurassic to early Cretaceous, rifting caused a block faulted terrain with topographic highs and lows. In fact, during that time southeastern Anatolia was an E-W trending topographic high (Yilmaz, 1993). As the

transgression flooded this high during the Aptian and Santonian the Mardin carbonates were deposited (Gorur et al., 1991). The Aptian Areban Formation, the base of the Cretaceous section in southeastern Turkey, is composed of mostly sandstone and it is overlain by the (Albian) Sabunsuyu Formation, a dolomite, and (Cenomanian-Turonian) Derdere Formation which is also highly dolomitized. During the Albian, Cenomanian and Turonian shallow shelf conditions prevailed throughout southeastern Turkey and a blanket of neritic carbonates were deposited and dolomitized (Sengör and Yilmaz, 1981) (Figure 5).

During the Campanian-early Maastrichtian interval the Kastel Foredeep basin formed to the south of Tauride orogenic belt. The Kocali and Karadut complexes tectonically overlie the Kastel Formation (Rigo de Righi & Cortesini, 1964; Sungurlu, 1974; Ala & Moss 1979) (Figure 5). The tectonic slices consisting of turbidities and olistostromes of the Karadut Unit, represent time equivalent units to the Mardin Group, and are deposited on the continental slope. Ophiolites of the Kocali Complex originate from the Tethyan ocean floor (Sengör and Yılmaz, 1981).

The Maastrichtian neritic limestone and marly limestone in the eastern and southern part of the basin were eventually covered by a shale and marl. During the Aptian-Lower Maastrichtian, southeastern Anatolia was characterized by intrashelf basins, which formed along the northern passive margin of the Arabian Plate (Yilmaz, 1993). The reefal buildups and shelfal limestones developed during Maastrichtian were finally buried in shale and marls (Figure 5). Restricted shallow marine environments were developed as a result of sea level changes throughout the late Maastrichtian. The allocthonous mass is the result of the obduction of rock masses that are believed to have originated from uplifted basins. Demirel, (2001) concluded that late Maastrichtian restricted shallow-marine shelf and relatively deep-marine environments were developed due to sea level changes in the southeast Anatolia while subduction continued.

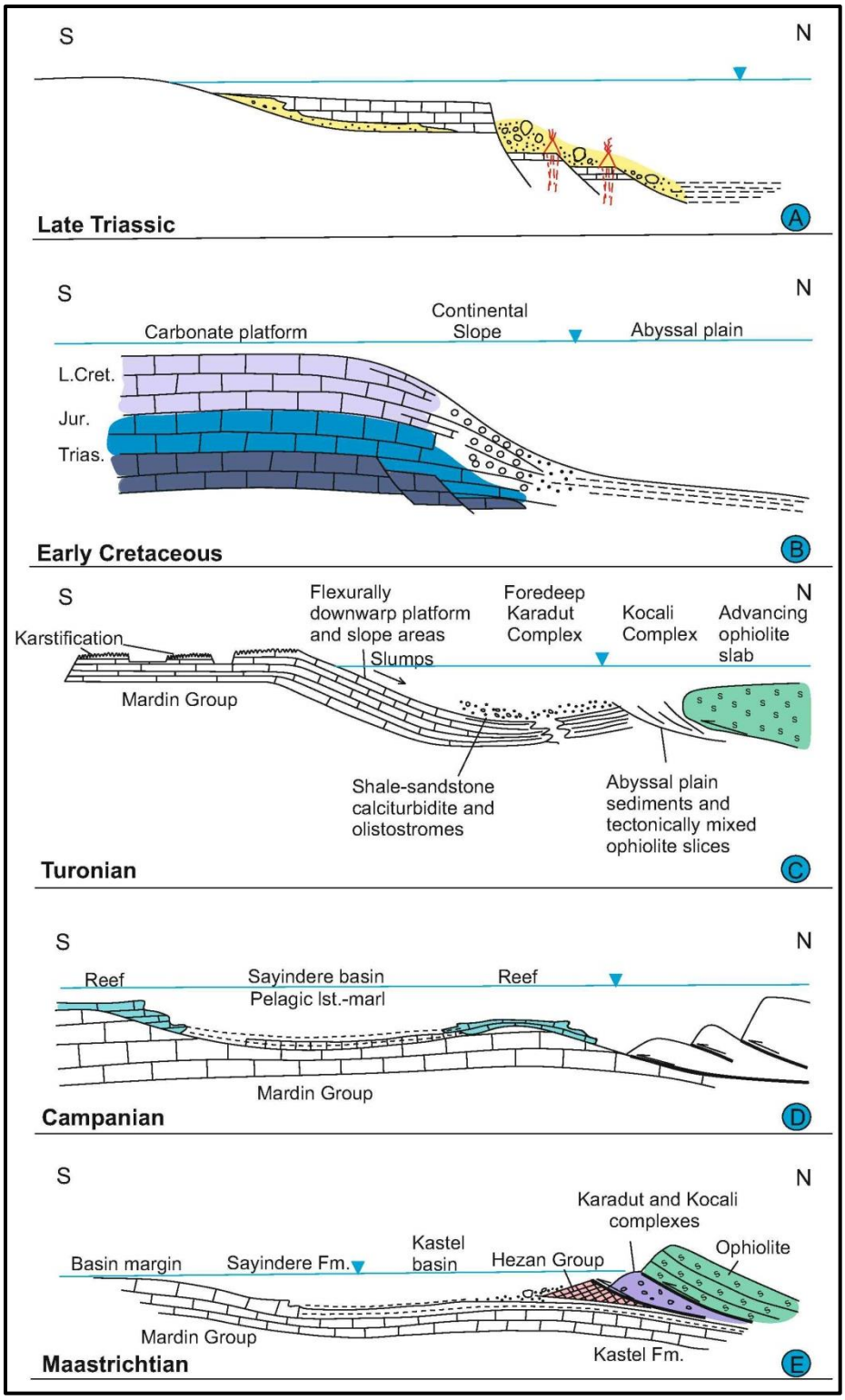

Figure 5: Plate-tectonic model for the Mesozoic evolution of southeast Anatolia (Modified from Yilmaz, 1993).

3. METHODS

To answer the three research questions above, this study examined the available subsurface data such as well logs and available cores from the oil-wells drilled by the TPAO (Turkish Petroleum Corporation).

The available cores (Cem-4, Cem-5, Cem-13, Cem-14, Cem-16, Cem-18, Cem-52 and Cem-54) were examined and thin sections were prepared and analyzed from the Karababa and Derdere formations of the Mardin Group rocks in the Cemberlitas oil field; to observe vertical and lateral petrographic changes within the two formations. Examination and interpretation of the available wireline logs (gamma-ray) were used; to construct structural cross sections to observe changes in identification and correlation of formations boundaries within the Mardin Group.

Petrel 2012 software was used for log interpretation and CorelDraw X6, Rockworks 15 were used for plotting and illustrations. Data from cores, well logs, and thin sections were used to construct depositional models for the Karababa and Derdere formations. The microfacies of the formations were identified based Dunham (1962). Wilson (1975) and Flugel (2004) facies belts and sedimentary models also were used. A sequence stratigraphic model of the Cemberlitas oil field is developed based on microfacies analyses. Sequence boundaries and system tracts were identified and correlated based on the well log interpretations and thin section analysis.

A total of 160 petrographic thin-sections from the Karababa and Derdere formations were examined. Twenty-five new thin-sections were made from core samples in the TPAO Research Center Petrographic Laboratory. Samples were chosen based on their location with respect to the significant lithologic changes within the stratigraphic succession. Thin section analysis was carried out by a transmitted light microscope. Microfacies were defined based on the major petrographic characteristics, such as relative abundance of major components, ratio of matrix versus cement, and rock texture.

32 wells were considered as the most useful and were used in constructing structural contour and isopach contour maps of the Karababa and Derdere units in the Cemberlitas oil field. Stratigraphic and structural cross-sections were also constructed based on available surface and subsurface data.

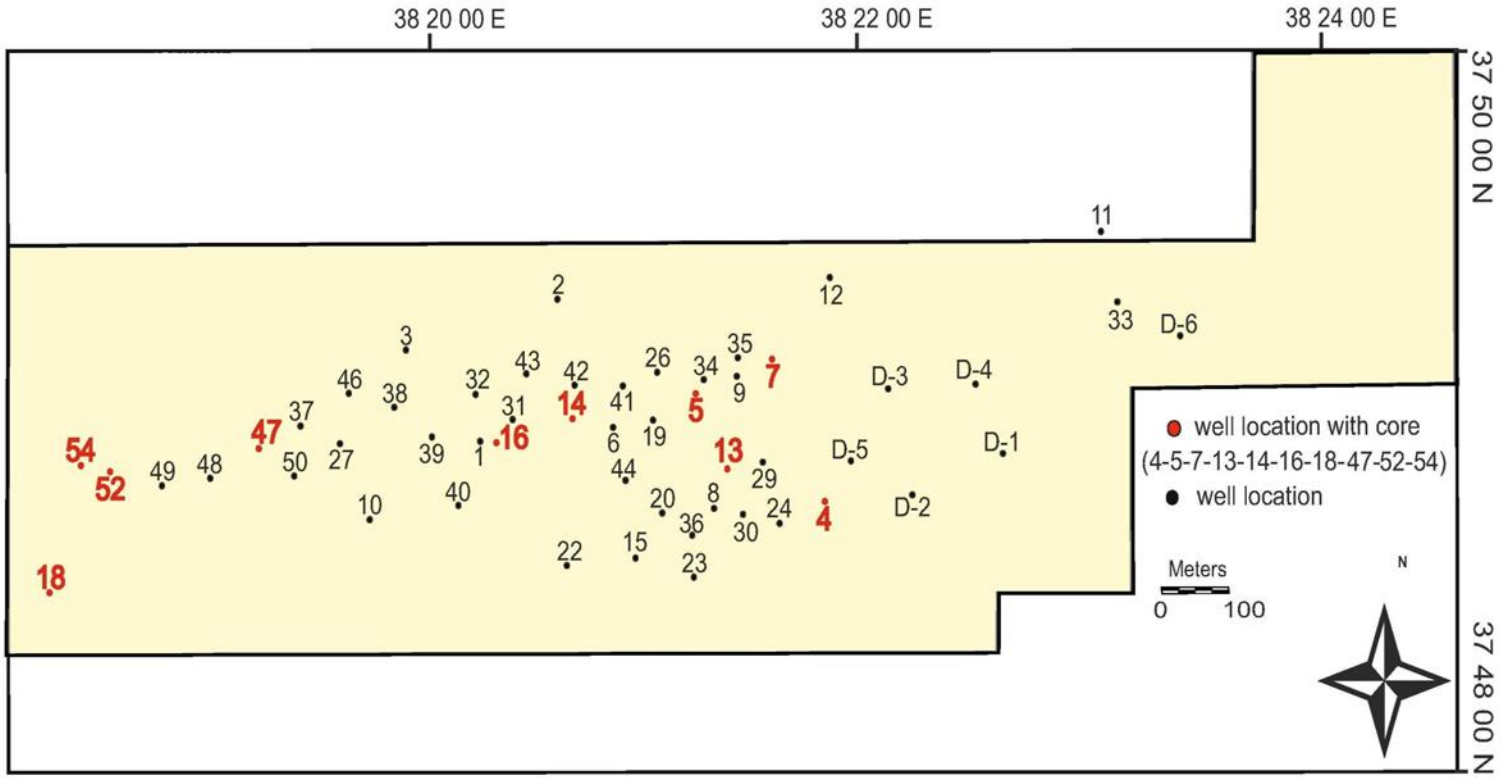

Figure 6: The base map of the Cemberlitas oil field showing studied wells used in the stratigraphic and sequence stratigraphic studies.

Well name	TD m	Karababa Fm Thickness m			Derdere Fm Thickness m	Karababa Fm top and base	Derdere Fm top and base	Core		Thin section Derdere Fm Karababa Fm	Log
		A	B	C				number	meter		
Cem-4	2398	47	52	18	56	2225-2342	2342-2398	5	43	12	SP
Cem-5	2402	41	40	16	112	2103-2200	2200-2312	5	42.5	36	GR
Cem-7	2757	51	62	20	21	2603-2736	2736-2757	1	3	8	SP
Cem-13	2399	53	55	17	112	2162-2287	2287-2399	5	37.5	12	GR
Cem-14	2419	34	46	14	107	2152-2246	2353-2419	10	81.5	20	SP
Cem-18	2497	54	55	16	87	2285-2410	2410-2497	5	30.5	38	SP
Cem-47	2409	62	45	12	13	2177-2296	2296-2409	4	8	1	SP
Cem-52	2303	52	55	24	31	2141-2272	2272-2303	2	18	4	SP
Cem-54	2345	27	50	18	57	2193-2288	2288-2345	5	32	27	GR

Figure 7: The wells used within the study are listed based on thin section number, stratigraphic position, thickness and log availability.

Figure 8: Photographs showing the condition of the cores in the Cemberlitas oil field.

4. RESULTS

4.1 Microfacies Analysis and Interpretations

Microfacies Associations

Microfacies associations are defined based on the microscopic features of the sedimentary rocks. In order to clarify the microfacies, a spread sheet was prepared for description of microfacies. There are two main microfacies associations; the Derdere and Karababa formations microfacies associations (MFA). They are comprised of eight microfacies (Table 1) and described below as follows:

Derdere Formation

The Derdere Formation contains four microfacies in study area. They are (1) fine-crystalline dolomite, (2) medium-coarse crystalline dolomite, (3) bioclastic wackestone and (4) lime mudstone (Table.1). These microfacies are essentially encountered in the middle and upper units of the Derdere Formation in the Cemberlitas oilfield (Figure 9).

	Facies code	Microfacies name	Components		Grain properties			Energy level	Facies belt
			Skeletal	Non-skeletal	Size	Sorting	Roundness		
Derdere Fm.	Mf1	Fine crystalline dolomite	——	——	Very fine	Poor	Poor	Low	Shallow subtidal to lower intertidal
	Mf2	Medium-Coarse Crystalline dolomite	——	——	Medium to coarse	Poor	Poor	Low	Shallow subtidal to lower intertidal
	Mf3	Bioclastic wackestone	Fine shells of bivalve Echinoid Benthic foreminifera	Rare peloids intraclast	Medium	Poor	Poor	Low to medium	Shelf lagoon
	Mf4	Lime mudstone	——	——	Fine	——	——	Low	Shelf lagoon
Karababa Fm.	Mf5	Phosphatic Glauconitic Planktonic Wackestone	Planktic foraminifera Bivalve	Phosphate and Glauconite grains	Medium	Medium to Good	Good	Medium to low	Deep subtidal
	Mf6	Planktonic Foraminiferous Wackestone/Packstone	Planktic foraminifera Bivalve	Phosphate grains	Medium	Good	Good	Medium to low	Deep subtidal
	Mf7	Dolomitic Planktonic Wackestone	Planktic foraminifera Bivalve Echinoid	Dolomite rhombs	Fine	Medium	Medium	Medium to low	Deep subtidal
	Mf8	Mollusks-Echinoid Wackestone/Packstone	Bivalve Echinoid Green algae	Rare peloids intraclast	Medium to coarse	Medium to Good	Medium	Low	Shallow shelf lagoon

Table 1: Microfacies types of the Derdere and Karababa formations in the Cemberlitas oil field.

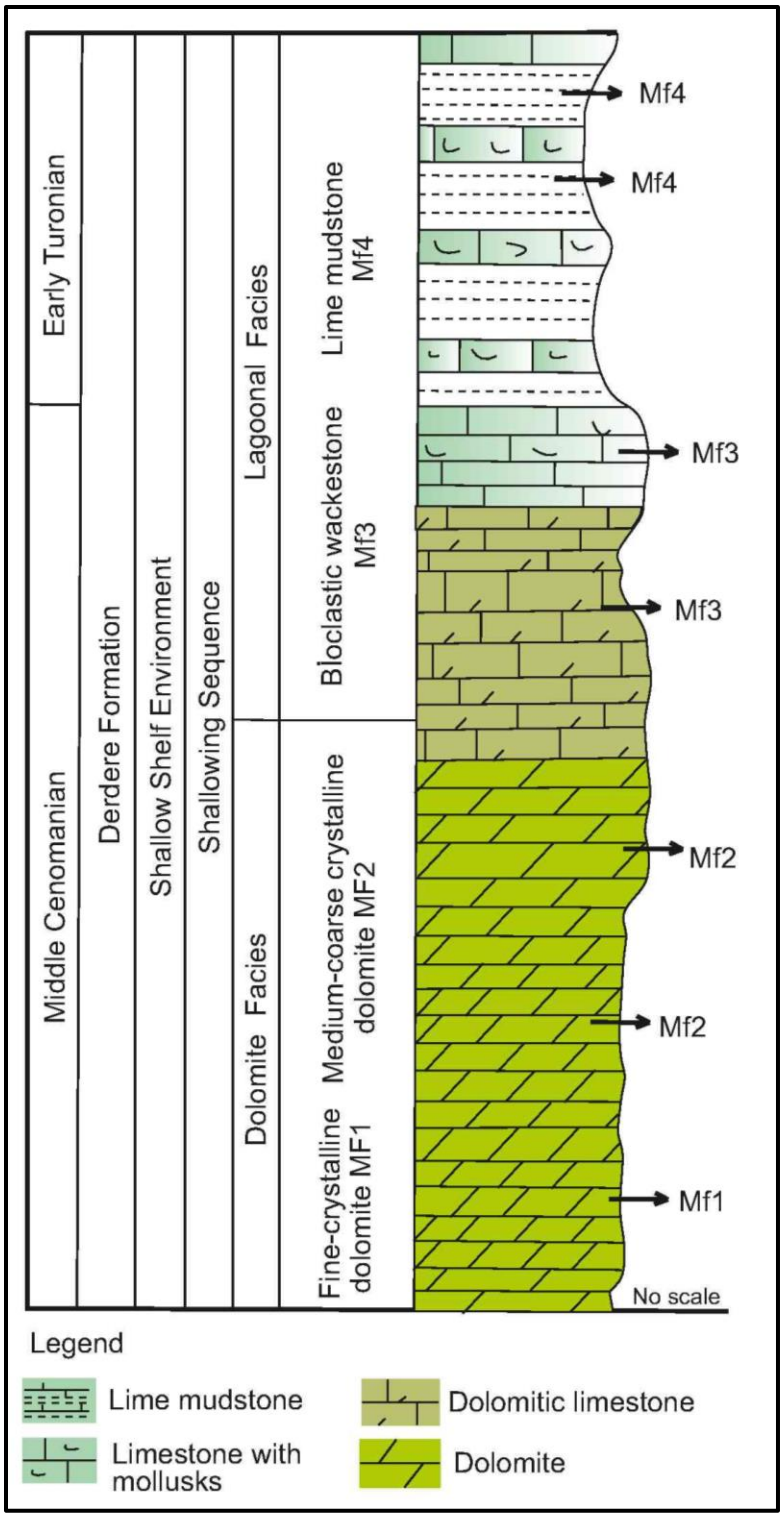

Figure 9: Generalized sketch of lithostratigraphy, facies, and depositional cycles of Derdere carbonates.

Fine Crystalline Dolomite (MF1)

Description: This type of dolomite is not widespread. Some dolomite rhombs have been calcitized (Figure 10). Fine-crystalline dolomite consists of subhedral to euhedral crystals, ranging from 10-60 μm. This type forms dense, dark mosaics of interlocking sub to planar-s crystals. The dense mosaics contain no recognizable allochems, and are probably associated with hydrocarbon. Stylolites are common in the dolomites (Figure 11).

Interpretation: The small crystal sizes (<60 μm), are restricted to peritidal environments (Amthor & Friedman, 1991). The fine crystal size is probably a result of an early replacement of precursor of peritidal lime mudstone or of neomorphism of a penecontemporaneous or early diagenetic dolomite (Zenger, 1983; Amthor & Friedman, 1991). Crystal size is controlled by the relation of two rate processes; the rate of nucleation and the rate of growth (Amthor & Friedman, 1991). Fine particles have a very large surface area in comparision to their volume and, therefore, they represent a rapid nucleation rate. If the nucleation rate is high compared to the growth rate, the resultant crystal size will be small (Amthor & Friedman, 1991). Experimental data (Sibley et al., 1987) indicate that the induction stage of dolomite formation increased with increasing crystal size. This may explain, along with other processes, such as porosity in a downdip direction on the ramp. Dolomite crystal size variations could be different, due to the selective dolomitization of finer crystalline calcium carbonate and early dolomitization of subtidal to supratidal lime muds (Amthor & Friedman, 1991). Thus, petrographic data compared with theoretical and experimental considerations allow interpretation of this facies as early-diagenetic dolomite replacing subtidal to intertidal carbonate muds. The sedimentary characteristics and facies associations of the fine crystalline dolomite reflect shallow subtidal to lower intertidal environments.

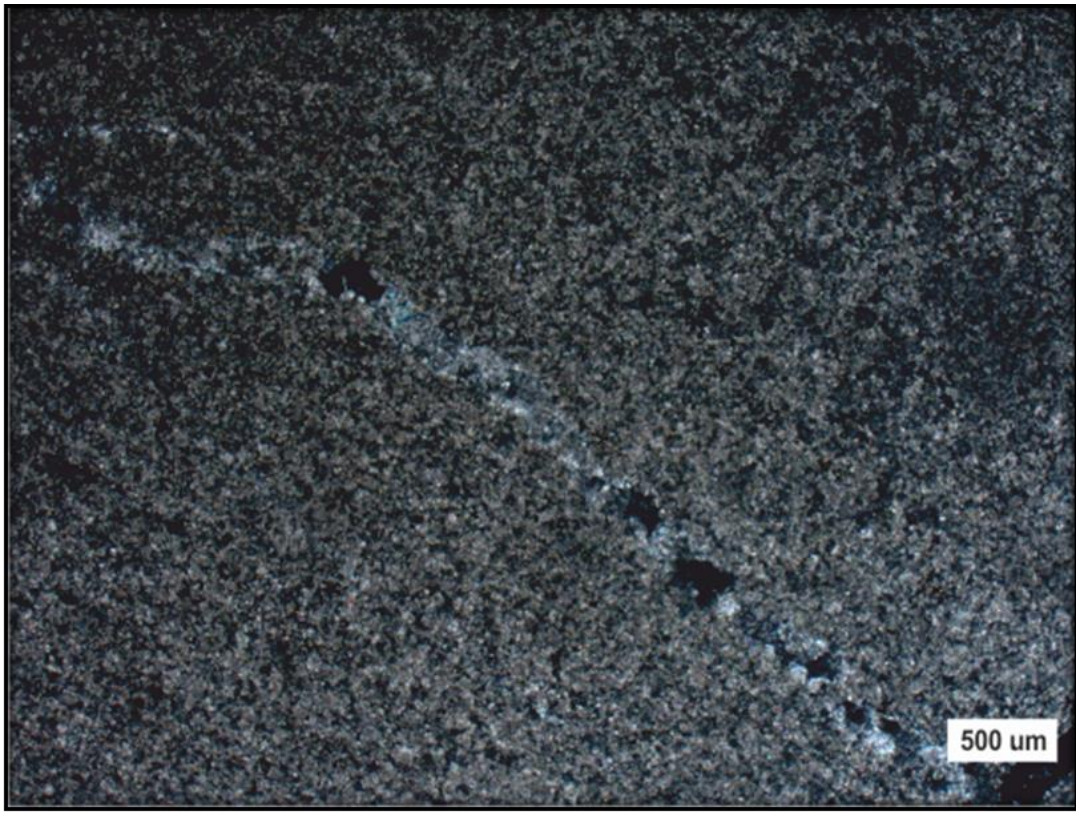

Figure 10: Photomicrograph (PPL) of fine-crystalline planar-s (subhedral) mosaic dolomite at a measured depth of 3118 meter. This type forms dense, dark mosaics of interlocking subhedral to anhedral crystals (Permit #Cem16).

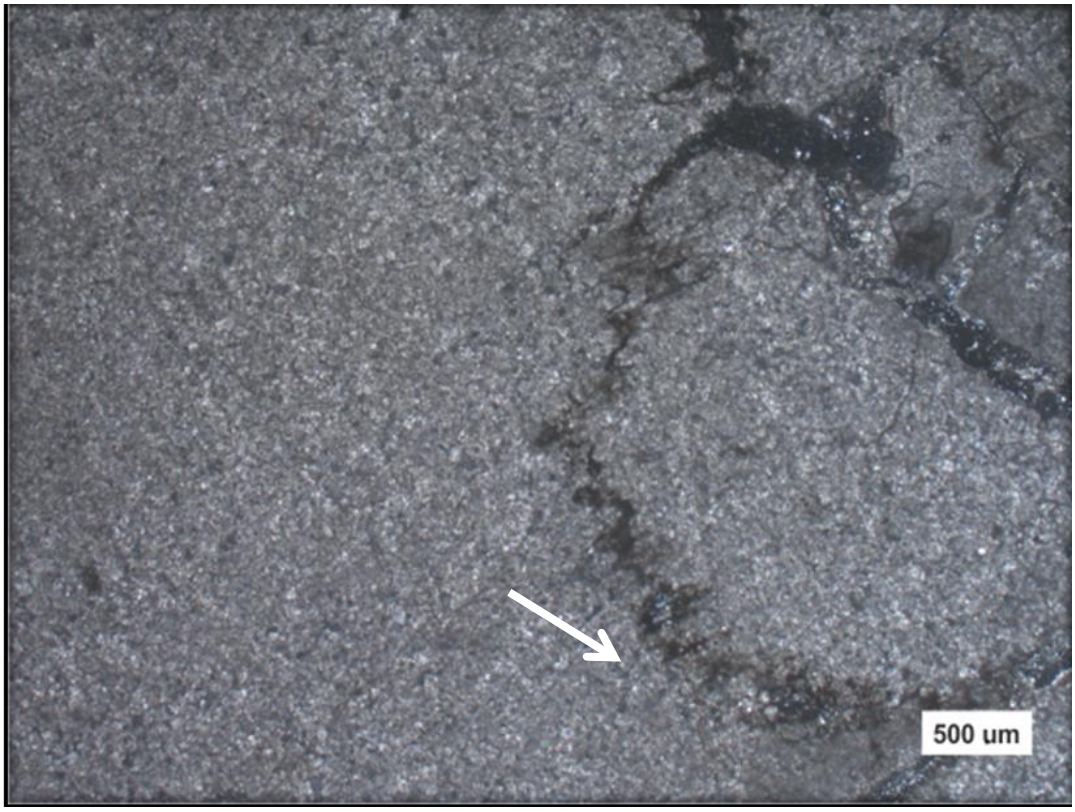

Figure 11: Photomicrograph (PPL) of fine-crystalline dolomite rhombs at a measured depth of 3010 meter. The dolomite rhombs may become calcitized into light calcite with stylolite (Permit #Cem5).

Medium-Coarse Crystalline Dolomite (MF2)

Description: Medium- to coarse-crystalline dolomite is the most abundant type of dolomite by volume in the Derdere Formation. This type forms dense mosaics of subhedral to anhedral planar-s crystals (70-600 μm) with well-defined crystal boundaries that are milky white, dark brown or grey clear. There are no fossils in this facies, while dissolution vugs and fractures are locally present in texture. This microfacies is present in the coarse crystalline dolomite terminating the C18 well sections. It consists mainly of interlocked calcitized dolomite rhombs. Some of the rhombs contain sucrosic features (Figure 12), and some stylolites cut across the fabric of the rhombs (Figures 13 and 14). The rhombs crystals contain clear or cloudy textures. No replacement textures can be observed.

Interpretation: This dolomite facies is interpreted to represent an intermediate to late-diagenetic replacement dolomite. The coarse crystal size suggests a major, probably long lasting, dolomitization event (Figure 14). Cloudy cores represent replacive dolomite, whereas the clear rims are zoned dolomite cements that occlude intercrystalline porosity (Amthor & Friedman, 1991). Preservation of primary sedimentary fabric, such as ghosts, requires that the volumetric rate of dolomite growth must be equal to the volumetric rate of calcite dissolution (Dockal, 1988; Amthor & Friedman, 1991). This type includes dolomite cement and dolomite replacing precursor cement. This dolomite type occurs together with fine crystalline dolomite types. Paragenetic relationships indicate that coarse crystalline dolomite is later than fine crystalline dolomite and contemporaneous (replacive dolomite). The sedimentary characteristics and facies associations of the medium-coarsely crystalline dolomite reflect shallow subtidal to lower intertidal environments.

Comprehensive dolomitization has occurred in the Derdere lithologies. These replacement dolomite crystals are coarsely crystalline and their shapes range from anhedral (xenotopic texture) to euhedral (idiotopic texture). These crystals are abundant and are considered to be the major element of the replacement-dolomite type (Figure. 14). It is commonly difficult to distinguish these replacement dolomite crystals from those dolomite crystals that developed by the process of neomorphism in the early stages of dolomitization (Zenger and Dunham 1988). Coarse-crystalline dolomites may occur as a replacement of limestone during late diagenesis in the deep subsurface (Machel and Anderson 1989) and this process may be controlled by the coarse-grained texture of the original deposits that are being replaced during late diagenesis (Sibley et al. 1993).

The origin of this replacement dolomite may have resulted from the invasion of the former limestone by magnesium rich fluid. The invasion could have happened through mega- and micro fractures, joints, faults, and pore spaces. The source of magnesium-rich solution that is responsible for these dolomitization processes is not fully understood.

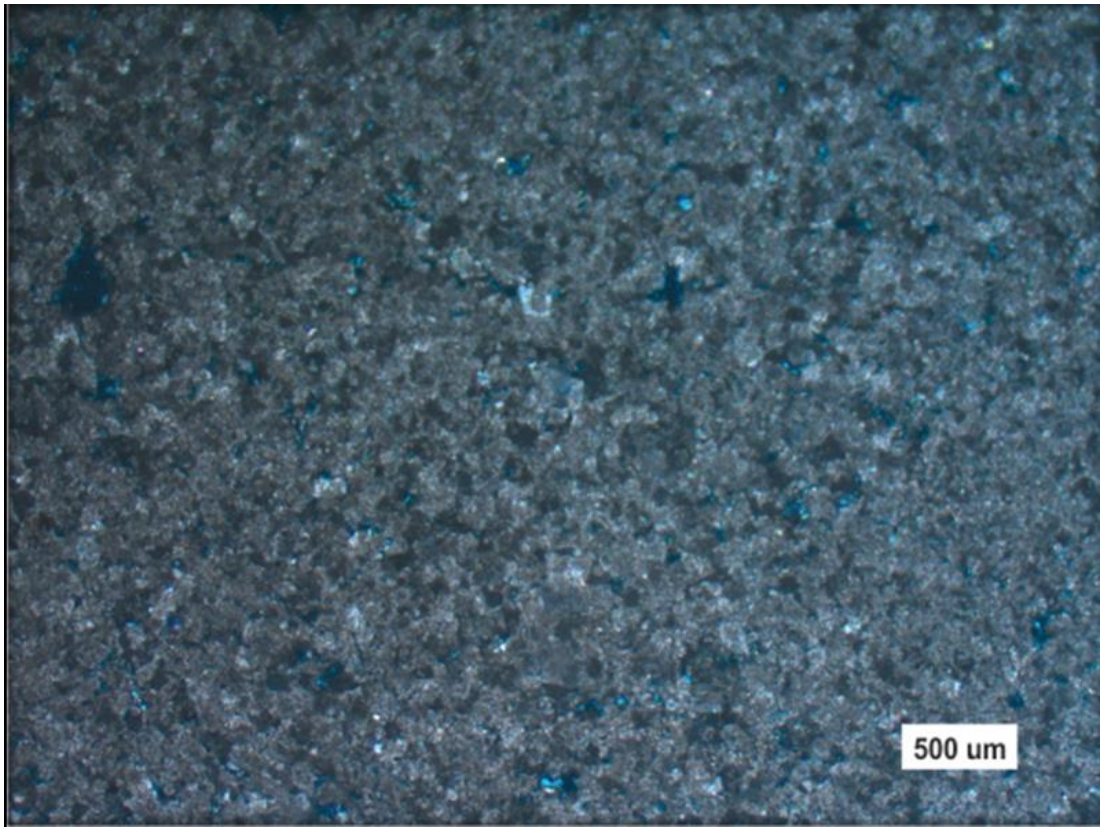

Figure 12: Photomicrograph (PPL) of medium-crystalline dolomite that consists of tightly interlocking mosaic of idiotopic, zoned dolomite rhombs at a measured depth of 3182 meter (Permit #Cem18).

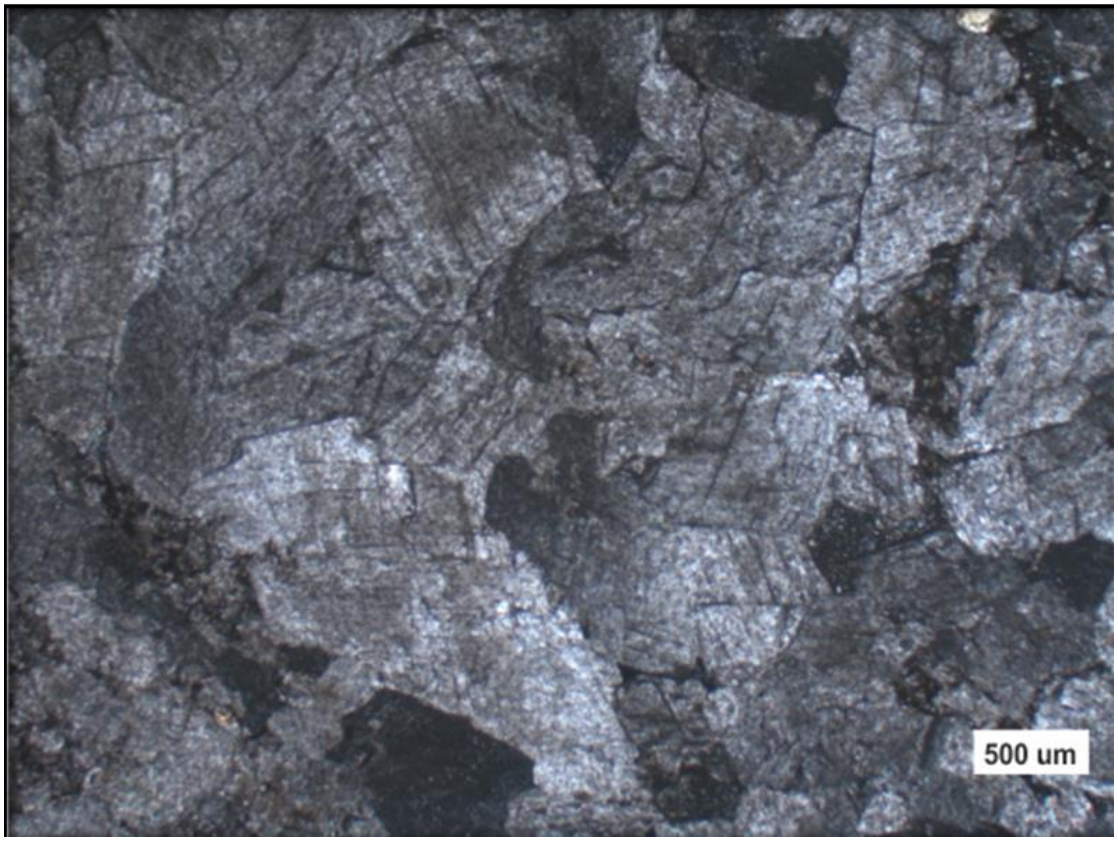

Figure 13: Photomicrograph (PPL) of coarsely crystalline planar-s (subhedral) dolomite at a measured depth of 3036 meter. This type forms patches and irregular bands (Permit # Cem5).

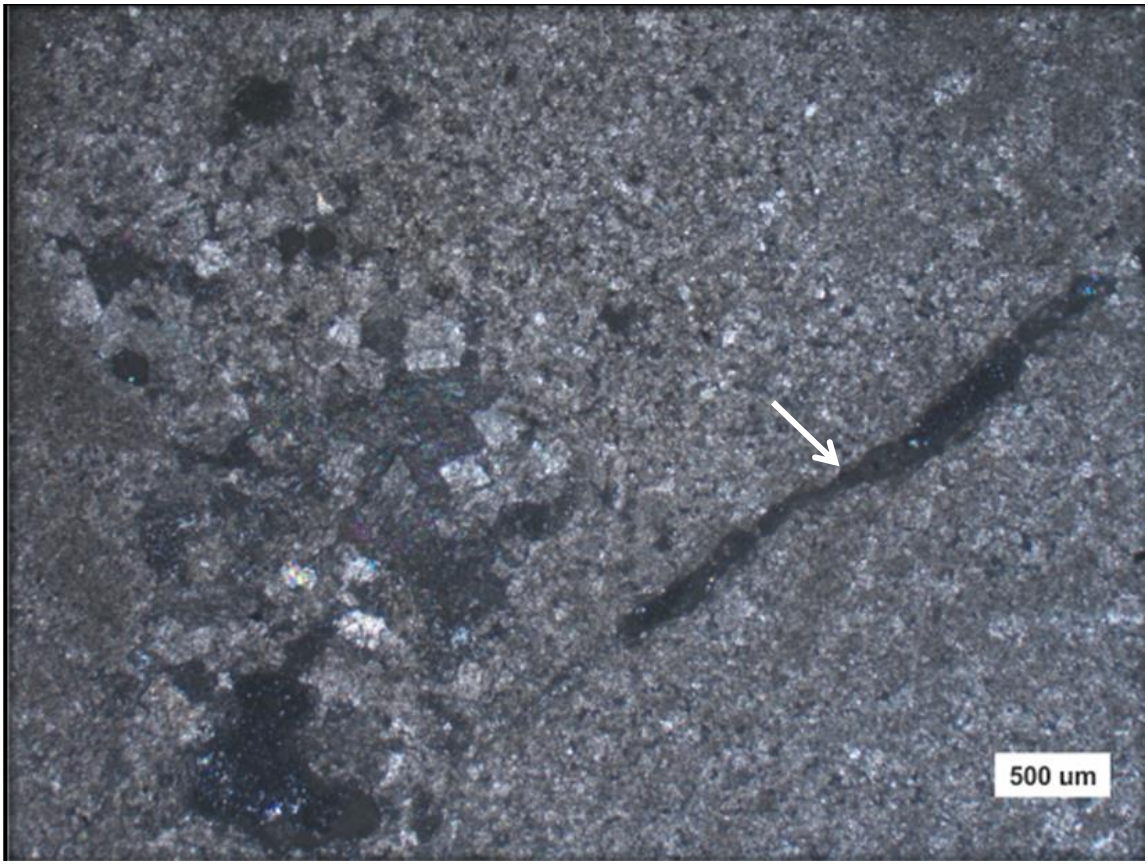

Figure 14: Photomicrograph (PPL) of MF2. These crystals are abundant and are considered to be the major element of the replacement-dolomite type. It also contains fracture-filling hydrocarbon at a measured depth of 3196 meter (Permit #Cem18).

Bioclastic Wackestone (MF3)

Description: This microfacies overlies the crystalline dolomite microfacies (MF1-2). Generally, the wackestones are mud-supported with various proportions of skeletal particles ranging generally from 30 to 40% and may reach to 60% in some thin sections. Allochems are diverse and include fragments of molluscs and echinoderms together with algae, and ostracodes. Specially, the shell fragments are highly recrystallized forming calcitespar of delicate high birefringence (Figure 15). The shell fragments show a wide range of sizes and the majority is less than 1 mm in length, showing no signs of wear. The algal fragments show cellular structure and were recrystallized to sparry calcite. The echinoderm fragments are composed of large single calcite crystals showing unit extinction and have a dusty appearance. The echinoid spines are easily distinguished by their radial stellate shape. The foraminifera are mainly benthic. The micrite matrix is selectively dolomitized, resulted in the development of very fine-to-fine, euhedral dolomite rhombs in an unaltered micrite matrix. In some instances, the shell fragments show some sort of arrangement indicating reworking and transportation directions (Figure 16).

Petrographic analysis of this microfacies included examination and point counting of 7 thin sections. In these 7 thin sections the percent of abundance of mollusks ranges from 13%-50%, benthic foraminifers range is from 1%-2%, matrix ranges from 68%-90%, and echinoid fragments range is from 1%-2% in this microfacies.

On average this microfacies is composed of 0.9% of echinoid fragments, 1% benthic foraminifers, and 14.8% mollusks (Figure 17 and 18). The major constituent of the microfacies is micrite matrix with 83.3% occurrence (Figure 18). The 3.3% of the fragments is stylolites. Within the facies algal fragments and corals were absent.

Interpretation: This microfacies type is comparable to FZ 7 and 8 of Wilson, 1975. They represent deposition in shelf lagoons. The predominance of bioclastic shell fragments in this microfacies indicates shallow subtidal, limited circulation, depth range 15-30 m. It also reflects shortlived periods of sea level fluctuation based on reworking and transportation. The presence of sparry calcite cement in some parts of MF 3, indicate that this microfacies is deposited in a moderate to high energy environment influenced by tidal currents near shoal. The other bioclasts present in this microfacies in small amounts are, benthic foraminifers (uniserial and biserial), micritic algae and bivalve shell fragments. Bioclasts and binding material are sometimes cut by stylolites with hydrocarbons (Figure 15).

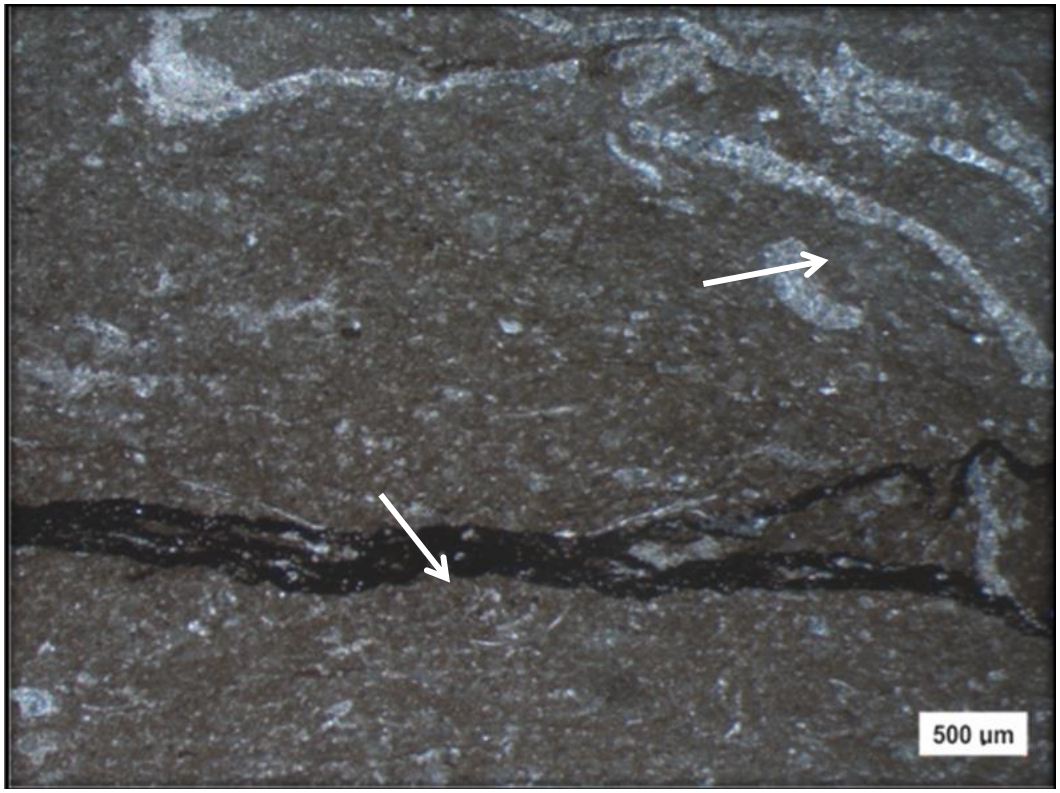

Figure 15: Photomicrograph (PPL) of bioclastic wackestone-packstone with ostracods, benthic bivalve fragments and calcareous algae. The matrix is dominated by fine-grained micrite. Sparry calcite cement is present in the matrix filling spherical to elliptical voids up to 0.3 mm and within anastomising veins. Cement also forms moulds of some bioclasts and appears within stylolite beneath some curved bioclasts at a measured depth of 3086 meter (Permit #Cem4).

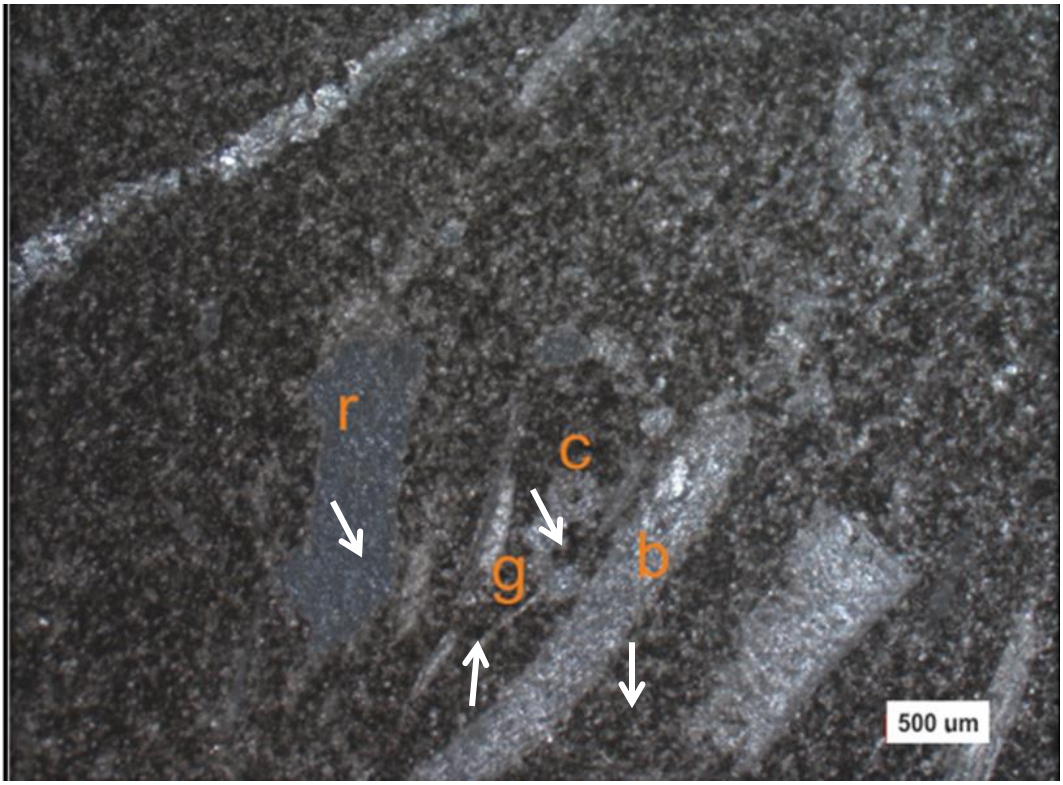

Figure 16: Photomicrograph (PPL) of bioclastic wackestone dominated by mollusc bioclasts in a fine-grained, micrite matrix. The bioclasts consist of fragments of molluscs, including (r) rudist, (c) crinoid, (b) bivalves and (g) gastropods up to 8 mm in size. The majority of bioclasts have been replaced by fine-grained sparry calcite at a measured depth of 3090 meter (Permit #Cem5).

Lime-Mudstone (MF4)

Description: This microfacies forms the top of the Derdere Formation. It is made up of very thin-bedded lime-mudstone which is dark to light grey, brown, fine-textured, and partly dolomitic. Texturally, lime-mudstone is formed of cloudy fine-crystalline calcite crystals, which have partially suffered from aggrading neomorphism into pseudospar. It contains many cavities filled with granular sparry calcite. The rocks are sparsely fossiliferous with poorly preserved bivalves. Some lime-mudstone beds are partly recrystallized into neomorphic spar (Figure 17). Scattered fine dolomite rhombs, 10–20 lm in size, may be present in remarkable amounts (10%, Figure 18). These early diagenetic dolomites are dense, cloudy and display hypidiotopic to idiotopic fabric with small dark center.

Interpretation: The lime-mudstone has been deposited in a low-energy, poorly fossiliferous environments which are common in shallow lagoonal areas of calm conditions with no water circulation (Flugel, 1982) that reduce the normal wave or current energy on the shallow marine carbonate shelf. They represent deposition in shelf lagoons. The restricted conditions are achieved by the low diversity of the faunal content. The relative absence of micro fauna strongly suggests deposition in near- shore domain at water depth less than 5m, where the near- shore ebb and tide condition cause the general decrease in faunal content. This is compatible with the standard microfacies SMF-23 of Wilson (1975). Therefore, the poorly fossiliferous lime–mudstone at Cemberlitas indicates deposition in shallow subtidal zone of lagoon. The flat lamination and diagnostic structures of the arid upper intertidal flat is indicative that the lime-mudstone was of lower intertidal origin. The abundance of the horizontal stylolitic seams in this microfacies strongly suggests dissolution and chemical compaction that probably took place during the diagenetic processes of the preexisting carbonates. The stylolite seams act as

impermeable barriers to prevent the movement of fluids perpendicular to the plane of the stylolites, but serve as channels to permit the fluid movement along the stylolite seams.

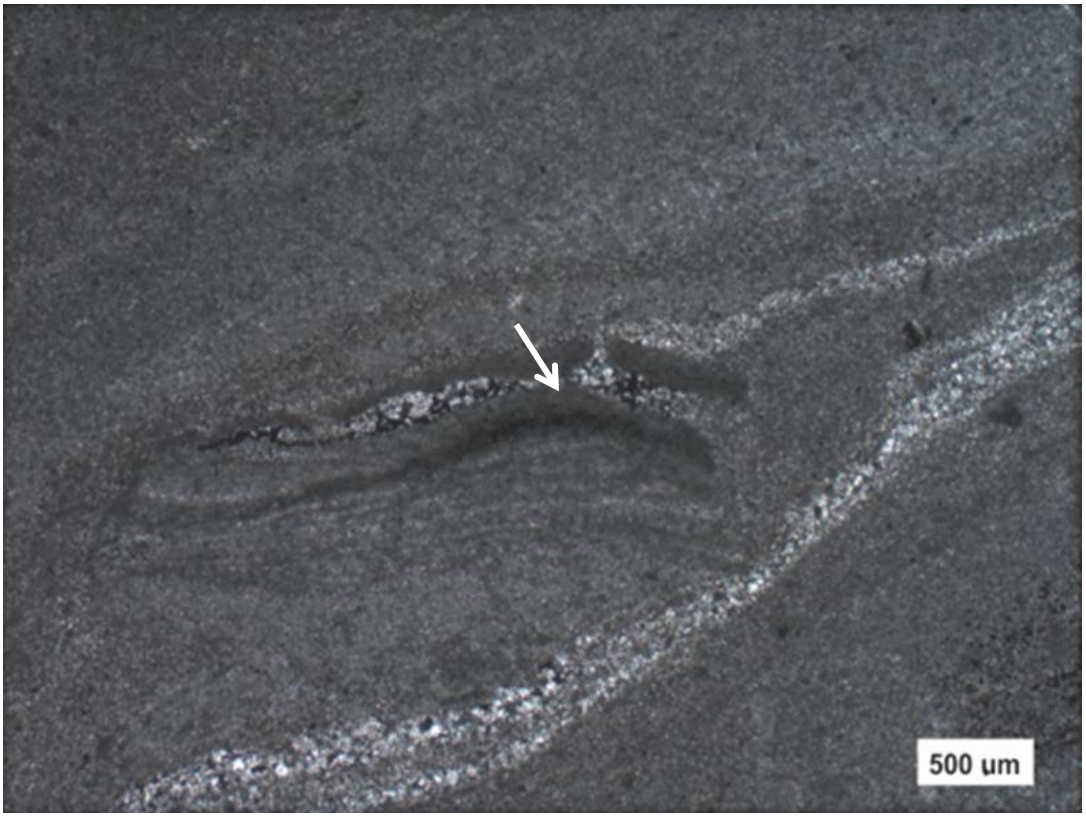

Figure 17: Photomicrograph (PPL) of fine neomorphic spar resulted from the aggrading neomorphism of a dense lime mud matrix, recrystallized lime-mudstone, and tiny black stringers which could be organic matter at a measured depth of 3178 meter (Permit #Cem18).

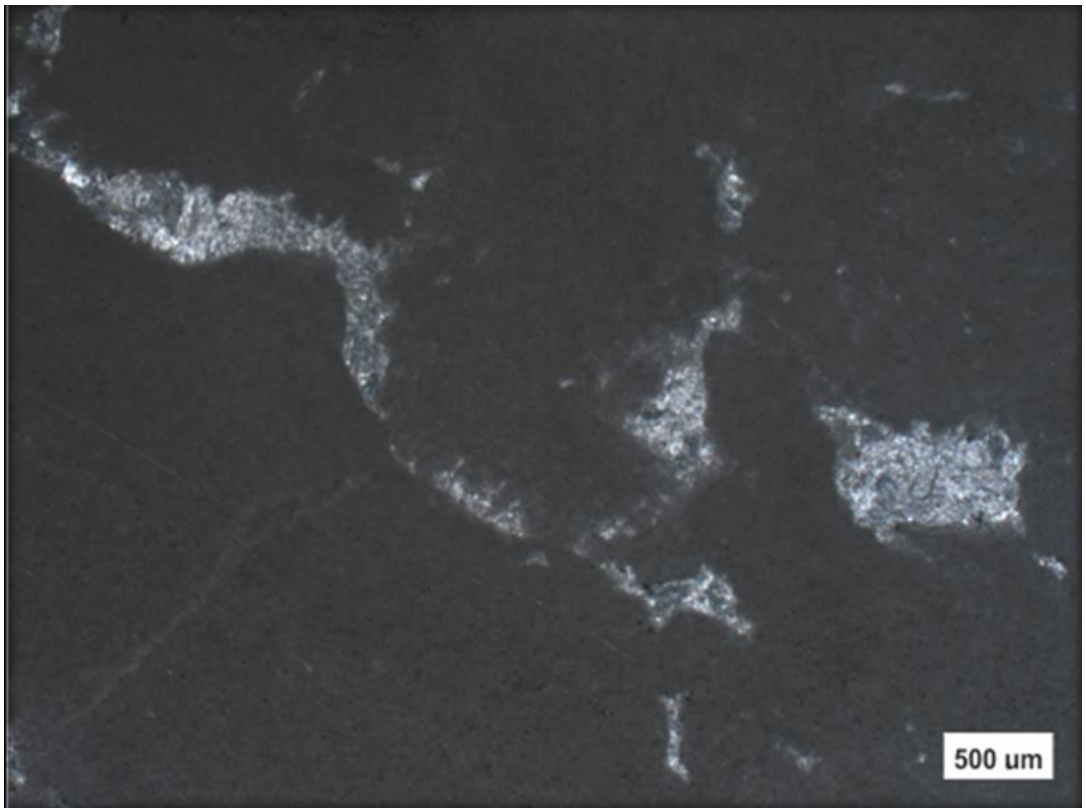

Figure 18: Photomicrograph (PPL) of lime-mudstone with sparry calcite filled voids at a measured depth of 3184 meter. The mud-limestone is considered to be intertidal in origin (Permit #Cem18).

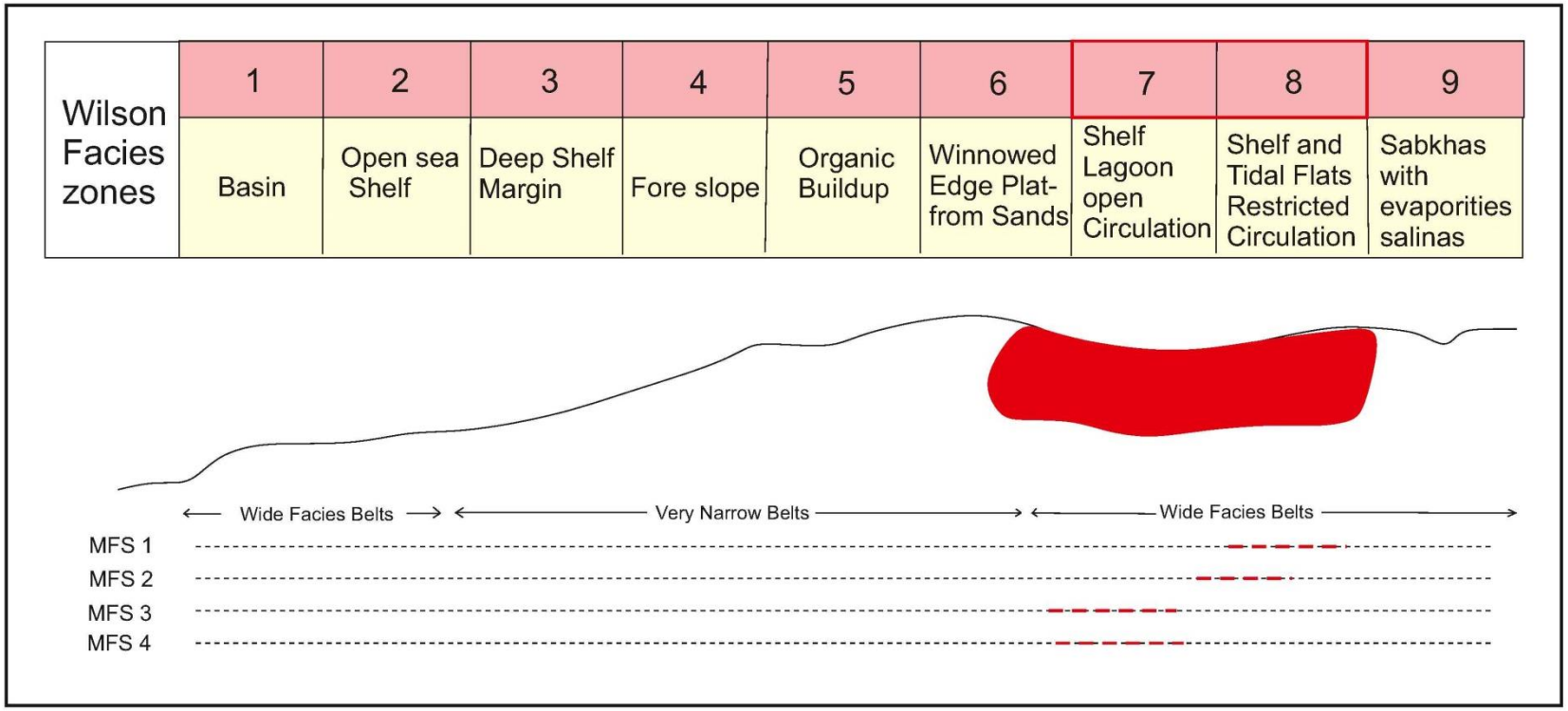

Figure 19: The MF 1, MF 2, MF 3, and MF 4 of the Derdere Formation present FZ 7 and FZ 8 in Wilson's facies belt.

Karababa Formation

The Karababa Formation is composed mainly of limestones (Figure 20). The thin section analysis under the transmitted light microscope revealed that there are four microfacies within the Karababa Formation in the Cemberlitas oil field. These include (1) phosphatic-glauconitic planktonic wackestone, (2) planktonic foraminiferous wackestone/packstone, (3) dolomitic planktonic wackestone and (4) mollusk-echinoid wackestone/packstone microfacies according to their fossil content and their location of deposition within the depositional realm of the formation. The major groups counted within the facies are: planktonic foraminifers, mollusks, glauconite and phosphate grains, echinoid fragments, gastropod fragments, benthic foraminifers, matrix, green algae and undifferentiated grains.

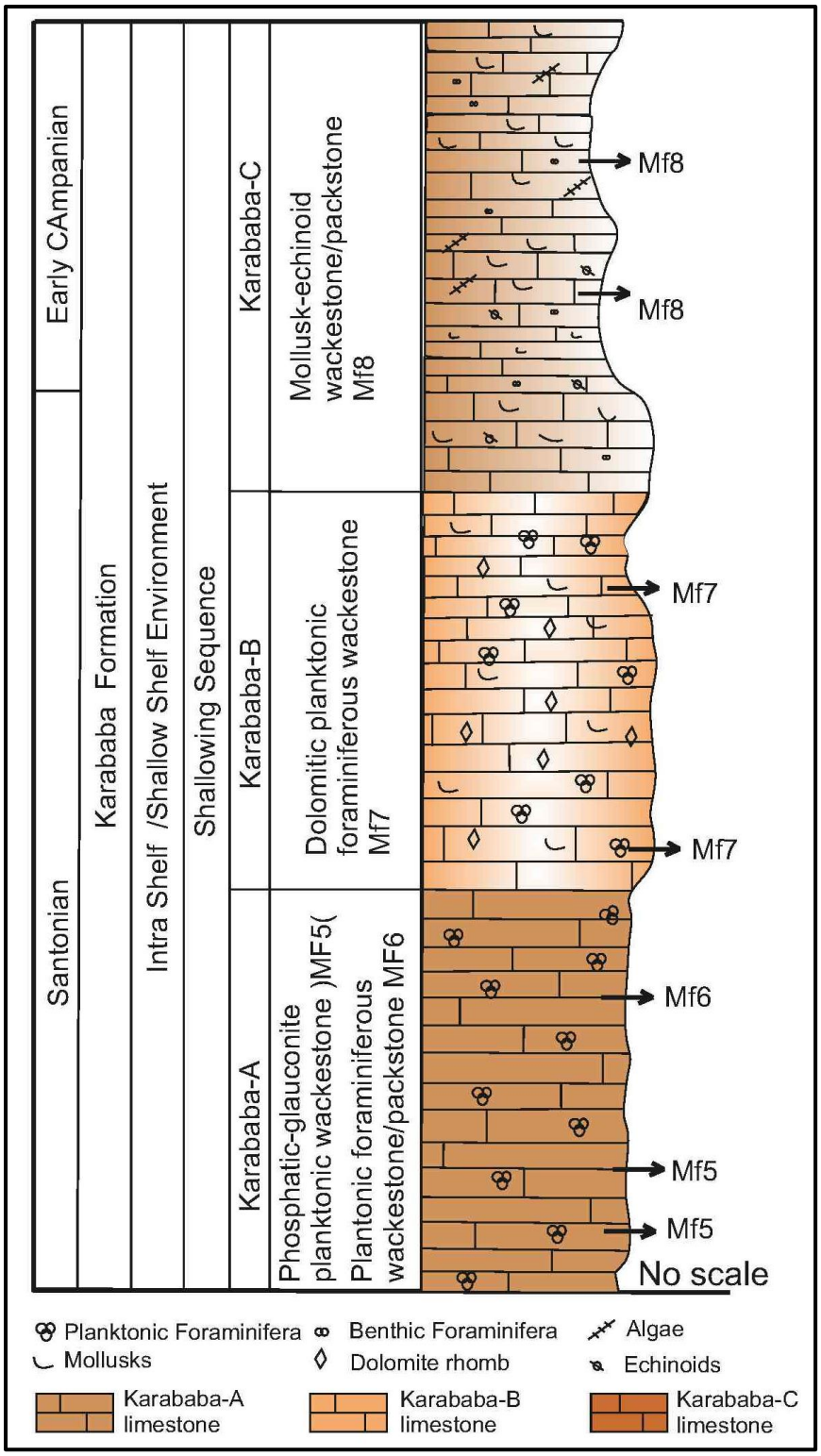

Figure 20: Generalized sketch of lithostratigraphy, facies, and depositional cycles of Karababa carbonates.

Phosphatic-Glauconitic Planktonic Wackestone (MF5)

Description: This microfacies typically underlies the planktonic-foraminiferous wackestone/packstone (MF6). It is composed of planktonic foraminifera, bivalves with less frequent glauconite and phosphate grains and patches are observed in the lower part of the Karababa Formation (Figure 21). All these components are embedded in a slightly recrystallized micrite or locally sparite, and stained argillaceous mud fragments are irregularly scattered throughout both the matrix and cement. The matrix is dominated by tiny bivalve fragments and organic matter (Figure 22). Small benthic foraminifera are less abundant than the planktonic foraminifera that dominate in the upper and lower levels. Planktonic fossils gradually decrease upwards in abundance with in this microfacies. The only grains deposited are observed to be acquiring green color is also present in some phosphatic wackestones. The abundance of glauconite and phosphate grains varies between 1-2%, and 2-3%, respectively.

Petrographic analysis of this microfacies included examination and point counting of 4 thin sections. The occurrence abundance of planktonic foraminifera range between 13%-50%., mollusks occur about 4-7%, other benthic foraminifera occurrence range is between 1%-10%, matrix existence range is between 45%-56%, echinoid fragments occurrence range is between 10%-15%, and ostracodes occurrence range is 1%-2%.

In average this microfacies is composed of 2.1% of echinoid fragments, 1.1% of benthic foraminifers, 1.2% of mollusks, and 50.9% of planktonic foraminifera (Figures 21 and 22). The major constituent of the microfacies is micrite matrix with 44.7% occurrence. 3.3% of the fragments are phosphate and glauconite affected by micritization, dolomitization or other diagenetic process. Algal fragments and corals were absent in the microfacies.

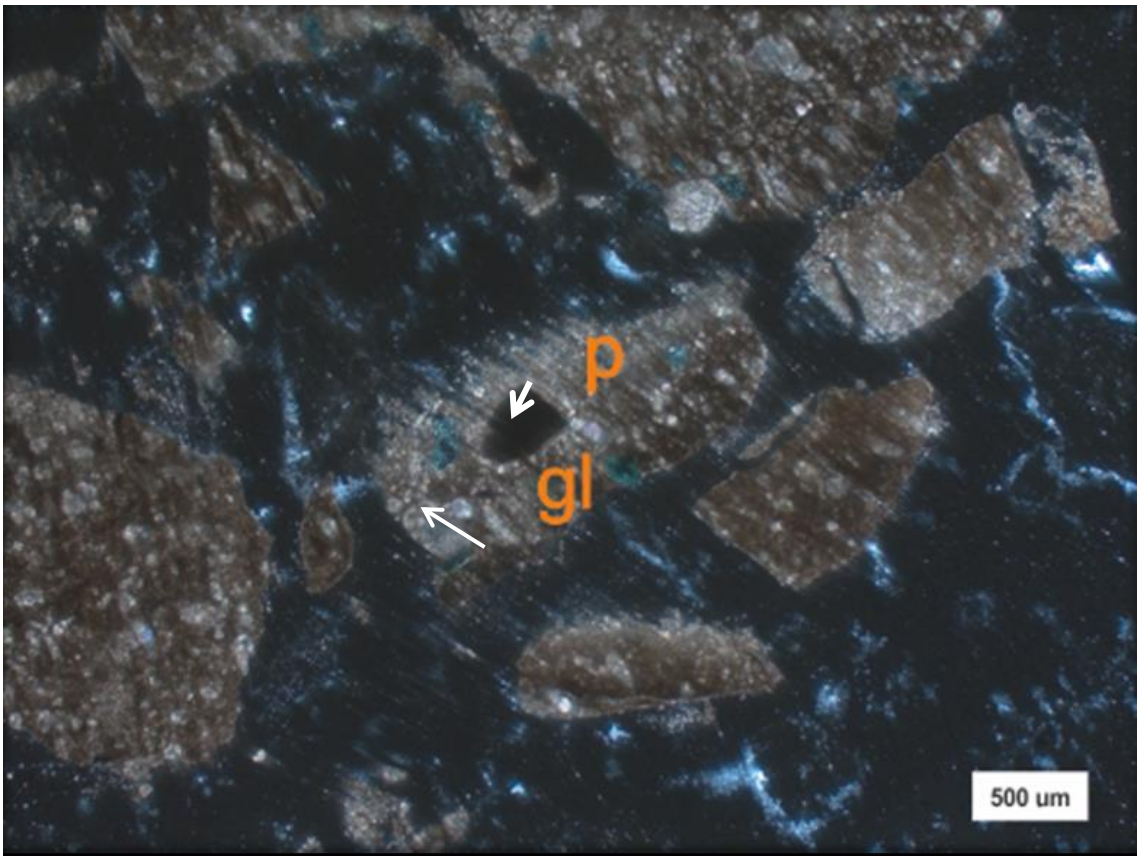

Figure 21: Photomicrograph (PPL) of Karababa- A Member (cutting sample) with phosphate and glauconite minerals at a measured depth of 3184 meter (P: phosphate, gl: glauconite) (Permit #Cem18).

Interpretation: This microfacies overlies the lime mudstone microfacies (MF4). It reflects deposition in a low energy, deep subtidal environment. The high abundance of fauna, especially, planktonic foraminifera, in this microfacies supports the interpretation of an open marine environment. The presence of echinoids and mud-supported fabrics (wackestone) indicate quiet water conditions.

Glauconite is an intra-basinal mineral that grows biochemically in the water of a depositional basin (Friedman et al. 1992). The presence of glauconite pellets strongly suggests that this lithofacies was deposited in an agitated shallow-marine setting of low sedimentation rate with temporary subaerial exposure (Logvinenko 1982). The glauconite-bearing strata are located at the base of transgressive/regressive cycles (Vail et al. 1991). The glauconite forms in a normal marine salinity or slightly alkaline solution (pH 7 ~ 8), warm water, slightly reducing conditions, and in the presence of phosphorites, iron sulphide, and decaying organic matter (Haq 1991). Initially, glauconite forms as an authigenic mineral in the marine environment by replacement of preexisting particles.

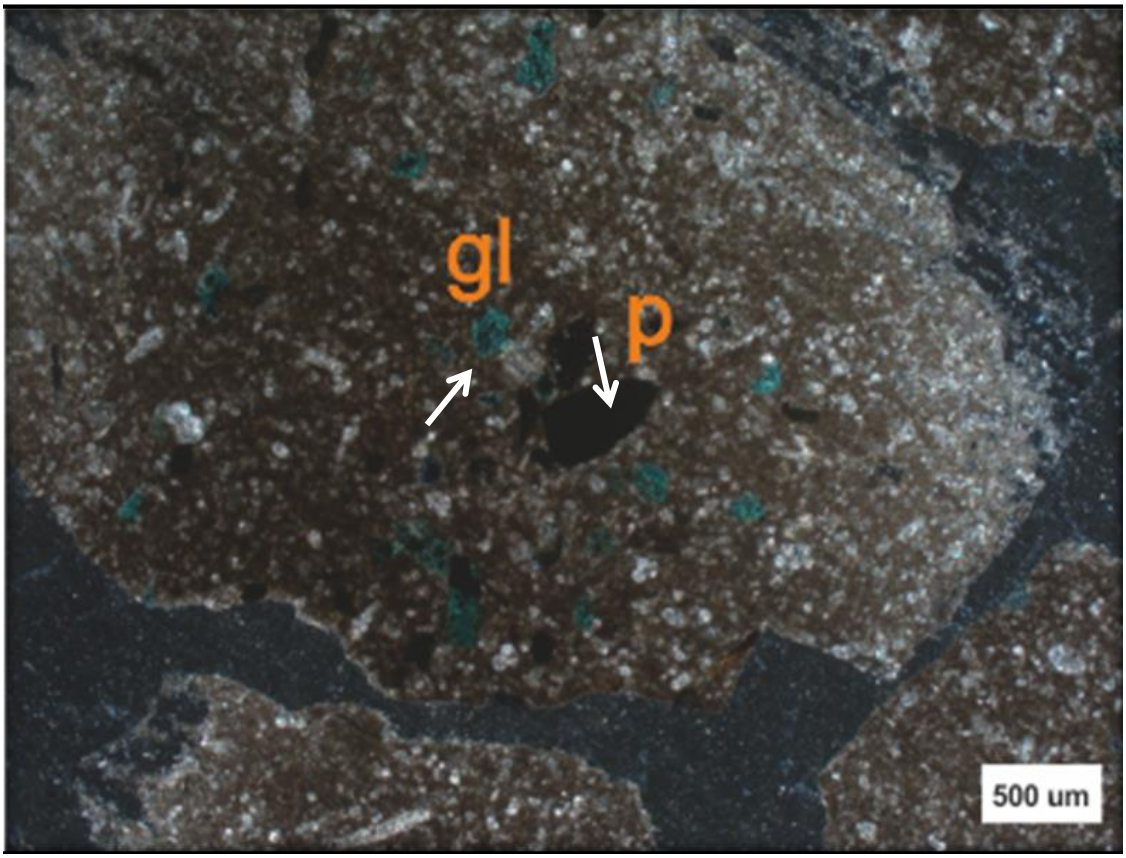

Figure 22: Photomicrograph (PPL) of tiny fossil fragments and organic matter with (GL) and (P) grains at a measured depth of 3184 meter (Permit #Cem18).

Planktonic Foraminiferous Wackestone/Packstone (MF6)

Description: The planktonic foraminiferous wackestone/packstone has similar characteristics as to those described above from (MF5). This microfacies is common at several horizons in the Karababa-A Member of the Karababa Formation in the Cemberlitas oil field. It consists mainly of dark brown and gray micrite contains rich-organic material, and is a slightly recrystallized into microspar exhibitions of few microfossils (Figure 23). It contains planktonic foraminifera and thin bivalve fragments, cemented by abundant micrite. Moreover, foraminifera is filled with fine sparry calcite and micrite cement, phosphate grains are scarce (≤1%), glauconite grains are absent, and micro-scale vertical size-grading occurs (Figure 24).

The major components of this microfacies are planktonic foraminifera (70%-80%) and matrix (20%-30%) whereas bivalves (1%-4%), other benthic foraminifera and ostracodes (1%) are less. On average this microfacies is composed of 70.2% planktonic foraminifera, 0.8% ostracodes, 0.5% echinoids, 1.8% bivalve fragments and 0.3% benthic foraminifers. The 24.6% of the microfacies consist of matrix (Figures 25 and 26). This microfacies accumulates in a deep subtidal to open marine environment. The microfacies occur near the base of the formation.

Interpretation: The sedimentary and fossil content of the Karababa Formation indicate it was deposited during the transgressive phase of a transgressive-regressive sequence, although there are small oscillations in sea level, the major trend is one of a eustatic sea level rise. This might be the reason why high energy microfacies are not observed in the Cemberlitas oil field. The microfacies are dominated by planktonic foraminifera, including the genera *Hedbergella* and *Heterohelex*, which occur in homogenous microcrystalline calcite. Many of the foraminiferal tests are replaced by subordinate sparry calcite such as *Globigerinelloides* and the pithonellid

calcispheres represents a planktonic assemblage that colonised shallow as well as deep, open, neritic environments.

This microfacies can be correlated with the FZ-2 and FZ-3 facies of Wilson (1975). It is interpreted as representing in a low energy deposition of a deep subtidal environment.

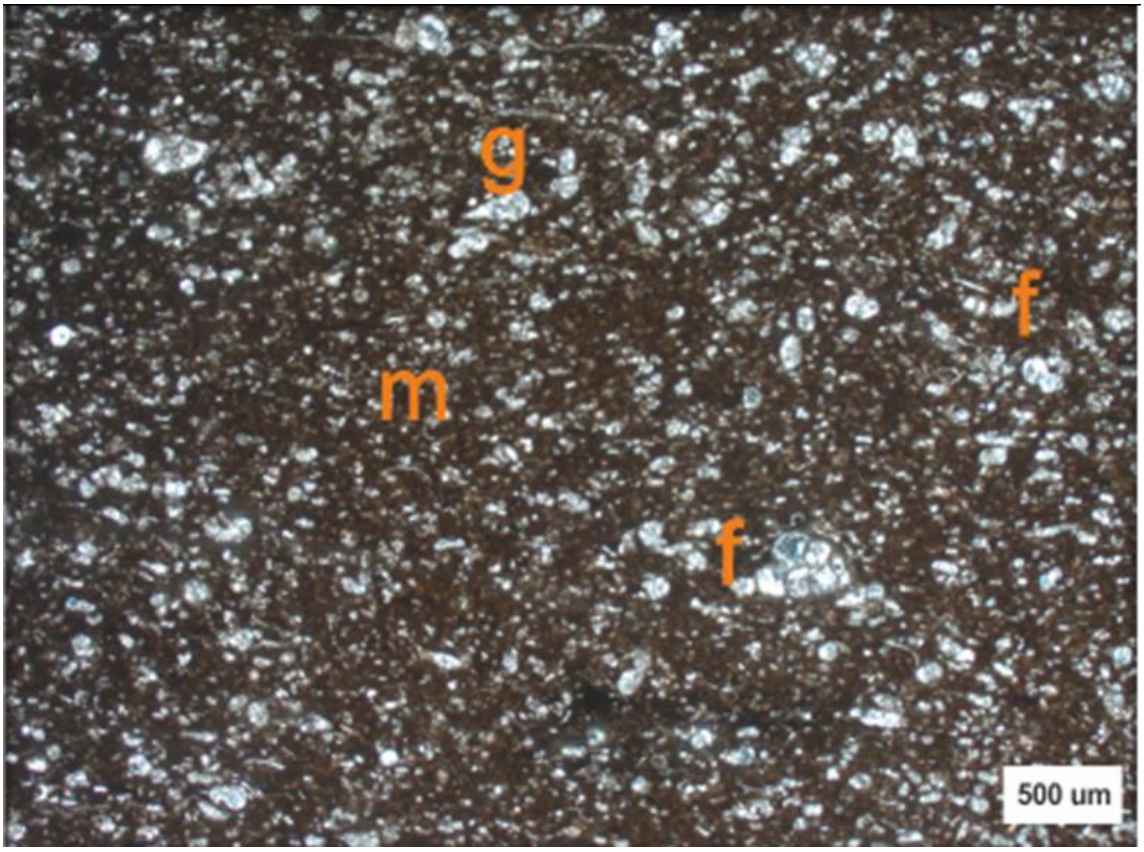

Figure 23: Photomicrograph (PPL) of Karababa-A limestone abundant planktonic foraminifera and thin bivalves fragments, cemented by micrite at a measured depth of 3184 meter (Permit #Cem18) (g: *Heterohelix* f: *Globigerinelloides*).

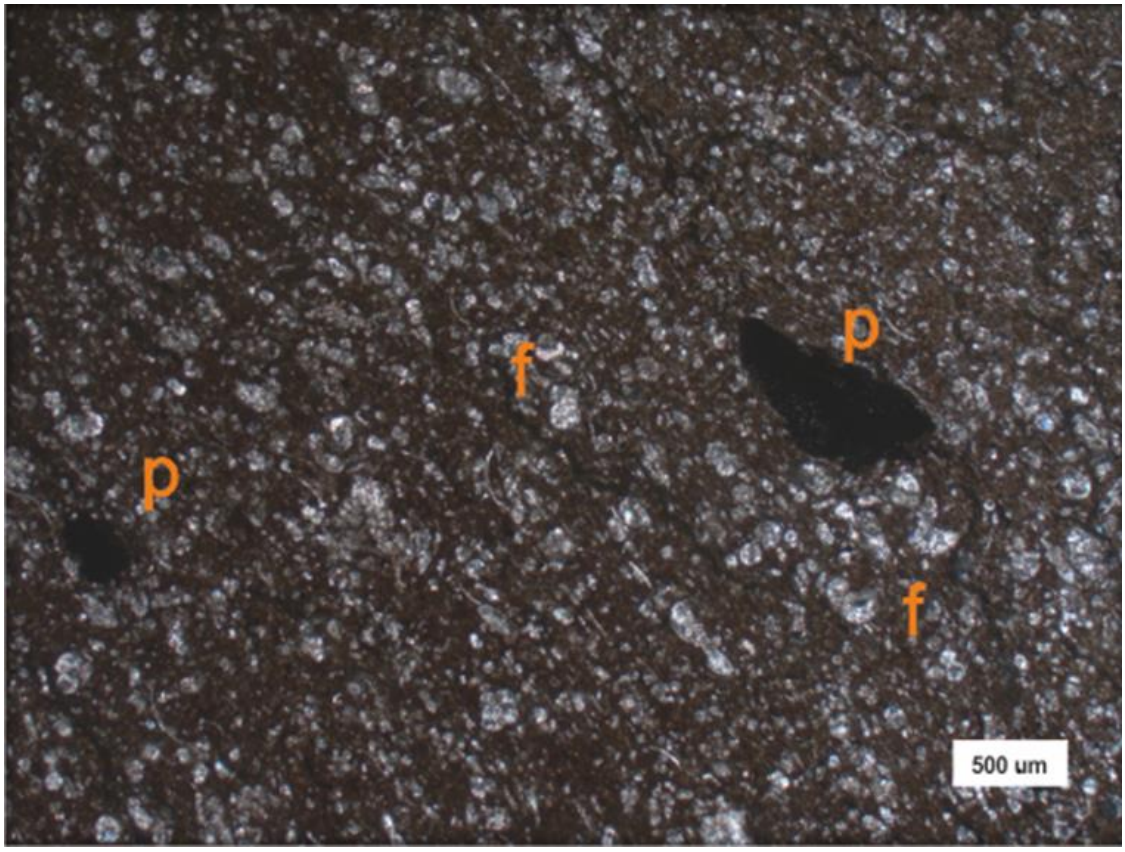

Figure 24: Photomicrograph (PPL) of Karababa–A limestone phosphate grains are scarce (≤4%), glauconite grains are absent, and micro-scale vertical size-grading is observed at a measured depth of 3184 meter (Permit #Cem18) (*g: Heterohelix f: Globigerinelloides).*

Dolomitic Planktonic Foraminifera Wackestone (MF7)

Description: The matrix consists of dolomicritic to very fine-grained anhedral crystals and fine-grained clear rhombic crystals. Where the cement is neomorphic calcite spar, it may consist entirely of extremely fine-grained crystals, or it may be fine- to medium-grained, subhedral crystals. In some places the matrix has a texture similar to that of the dolomicritic of the lower cherty dolomitic limestone, with extremely fine-grained anhedral crystals mixed with very fine- to fine-grained calcite rhombs. In places, clear, fine-grained, rhombic dolomite occurs in these samples (Figure 25). Fossils in this wackestone include planktonic foraminifera, echinoid fragments and mollusks. Generally, no more than three types are present at any given location, and usually there are only one or two varieties of fossils. Planktonic foraminifera are the most common, followed by echinoids and mollusks. The shells and tests of the fossils typically are calcite but may be partially or completely replaced.by dolomite. Occurrence of calcite is affected by dolomitization with the development of scattered subhedral to euhedral dolomite crystals, which form about 2% of the rock volume. The dolomite crystals range in size from 50 to 80 microns (fine to medium crystalline). They are rarely zoned with turbid cores and clear peripheries.

Petrographic analysis of this microfacies included examination and point counting of 32 thin sections. In 32 thin sections, the percent of planktonic foraminifera range from 2%-10%, echinoids range from 1-6%, mollusks range from 1%-3%, and matrix material ranges from 85%-97%. On average this microfacies is composed of 1.2% of mollusks, 5.1% of echinoid fragments, 8.6% of planktonic foraminifera, (Figures 25, 26 and 27). The major constituent of the facies is consisting of 85.1% of the rock (Figure 27). 1.3% of the rock composition is undifferentiated because of silicification and dolomitization.

Interpretation: This microfacies suggest deposition in shallow low-energy, open subtidal environments. It suggests deposition in shallow neritic water of open circulation at or just below wave base (FZ 3). These sediments accumulated in a low energy open shelf subtidal environment. In general, the degree of dolomitization of the original matrix increases as the number of fossils decreases. This suggests that the depositional environment became more restricted, possibly as to with circulation effects on increase or decrease in salinity that promoted penecontemporaneous dolomitization.

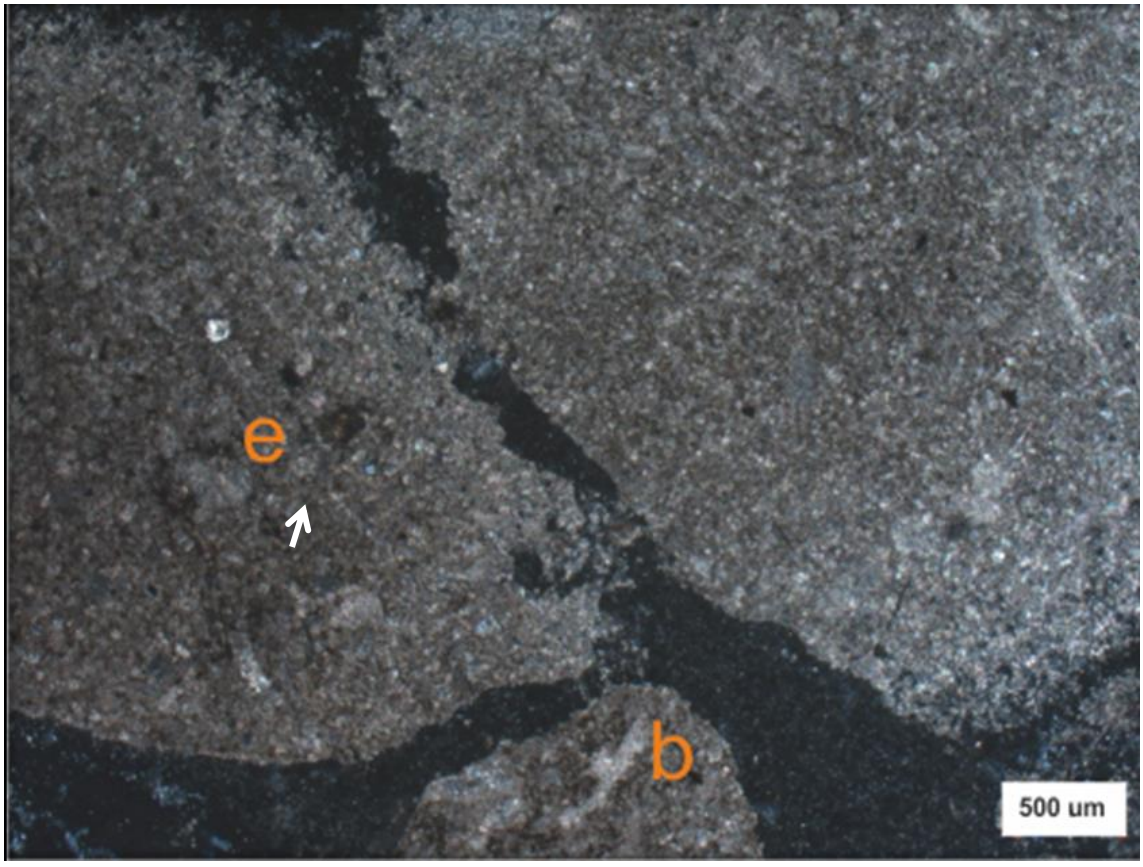

Figure 25: Photomicrograph (cutting sample) (PPL) of dolomitic wackestone facies of the middle Karababa Formation at a measured depth of 3184 meter. Note that the matrix has been partially dolomitized (Permit #Cem18).

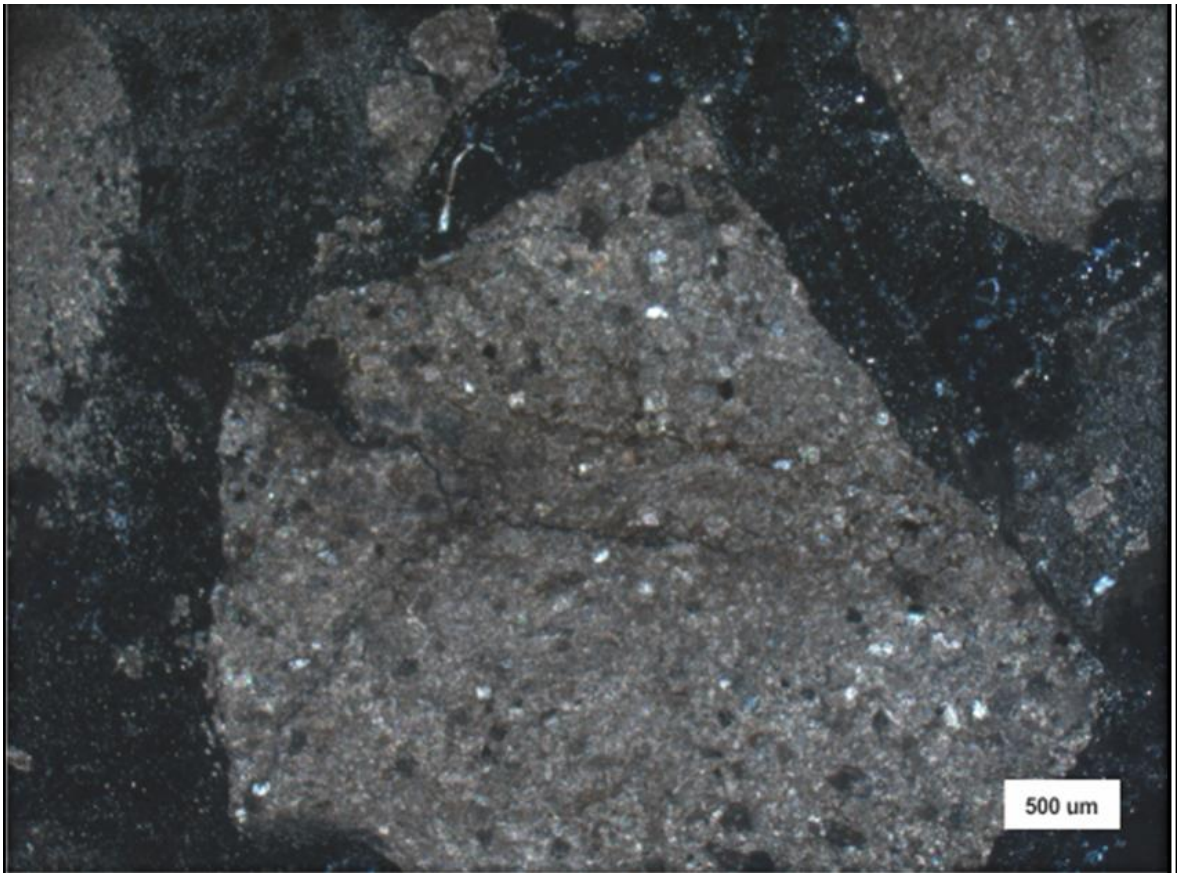

Figure 26: Photomicrograph (cutting sample) (PPL) of homogeneous microcrystalline calcite contains fine hypedomorphic monotopic dolomite crystals at a measured depth of 3184 meter. The dolomite rhombs might be formed by the later diagenetic dolomitization of the limestone (Permit #Cem18).

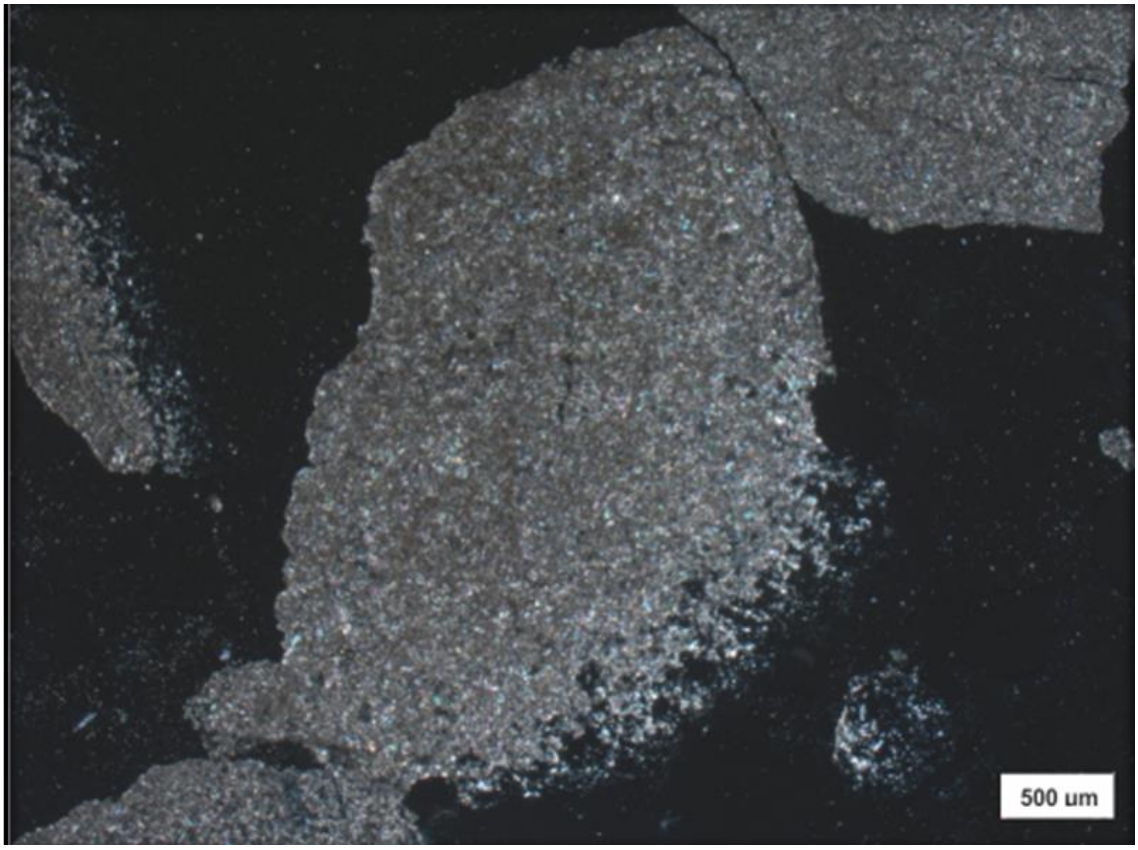

Figure 27: Photomicrograph (cutting sample) (PPL) of homogeneous microcrystalline calcite contains fine hypedomorphic monotopic dolomite crystals at a measured depth of 3184 meter. The dolomite rhombs might be formed by the later diagenetic dolomitization of the limestone (Permit #Cem18).

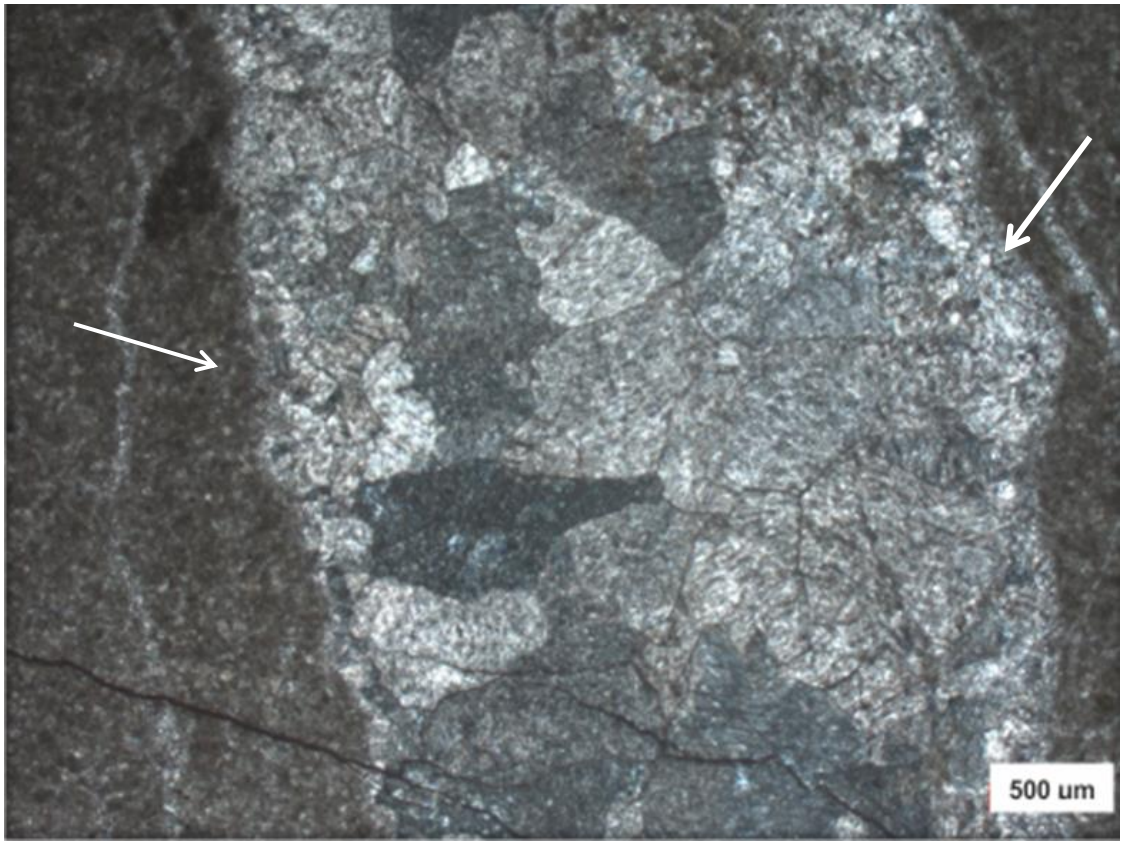

Figure 28: Photomicrograph (PPL) of major structure is partly filled in coarse crystalline dolomite which forms zone of large crystals (middle) at a measured depth of 3184 meter (Permit #Cem18).

Mollusk-Echinoid Wackestone/Packstone (MF8)

Description: Fossils in this microfacies include mollusks, echinoids, dasyclad algae, and planktonic and benthic foraminifera with phosphatic grains. Only a few phosphatic grains are present in each sample. The shells and test of fossils which were originally calcite generally remain calcite. Bivalve fragments and echinoids are most commonly calcified. Some fossils, usually echinoids, can be dolomitized and may be replaced by a single crystal of dolomite or by many fine rhombs (Figure 29).

Petrographic analysis of this microfacies included examination and point counting of 22 thin sections. The percent of mollusks range from 11%-65%, echinoids ranges from 5-32%, green algae ranges from 4%-26%, benthic and planktonic foraminifera range from 1%-2%, and matrix material ranges from 21%-95%.

On average this microfacies is composed of 50.3% of mollusks, 8.4% of echinoid fragments, 2.1% of benthic and planktonic foraminifera, and 7.1% of green algae (Figure 29, 30). The major constituent of the microfacies is micrite matrix with in average of 32.1%. 2.7% of the fragments are undifferentiated because of micritization, dolomitization or other diagenetic processes.

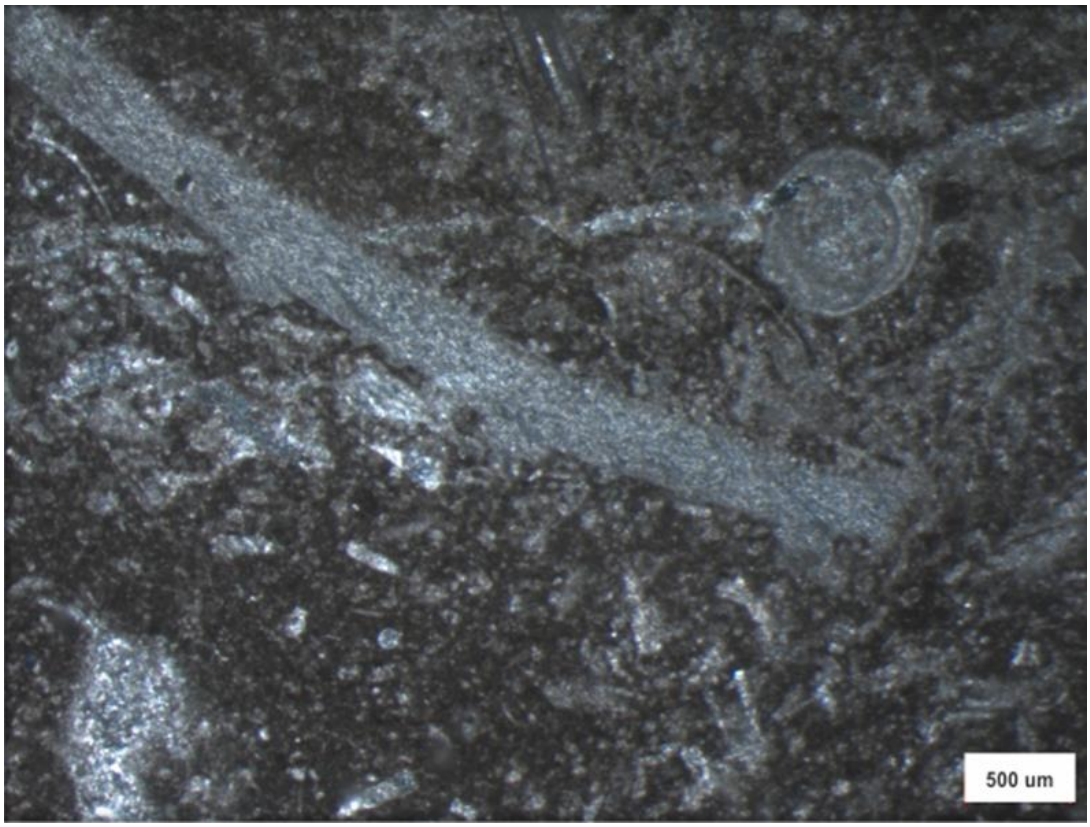

Figure 29: Photomicrograph (PPL) of mixed-skeletal wackestone facies of the upper parts of limestone. Note that the matrix has been partially calcitized at a measured depth of 3184 meter (Permit #Cem18).

Interpretation: Wackestones containing well preserved bivalves (Figure 29) reflect a low-energy depositional environment below fair-weather wave base. The excellent preservation of these shells indicates that they are replacing rather than reworked on the sea floor. Also no preferential of shells orientation is observed in this microfacies. The echinoids found in this subtidal environment are broken and transportation indicating and reworking by wave energy. Echinoids became a major constituent of shallow water benthic communities during the Cretaceous and particularly in deep water environments in late Cretaceous (Flugel, 2004). This microfacies can be correlated with the FZ- 8 facies of Wilson (1975). (Figure 30) that idealized the distribution of various algal groups shows that a predominance of dasycladacean green algae occurs in shallow shelf and lagoonal environments.

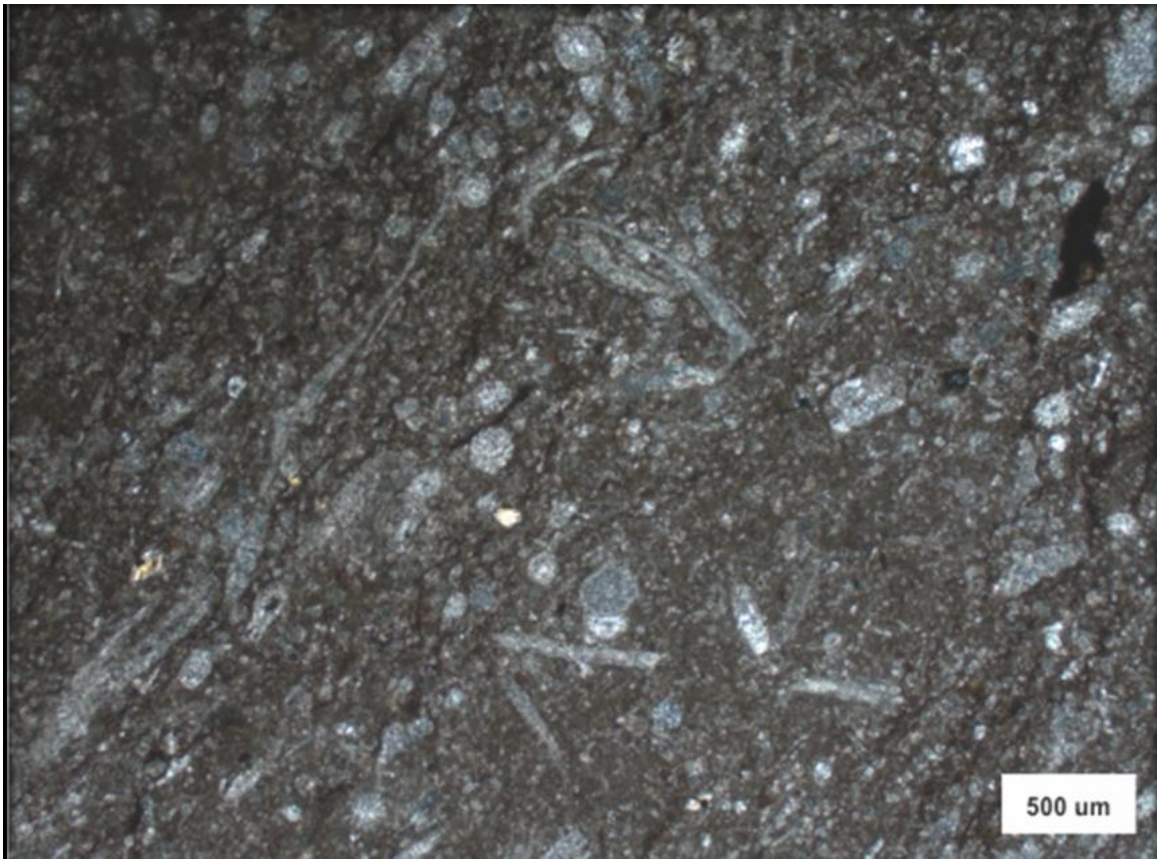

Figure 30: Photomicrograph (PPL) of remobilized and broken fragments with calcispheres and phosphatic grains at a measured depth of 3184 meter (Permit #Cem18).

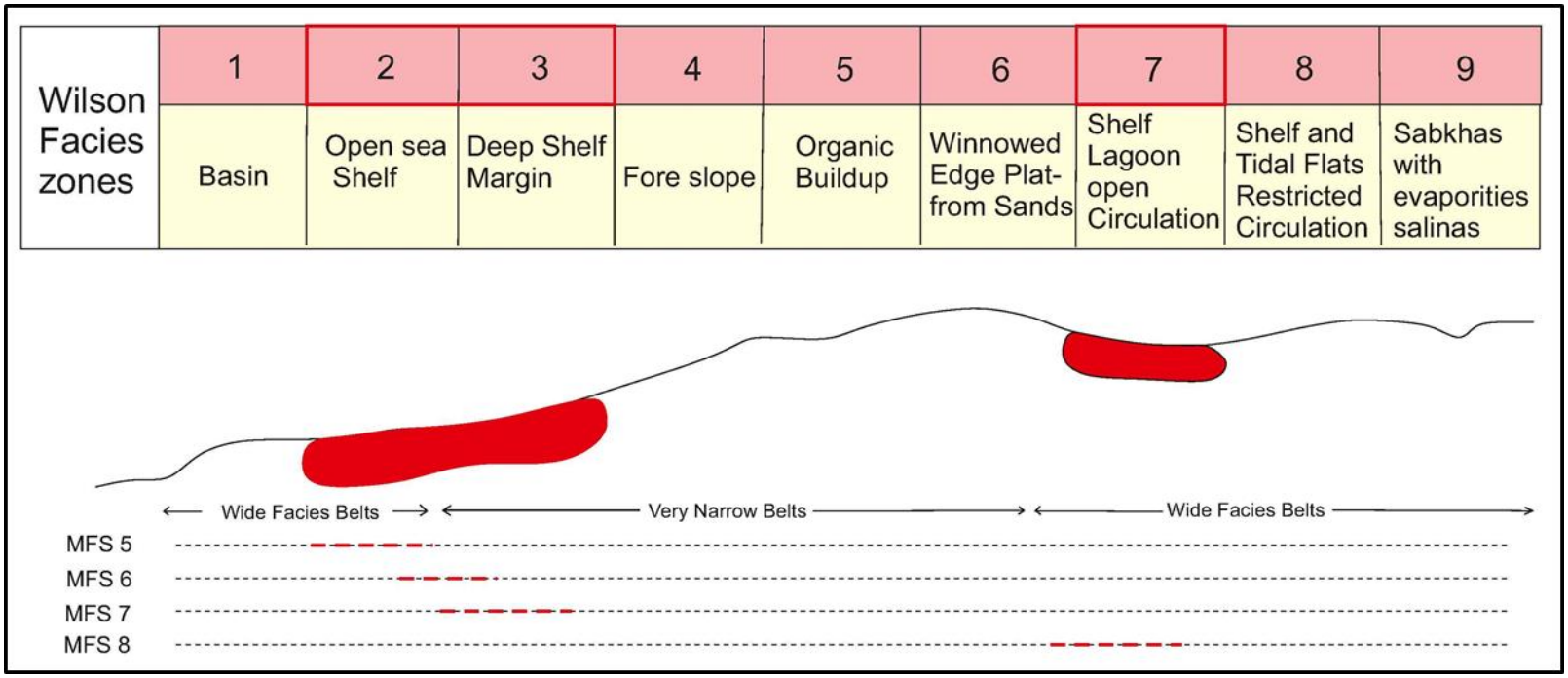

Figure 31: The MF 5, MF 6, MF 7, and MF 8 of the Karababa Formation present FZ 2, FZ 3 and FZ 8 in Wilson's facies belt.

4.2 Depositional Environments

Depositional Setting of the Derdere Formation

The characteristics of the microfacies of the Derdere Formation suggest deposition in a shallow shelf to marine lagoonal depositional environment. The presences of sedimentary textural characteristics such as coarser bioclastic fragments from mollusks suggest, low latitudes where sea water temperatures are always over 15°C and the salinity is normal. In this type of environment, calcareous green algae are common and along with numerous other organisms form a chlorozoan assemblage. The formation locally contains lime mudstone microfacies. The absence of larger foraminifera, textulariids, and open marine fauna is consistent with a shallow shelf to marine lagoonal environment (Figures 32 and 33). The lagoonal conditions were wide spread occurring in an epeiric shallow shelf setting that included local protected areas on the shelf associated with bivalve banks (Figure 33).

It has been suggested by many researchers that shallow marine sedimentation occurs in non-oceanic epeiric seas where great width of shelves and extreme shallowness of the waters are sufficient to restrict or eliminate circulation (e.g. Irwin, 1965; Harries, J.P. and Kauffman E. G., 1990). Depositional environments during the Derdere deposition included shallow water depths in the photic zone, warm temperatures, normal salinities and low to moderate water energy as evidenced by the presence of a high content of euphotic and stenohaline organisms, such as calcareous algae (dasyclad), ostracodes and bivalves. Such a faunal assemblage is characteristic of shallow marine deposition (Flugel, 2004). Shallow-lagoonal bivalve banks may be reworked by storms and/or affected by strong bio-erosion occur in this shelf-lagoon setting.

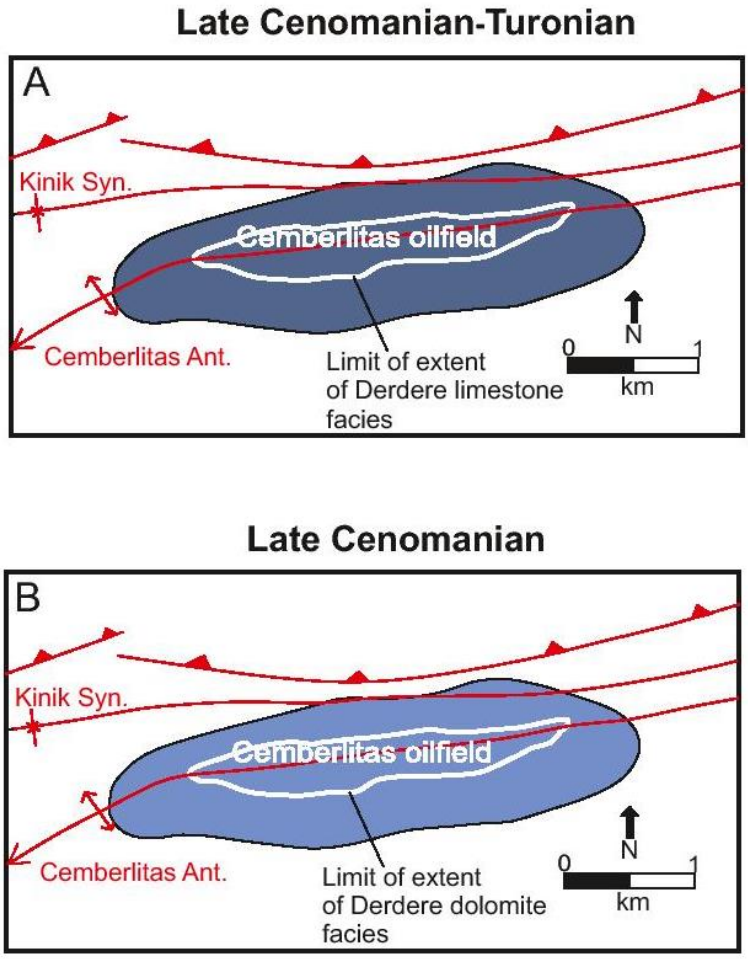

Figure 32: Facies distribution of the Derdere Formation (Cenomanian-Turonian) in the Cemberlitas oil field area. A) Derdere limestone facies and B) Derdere dolomite facies.

The abundance of suspension- and deposit-feeding macrobenthos of bivalves and echinoids of the Derdere Formation indicate eutrophic conditions that may account for the lack of hermatypic corals and patch reefs. Nevertheless, the lagoonal carbonate factory mainly consisting of heterotrophic biota (especially bivalves) and calcareous algae produced sufficient carbonate sediments to fill the available accommodation space. The topmost beds of the Derdere Formation represent a slightly restricted environment characterized by elevated salinities and

very shallow water environment. An absence of macrofauna and the occurrence of low diversity microfauna predominated by benthic foraminifera (miliolids) support this interpretation.

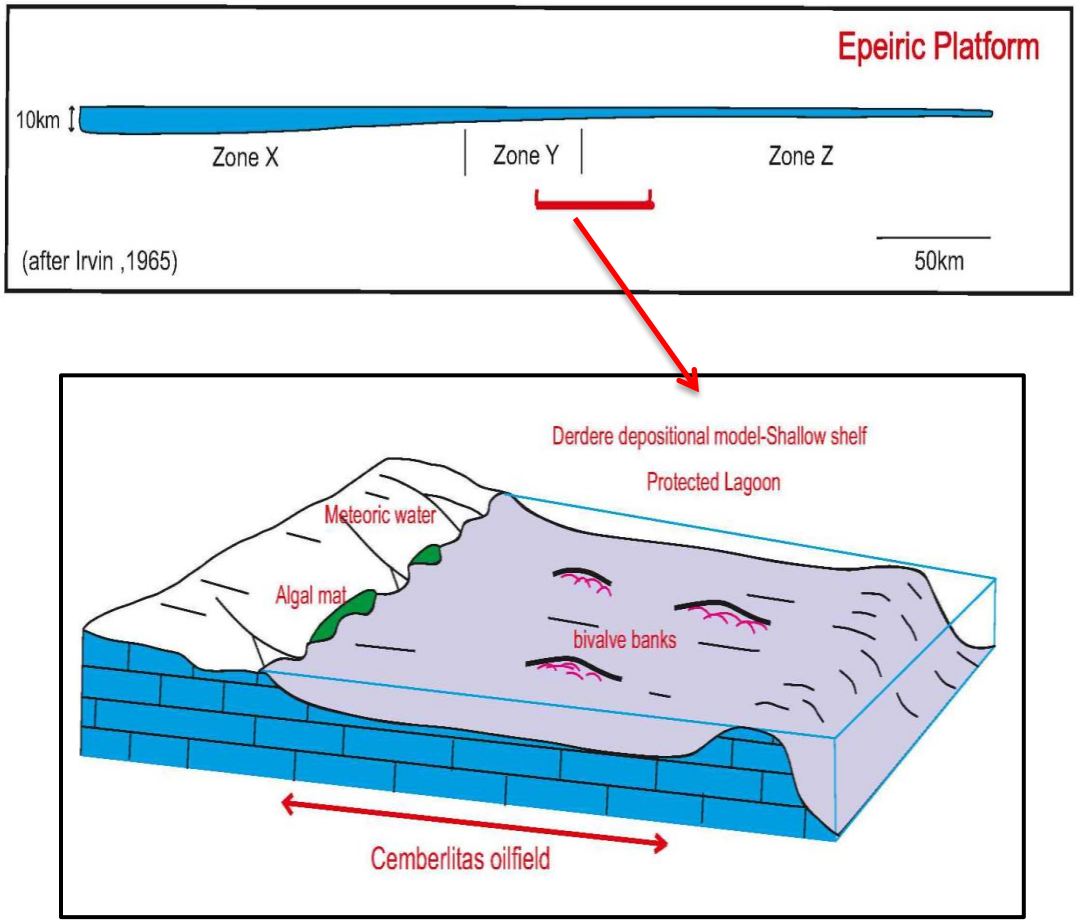

Figure 33: Depositional setting of Derdere Formation in the Cemberlitas oil field (based on Irwin 1965 and Flugel, 2004 epeiric shallow marine model).

Factors Restricting Circulation in Lagoonal Environments

The tectonic framework may have directly affected the water circulation in the study area. Small topographic relief may have had disproportionately large effects. A relief of tens of meters may have mimicked the restrictive effects of hundreds of miles of horizontal distance (Shaw, 1964; Flugel 2004).

Almost any elevation of the sea floor may have caused the development of many features commonly attributed to barriers such as bivalve banks (Figure 33).

In quiet water areas, behind barriers, or across broad shallow water shelves restricted circulation and climatic factors may strongly influence the type of carbonate sedimentation in a unique way. Insufficient circulation results in restricted environments for most marine organisms. It also results in more variability when it occurs in shallow epeiric sea areas. In epeiric seas, it is unlikely that movement of water in the form of high currents of the type characteristics of today's open oceans could even have existed (Harries, J.P. and Kauffman E. G., 1990).

Harries, J.P. and Kauffman E. G., (1990) stated that ''the shallowness of the seas in Derdere time would have dissipated the energy of the current through friction on the seafloor. The shallow depth of water would probably have precluded the transfer of such large values except at very slow speeds. This is not to infer that epeiric seas during deposition of the Derdere Formation were without currents and always stagnant. Currents were probably created largely by wind. Prevailing winds could have moved some water persistently, setting up epeiric currents. If such winds blew consistently from the open ocean onto the shallow epeiric shelf, they could extend the effects of normal marine salinities somewhat beyond the limit of tidal exchange. In this case, however, the existence of the current would only flatten the salinity gradient, because as once the water in the current passed beyond the zone of tidal exchange, it would come under the inexorable forces of evaporation, and the salinity would increase as the water was further removed from its source of replenishment.''

Movement does not prevent evaporation; waters in motion are as much subject to increased salinities as still water. In addition to supporting generally restrictive circulation conditions, preferred structural orientation of positive features or uplifts within the epeiric sea floor normal to prevailing wind and current direction may result in a vortex situation. The resultant constriction may cause an increase in current velocity through the aperture, which when combined with shallowing of water depth intermittently increases the energy level of bottom water in the shelf region and leads to periods of erosion and minimal net sedimentation (Bottjer and Bryant, 1980).

Dolomitization

As discussed above, the carbonate rocks of the Karababa and Derdere formations were deposited on a shallow marine environment. No features suggestive of sabkhas and supratidal conditions are found in the Cemberlitas oil field area. Amthor and Friedman (1992) stipulated that the fluid available for and capable of extensive dolomitization in early diagenetic stage is seawater of normal or elevated salinity. Vahrenkamp et al. (1991) stated that the formation of massive dolomite requires a long residence time for the dolomitized body near sea level and the optimal situation for dolomitization is prolonged sea-level highstands and slow subsidence (during times of minimum sea-level fluctuation). In addition, the only major source of magnesium for penecontemporaneous and shallow-burial dolomitization may be seawater (Lee & Friedman, 1987). Magnesium for deep-burial conditions can be supplied from (1) connate waters (trapped seawater); (2) dissolution of unstable original minerals; (3) pressure solution (stylolitization); (4) compaction of underlying shales; and (5) basinal brines (Lee & Friedman, 1987).

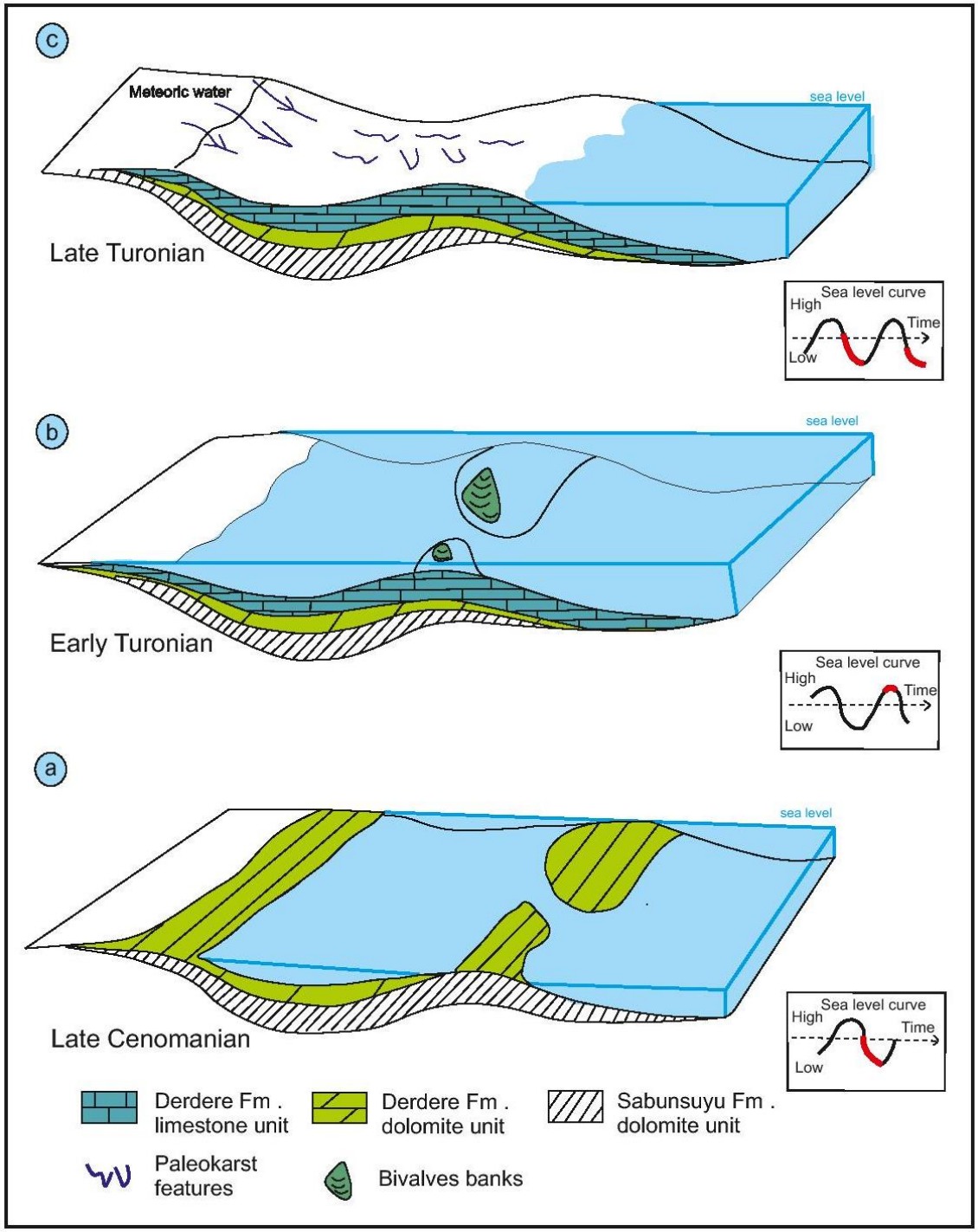

Figure 34: Diagrams showing of Derdere depositional environments in the Cemberlitas oil field area. The presence of a subaerial unconformity on the top of the Derdere Formation shows that paleokarst features were developed on surface.

In the Cemberlitas oil field area, dolomitic carbonates are almost entirely restricted to the shelf interior which is interpreted to have been covered by restricted lagoons favourable for the deposition of lime muds. Dolomitization was brought to an end by flooding of the lagoonal area during relative sea-level rise when the bivalve bank facies of the Derdere Formation was deposited (Figure 34b). Subsequent sea-level fall led to exposure of the Derdere Formation to the surface (Figures 34a, 34c).

The thickness variations of the Derdere Formation may explain the karstification and the absence of evaporites in the Derdere Formation. The dissolution phase also accentuated by well-developed secondary porosity in dolomite facies, making it one of the most important reservoir rocks in the Cemberlitas oil field.

In southeast Anatolia, the late Cretaceous dolomites can be linked with sea-level changes since they occur at the top of transgressive regressive depositional sequences, and just below unconformities that form the sequence boundaries. This is particularly true for the dolomites in the Cemberlitas area which are located at the top of a middle Turonian depositional cycle, (Figure 34), just below a subaerial exposure surface which correlative with the global 90.5 Ma sea-level fall. The sea-level lowering basically led to the establishment of seawater - meteoric water mixing with a progressive dilution that controlled the dolomitization.

Depositional setting of Karababa Formation

Intrashelf basins were common on the shallow margins of the Arabian Plate in Cenomanian-Turonian time (Yilmaz, 1993 and van Buchem et al., 1996). Aigner et al., (1989) suggests that these relative shallow depressions are formed by a combination of load-induced, isostatic sagging of the platform interior and a major rise in sea level. Since these basins occur in

tectonically stable areas and are controlled mainly by high-frequency sea-level changes, they tend to be geologically short-lived and filled during subsequent sea-level cycles. The infill of intrashelf basins often consists of storm-generated sequences of sediments derived from the surrounding platform (Read, 1985); in deeper parts of the basins, organic-rich sediments may accumulate, which can form source rocks for hydrocarbons (Ayres et al., 1982).

The Coniacian-lower Campanian Karababa Formation is considered to be one of the major source rocks in southeastern Turkey (Gorur, 1985) because it consists of organic-rich limestones. In places, glauconite occurs locally scattered throughout the sediment. The deposition of the Karababa source rocks took place in an intrashelf basin on the broad, epeiric, shallow-water carbonate platform which extended over much of southeastern Turkey.

The Karababa Formation was probably deposited in intrashelf settings under wet climatic conditions. The organic-rich Karababa limestone is *Heterohelix*-bearing and marly limestone which reflects a combination of climatic influences including, variable nutrient levels and eustatic sea level changes during the deposition of the Karababa–A Member (Figure 35d). The association of non-keeled planktonic foraminifera such as *Globigerinelloides* calcispheres represents a planktonic assemblage that colonised shallow as well as deep, open, neritic environments. This facies is interpreted as the deepest intra-shelf basinal environment with an estimated water depth in the order of 60–150 m, based on geometrical reconstructions, with bottom-water conditions that varied from well oxygenated to dysaerobic (Van Buchem et al. 2010).

This type of facies occurs in the third-order transgressive phases at the base of the Karababa-A member. The abundance of the *Heterohelix* calcispheres indicates transgressive episodes. The *Heterohelix* and *Globigerinelloides* calcispheres are found to dominate in the limestone and are considered as indicators of eutrophic conditions. The presence of marly limestones is considered as an indication of wet episodes when abundant run-off would have generated sediment-laden brackish water bodies (Van Buchem et al. 2010). Limestones represent periods of high productivity of calcareous planktonic skeletons and the marls represent times of low productivity. Microscopic observations of this Karababa-C facies showed the presence of mollusks, echinoids, green algae and small benthic foraminifera. This facies occurs in the regressive part of the third-order sequences with a paleowater depth just above or around storm wave base. Therefore, it is interpreted as a shallow water, well-oxygenated, intra-shelf basinal environment, with an estimated water depth in the order of 10–40 m. (Figure 35f)

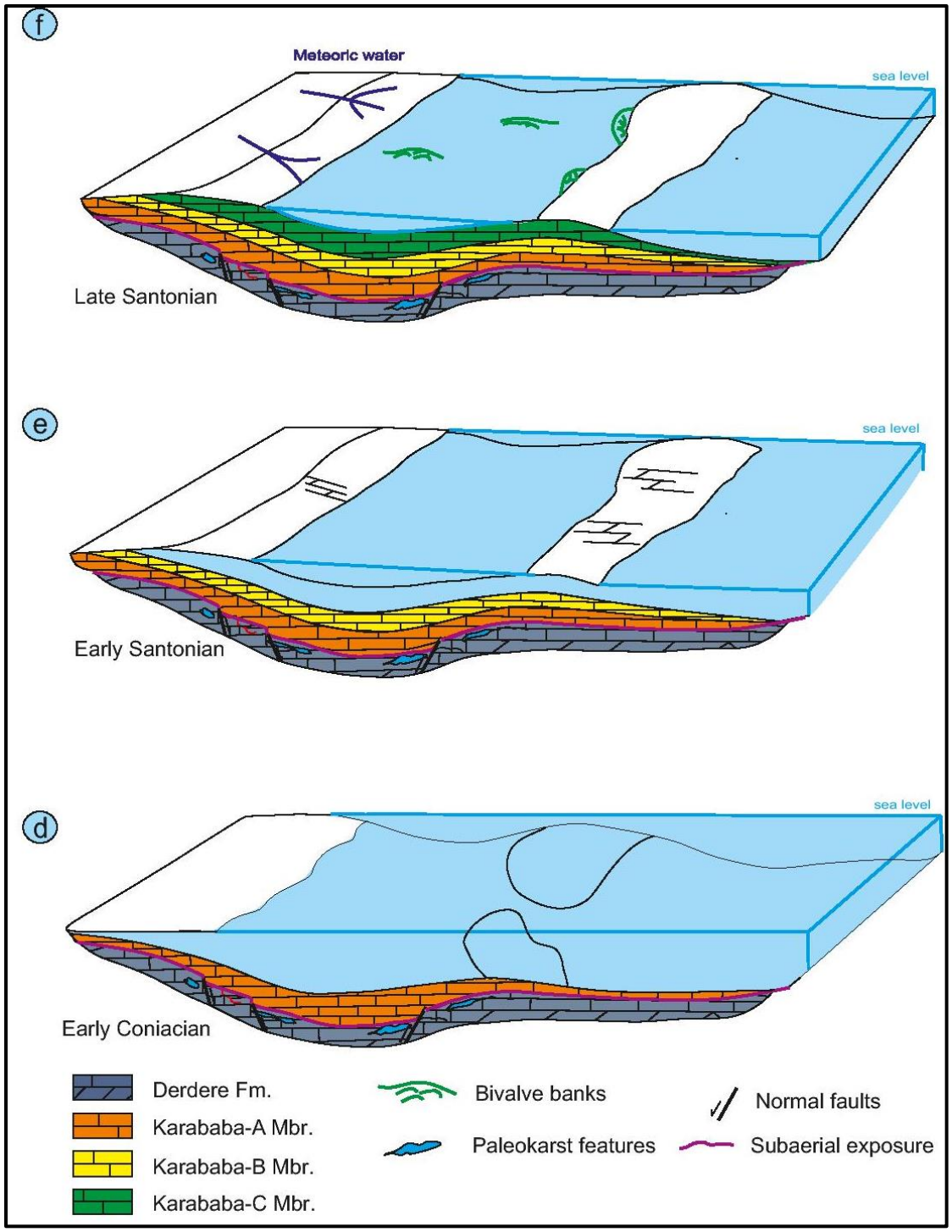

Figure 35: Diagrams showing possible Karababa depositional environments in the Cemberlitas area.

Sedimentary environments interpretation

The regional correlation of the Karababa Formation shows that deposition took place within a basin surrounded by a shallow-water carbonate platform (Perincek, 1980). The biota of the sediments gives little indication of the depositional water depths. The absence, or sparse occurrence, of planktonic foraminifera could be due to shallow water depths or other unfavorable environmental conditions or due to diagenetic processes. This does not necessarily indicate a "deep" water setting. Moreover, abundant calcareous planktonic foraminifera are also known to occur in lagoonal areas with water depths of less than 40 m (Scholle and Kling, 1972; Mancini, personal comm. 2013). The fine-grained and muddy textures, in lithofacies suggest a low-energy sedimentary environment, mostly below fair-weather wave base. The abundant preserved marine organic matter suggests poorly oxygenated to anoxic bottom water conditions. In contrast, the abundance of various agglutinating benthic foraminifera, bivalves and dasycladacean- like algae and bioturbation indicates a shallow marine, well-oxygenated environment for the sediments of Karababa-C. The presence of echinoids in many intervals suggests that "normal" marine salinities were common. From the above, a shallowing upwards trend can be observed going from the dark, organic-rich to the light organic-poor to the Karababa-C intervals. The vertical distribution of these intervals observed in this study suggests that the formation consists of one transgressive- regressive cycle (Figure 35).

Hardgrounds and Upwelling currents

The development of hardgrounds (Figures 21 and 22) and related glauconitic- phosphate crusts in the Cemberlitas oil field area (see. MFA- Karababa) may be attributed to depositional isolation on submarine paleotopographic or structural highs, or the activity of bottom currents

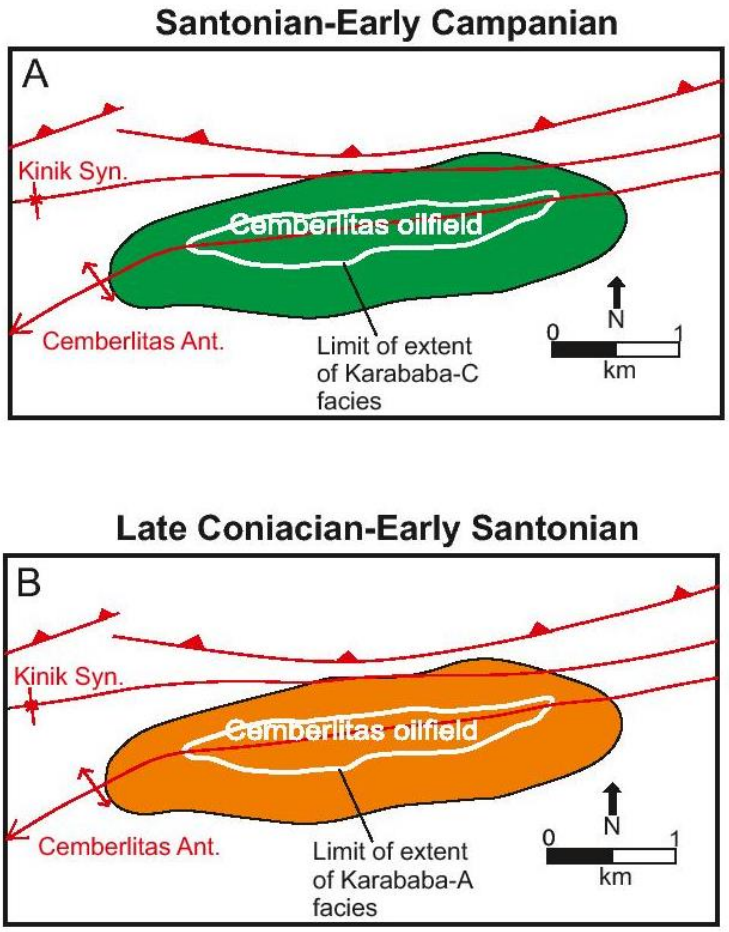

Figure 36: Facies distribution of the Karababa Formation (Coniacian-lower Campanian) in the Cemberlitas oil field area. A) Karababa-C facies and B) Karababa-A facies.

that may influence the depositional surface of the outer continental shelf. The benthic edges of the cavities within the hardground are replaced by green authigenic glauconite and the pore spaces are filled with pelagic wackestone. Phosphate crust covering submarine paleotopographic highs are characteristics of depositional hiatuses (Clari et al., 1995; Hillgartner, 1998). The close relationship of glauconitic phosphate crusts with hardgrounds (Figure 24) clearly indicates that glauconite and phosphate were both formed at the interface of the hardground with marine water in the Cemberlitas oil field area. Solution cavities within the hardground were freely connected to the open-sea floor. The cavities within the hardground evidently were produced by the

dissolution of carbonate in a subaqueous environment, in the presence of decomposing organic matter, and partly by biological erosion. While the condensed glauconitic-phosphatic limestone unit in the Cemberlitas oil field area is mainly attributed to sediment starvation and upwelling associated with eustatic sea-level rise, tectonic factors also appear to have played a significant part (e.g. Clari et al., 1995; Hillgartner, 1998).

Condensed section

In Cemberlitas oil field area Karababa-A Member is a condensed section. Condensation mechanism show that rapid sea level rise brings about the transformation of shallow water and nearshore sections into pelagic ones, decline in the erosion rate, and a decrease of erosion area. This is, naturally, the principal reason for condensed section (Loutit et al., 1988). Shallow water hemipelagic and pelagic condensed sections originate during rapid sea level rise under shelf or epicontinental basin conditions. Anoxic pelagic deep sea and shallow water epicontinental condensed sections can also occur (Einsele, 2000) such as Karababa-A Member condensed section. Even a small sea level rise in an epicontinental basin with a thin sedimentary cover and low topography is sufficient for flooding sources of sedimentary material supply and for development of a condensed section. A rise in sea level is usually accompanied by an upwelling of cold oceanic water on the shelf. This process results not only, in the formation of a shallow water hemipelagic condensed section with glauconite and phosphate but also, in an additional decline in sedimentation rate due to sediment rewashing.

4.3 Sequence Stratigraphy

The carbonate microfacies of the Derdere-Karababa formations contain a distinctive assemblage of facies and stratigraphic surfaces that can be used to define depositional sequences and systems tracts. During this study, a special attention was given to the determination of surfaces indicating subaerial exposures, such as hardground development, and abrupt juxtaposition of contrasting facies. The sequence stratigraphic terminology of Van Wagoner et al. (1988) and Sarg (1988), were used under the light of the by concepts developed by Catuneanu (2002) and Schlager (2005).

The Derdere and Karababa formations in the subsurface can be subdivided into two third-order sequences that were deposited from the middle Cenomanian to the early Campanian (Tardu, 1991). Each depositional sequence is bounded by an unconformity and its correlative conformities and contains transgressive and regressive facies. Within each sequence, deepening trends define the transgressive system tract (TST), and shallowing trends define the highstand system tract (HST). Transition from deepening to shallowing successions appears to define downlap surfaces, which also are interpreted as maximum flooding surfaces (MFS) (Figure 37).

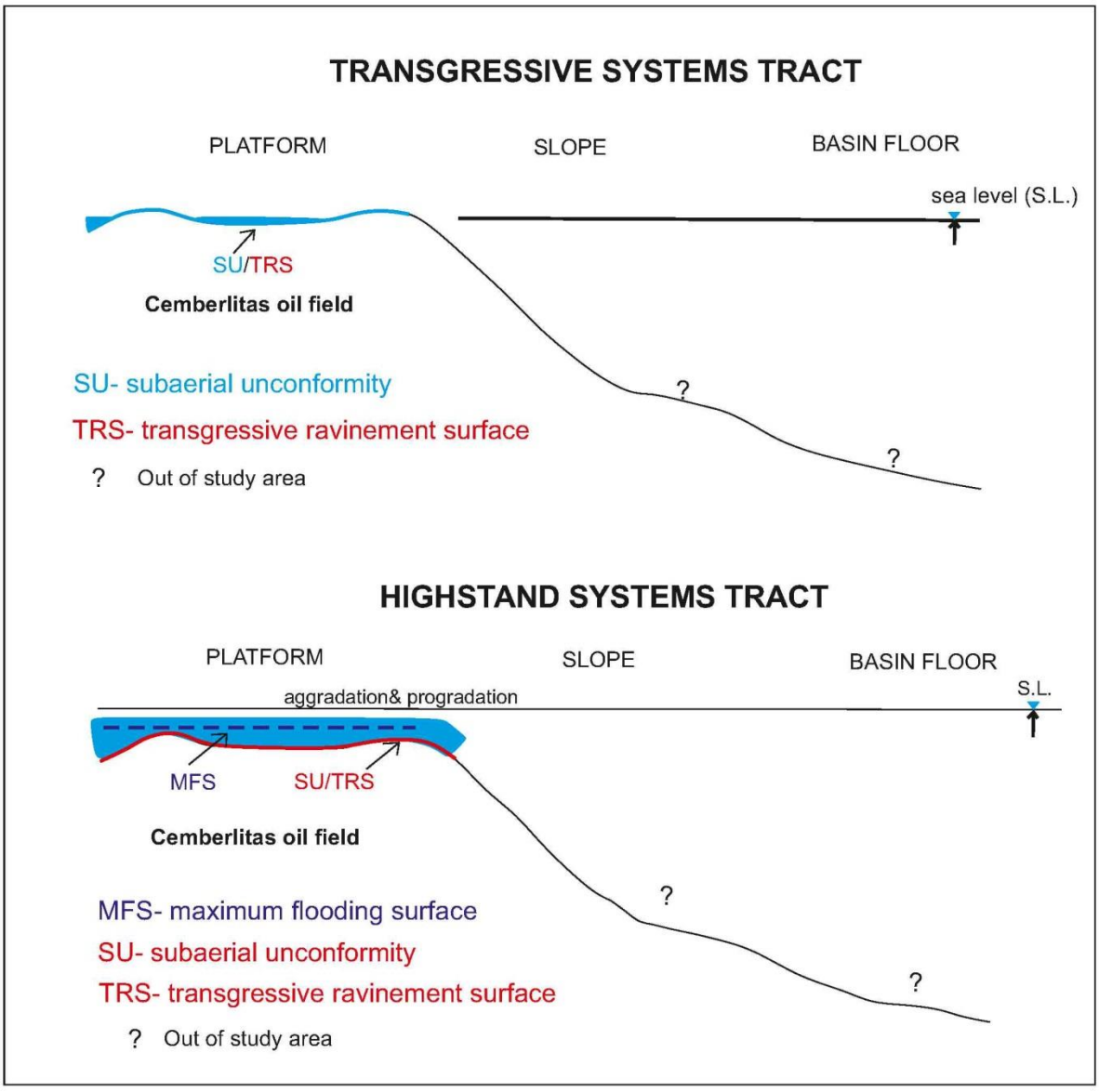

Figure 37: Schematic models showing development of system tracts for the Cemberlitas oil field (after Slowakiewicz, 2009).

Sequence boundaries (SB)

During this investigation, sequence boundaries were located where there are surfaces indicating abrupt facies changes, such as submarine hardgrounds or subaerial exposures. The following sequence boundaries are distinguished.

Lower sequence boundary (SB1) of the Derdere sequence

In the Cemberlitas oil field area, the lower sequence of the Derdere Formation is traced between the shallow carbonate deposits (lagoon) of upper Turonian Derdere Formation and the deep subtidal (intra shelf) carbonate deposits of the underlying Santonian-Coniacian Karababa Formation (Figure 38). The surface contains features suggesting solution widened fractures, collapse breccia, vugs and cave floor deposits development at time of subaerial exposure (Wagner, 1987). This surface is recognized as a subaerial unconformity. This recognition is similar to that described in the sequence boundaries in the Jurassic and Cretaceous shallow-marine carbonate platform of France and Oman by Hillgärtner (1998), and Immenhauser et al. (2001), respectively who ascribed the brecciation in the carbonate platforms to their karstification during an episode of sea-level fall and exposure. Also, the occurrence of shallow marine deposits above this subaerial unconformity surface represents a transgressive surface of erosion (Van Wagoner et al., 1988) or a ravinement surface (Catuneanu, 2002).

Both phosphate and glauconite are commonly associated with hardgrounds. The presence of hardground does not necessarily indicate emergence of the sea floor. Hardgrounds may have developed during a minor break in sedimentation or a very slow rate of marine sedimentation accompanying by a short-term sea-level fall. This surface of phosphate and glauconite could be formed during a short period of sea-level fall in the carbonate platform (Sarg, 1988). In the study

area, this lower sequence boundary is delineated Karababa-A Member of the Karababa Formation (Figure 38).

Upper sequence boundary (SB2) of the Karababa sequence

Within the study area, the second sequence boundary is Santonian/Campanian in age. It is a sharp boundary and is easily traced at the top of the Karababa-C Member due to obvious variations in facies (Figure 38). It is traced between the shallow marine carbonate deposits of the basal part of the Santonian Karababa Formation and the deep marine deposits of the underlying Campanian Karabogaz Formation. This contact marks an intense hardground in the study area possibly due to a minor sedimentation break in association with a short-term fall in sea-level. Correlation with the sea-level curve given by Luning et al. (1998) for the central-east Sinai shows some similarities especially for the sea-level falls associated with the Santonian/Campanian boundary (Figure 38).

Although not directly observed, circumstantial evidence suggests that the transgressive-regressive cycle of the Karababa Formation is bounded by subaerial erosion surfaces in marginal areas. Therefore, this one can be considered as depositional sequences of which the maximum flooding surfaces coincide with the peak in organic-rich sediment occurrence (Figure 38). The drowning surface that forms the boundary between the Derdere and Karababa formations would be the transgressive surface of the lower cycle. The drowning surface of the upper cycle is more difficult to recognize in the basinal sections, however in the marginal areas an interval of hardgrounds occurs in the source rock interval. Karstic deposition related to subaerial exposure in at least some marginal areas could represent sequence boundaries.

Depositional sequences

On the basis of their stratigraphic setting, facies changes and sequence boundaries, the Derdere/Karababa formations display two depositional sequences formed in response to eustatic sea-level changes (Figure 38).

Subsurface section (depositional sequence)

The two-third-order depositional sequences at the subsurface section are:

Sequence-1

This depositional sequence includes the middle and upper units of the Derdere Formation. Facies of this sequence can be grouped into transgressive and highstand systems tracts (Figure 38). The TST includes the middle part of the formation. The TST interval of this sequence consists of fine crystalline and medium-coarse crystalline dolomite microfacies. The bioclastic wackestone facies represents beds associated with the MFS1. The overlying facies of MFS1 are interpreted as HST. The HST constitutes the uppermost part of the upper unit of the formations. It shows an upward shallowing trend relative to the deepening upward trend observed in the underlying TST. The upper part of the HST is mainly represented by shallow subtidal lagoonal facies. This is because the rate of eustatic sea-level fall is greater than it was during the deposition of the underlying HST beds.

The occurrence of dolomites above the shallow subtidal carbonate platform beds has been interpreted to indicate a relative progressive shallowing of water depths due to a decrease in the rate of sea-level rise. This is similar to that described in the HST of the carbonate platform beds of the Karababa Formation. A transgressive surface (TS1) overlies these HST beds.

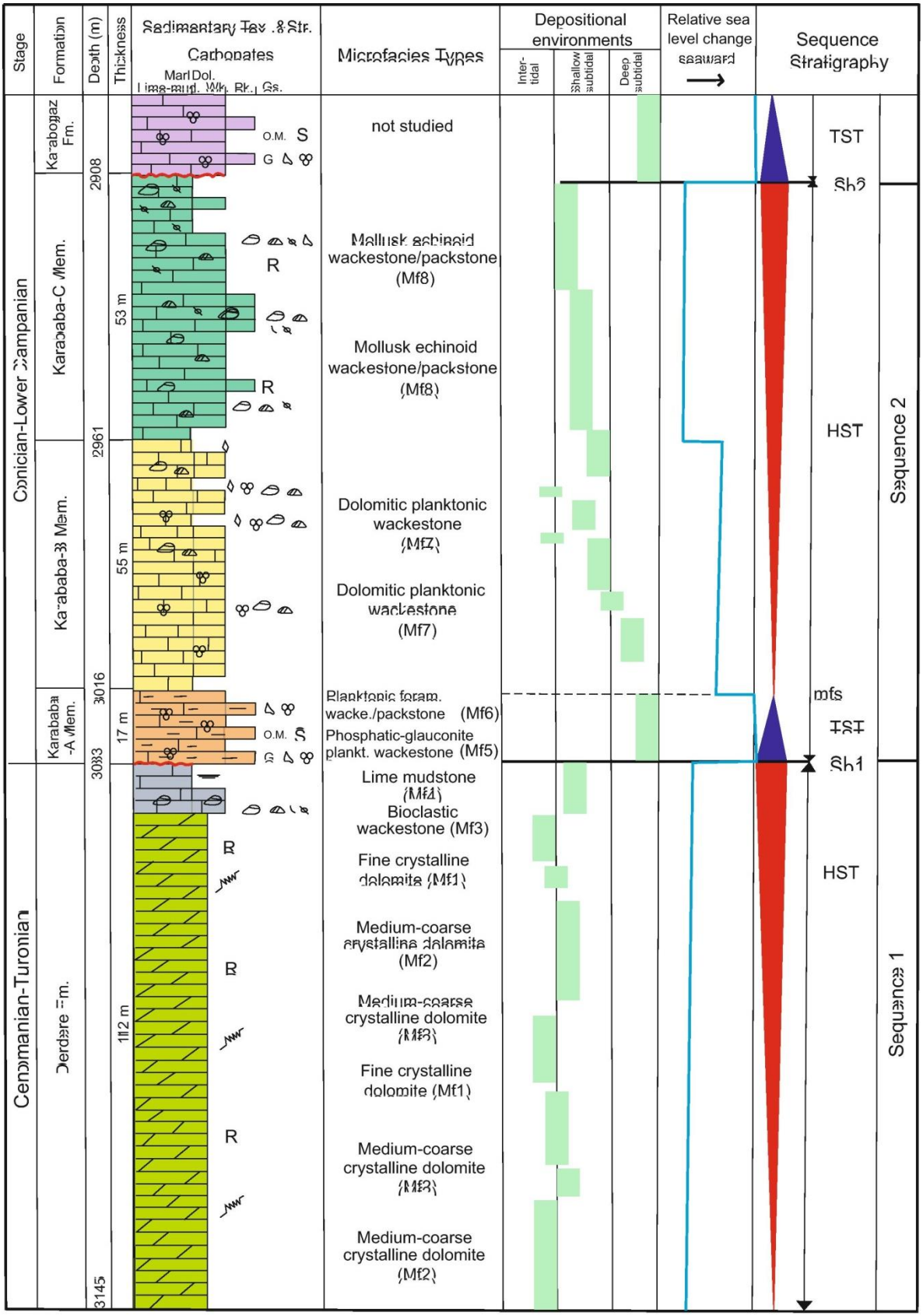
Stage
Formation
Depth (m)
Thickness
Sedimantary Tex. & Str.
Carbonates
Marl Dol.
Lime-mud. Wk. Pk. Gs.
Microfacies Types
Depositional environments
Inter-tidal
Shallow subtidal
Deep subtidal
Relative sea level change seaward
Sequence Stratigraphy
Coniacian-Lower Campanian
Karabogaz Fm.
Karababa-C Mem.
Karababa-B Mem.
Karababa -A Mem.
Cenomanian-Turonian
Derdere Fm.
2908
2961
3016
3033
3145
53 m
55 m
17 m
112 m
O.M.
S
G
R
not studied
Mollusk echinoid wackestone/packstone (Mf8)
Mollusk echinoid wackestone/packstone (Mf8)
Dolomitic planktonic wackestone (Mf7)
Dolomitic planktonic wackestone (Mf7)
Planktonic foram. wacke./packstone (Mf6)
Phosphatic-glauconite plankt. wackestone (Mf5)
Lime mudstone (Mf1)
Bioclastic wackestone (Mf3)
Fine crystalline dolomite (Mf1)
Medium-coarse crystalline dolomite (Mf2)
Medium-coarse crystalline dolomite (Mf3)
Fine crystalline dolomite (Mf1)
Medium-coarse crystalline dolomite (Mf3)
Medium-coarse crystalline dolomite (Mf2)
TST
HST
mfs
TST
HST
Sequence 2
Sequence 1

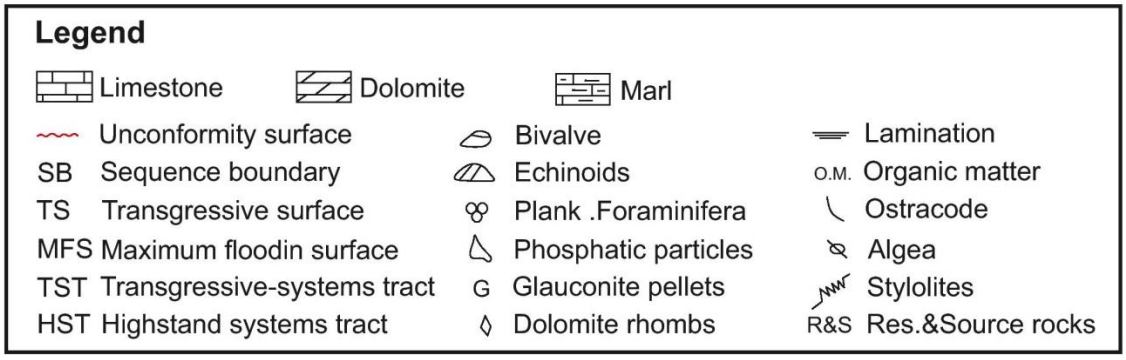

Figure 38: Representative stratigraphic section showing the microfacies, depositional environments, relative sea-level curve, depositional sequence and system tracts and sequence boundaries of the Derdere and Karababa formations in Cemberlitas oil field area, based on the detailed study of the well#13.

This surface is recognized where the quiet, deep subtidal marine facies of the lower Santonian Karababa Formation drowned the HST carbonate shallow shelf beds of the mid-Cenomanian–Turonian succession (Figure 38).

Sequence 2

This depositional sequence is basically the Karababa Formation. Its lower boundary is delineated by the Turonian- Coniacian sequence boundary SB1 and its upper boundary is TS2. The sequence starts with deposition of deep subtidal planktonic foraminiferous with shallow subtidal mollusks wackestone/packstone beds due to a gentle drop in relative sea-level during the late Santonian. Facies of this sequence can be grouped into transgressive and highstand systems tracts (Figure 38). The transgressive surface at the base of this transgressive systems tract (TST) coincides with sequence boundary 2 (SB2). The TST includes the lower part of the Karababa Formation. The TST interval of this sequence consists of sediments of deep subtidal limestone

and foraminiferal wackestone/packstone beds. The maximum flooding surface (MFS2) is identified at the top of the deep subtidal units. The MFS2 is recognized by a facies change from the underlying deepening upward trend observed in the foraminiferal wackestone facies to a shallowing upward trend seen in the overlying strata of the HST (Figure 38). This HST constitutes the uppermost part of the middle unit and the upper unit of the formation. The HST strata are overlain by thick aggradational shallow subtidal units. These shallowing upwards units represent highstand systems tract (HST) deposits that formed due to a normal regression associated with a sea-level highstand. A highstand normal regression occurs when the rate of sediment supply to a given shoreline exceeds the rate of accommodation space (Posamentier et al., 1992). This HST interval consists of shallow subtidal units of dolomitic planktonic wackestone and mollusk-echinoid wackestone/grainstone at the top. Such an occurrence of dolomites above intertidal-shallow subtidal carbonate platform beds has been interpreted to indicate a relative progressive shallowing of sea-level. The occurrence of early diagenetic dolomite concomitant with a short-term hiatus signals the accumulation of deep marine deposits of the next sequence. Sequence 2 is terminated with a short-term relative sea-level fall in the late Santonian which caused emersion and subaerial diagenetic processes (SB2).

4.4 Structural Geology

The geology of Cemberlitas, like the overall geology of the Adiyaman region, is characterized by nearly flat sedimentary rocks of the Mardin and Adiyaman Carbonate Groups (Figures 43 and 44). However, well log correlation and subsurface contouring around the Cemberlitas oil field reveal presence of normal faulting in the Derdere and Karababa formations. In the northeast part of the Cemberlitas area, there are two normal faults that may have been identified through subsurface geologic studies (Figures 39, 40 and 41). These faults trend in a northeast/southwest direction. The faults may have created or affected hydrocarbon traps in the near vicinity of the Cemberlitas oil field area. These normal faults were probably formed in late Cretaceous due to flexural bending associated with the closure of southern Neotethys Ocean (Perincek and Cemen, 1993, and Cemen, Personal Comm., 2013).

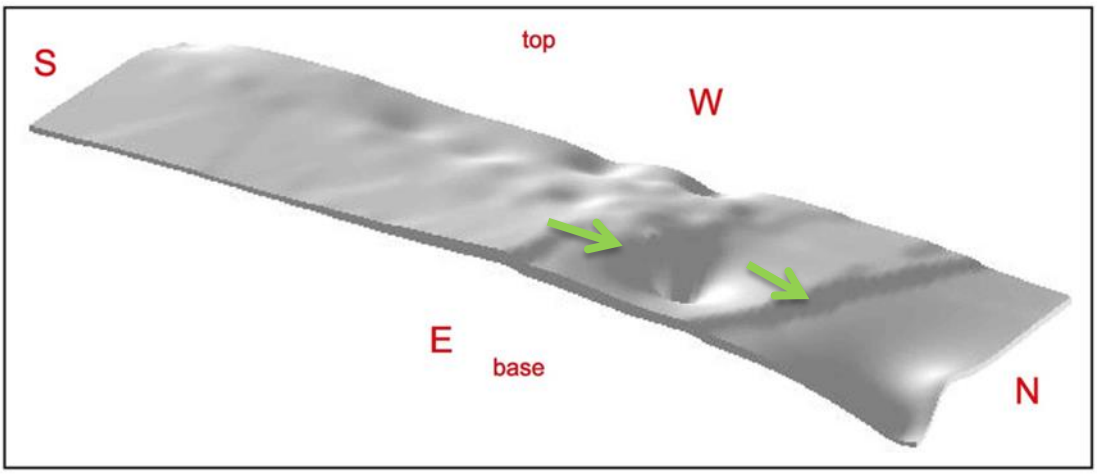

Figure 39: Extent of the Derdere Formation in the study area and the control of the northeast faults (green arrows) as manifested from well data.

Figure 40 is a two-dimensional shaded relief structural contour map of the top of the Derdere Formation that uses colors to represent changing elevations. A major normal fault is shown clearly in the northern part of the area figure 40.

Structural Contour Map on the Top of the Karababa Formation

The subsea elevations on top of the strata representing Coniacian-lower Campanian Karababa Formation in the Cemberlitas oil field range from 2100 to 2700 meter. A structural high is present in the central part of the Cemberlitas area. Erosion of Karababa Formation over the structural highs is evident along the cross sections.

Structural Contour Map on the Top of the Derdere Formation

The subsea elevations on the top of the strata representing late Cenomanian- Turonian Derdere Formation in the Cemberlitas oil field range from 2200 to 2800 meter. A structural high is present in the central part of the Cemberlitas area. Erosion of Derdere Formation over the structural highs is evident along the cross sections (Figures 41 and 44).

Isopach Map of the Karababa Formation

The Karababa Formation is present in subsurface throughout the Cemberlitas oil field are in Adiyaman. The maximum thickness of Karababa deposits penetrated in the thesis area is 130 meter in the Cemberlitas oil field in wells Cem-52, Cem-7. The thinnest well section is Cem-15 where the Karababa Formation is 55 meter (Figure 42).

There is minor thickening in the west and northeastern part of the area. This thickening is aligned in a southwest-northeast direction. This thickening may be due to a topographic low that was present on the pre-depositional Karababa surface.

Structural and Stratigraphic Correlation

During this investigation, structural and stratigraphic cross-sections and structural elevation diagrams were prepared to determine the structural and stratigraphic configuration of the late Cretaceous units in the subsurface of the Cemberlitas oil field area (Figures 43 through 46).

The existence of normal faulting in the Cemberlitas oil field was confirmed by the structural map of the Derdere and Karababa formations displayed in figures 40 and 41. Figures 45 and 46 show structural cross-sections and suggest the presence of a normal fault beneath well Cem-16, Cem-7, Cem-.44, Cem-13 and Cem-11. The structural cross- sections done in this part of the study helped in determining a possible trapping structure in the area of study.

Stratigraphic cross-section constructed during this study reveal the thickness, lithologic sequences, and stratigraphic correlations of the Mardin and Adiyaman Groups logged in the Cemberlitas oil field. The Karabogaz Formation was chosen as a datum because it is an identifiable stratigraphic unit that is easily recognized in the subsurface from geophysical well logs. In the section that already has shown in Figures 43 and 44. Note that the Karabogaz Formation is relatively thin in Cem-5 well. This suggests that this area may have already been a structural high when the Karabogaz was deposited.

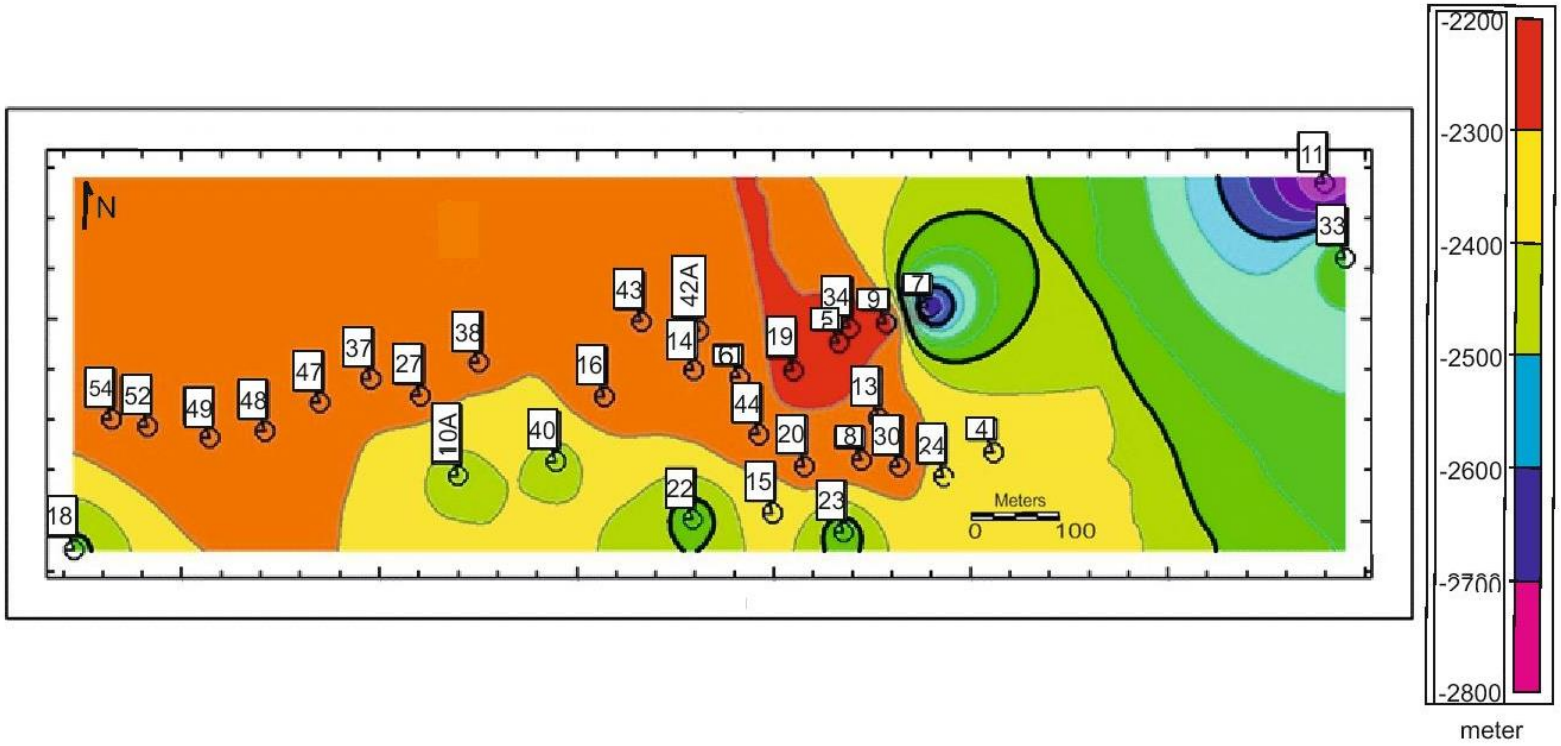

Figure 40: Structural contour map on the top of the Derdere Formation (scale: elevation-meter)

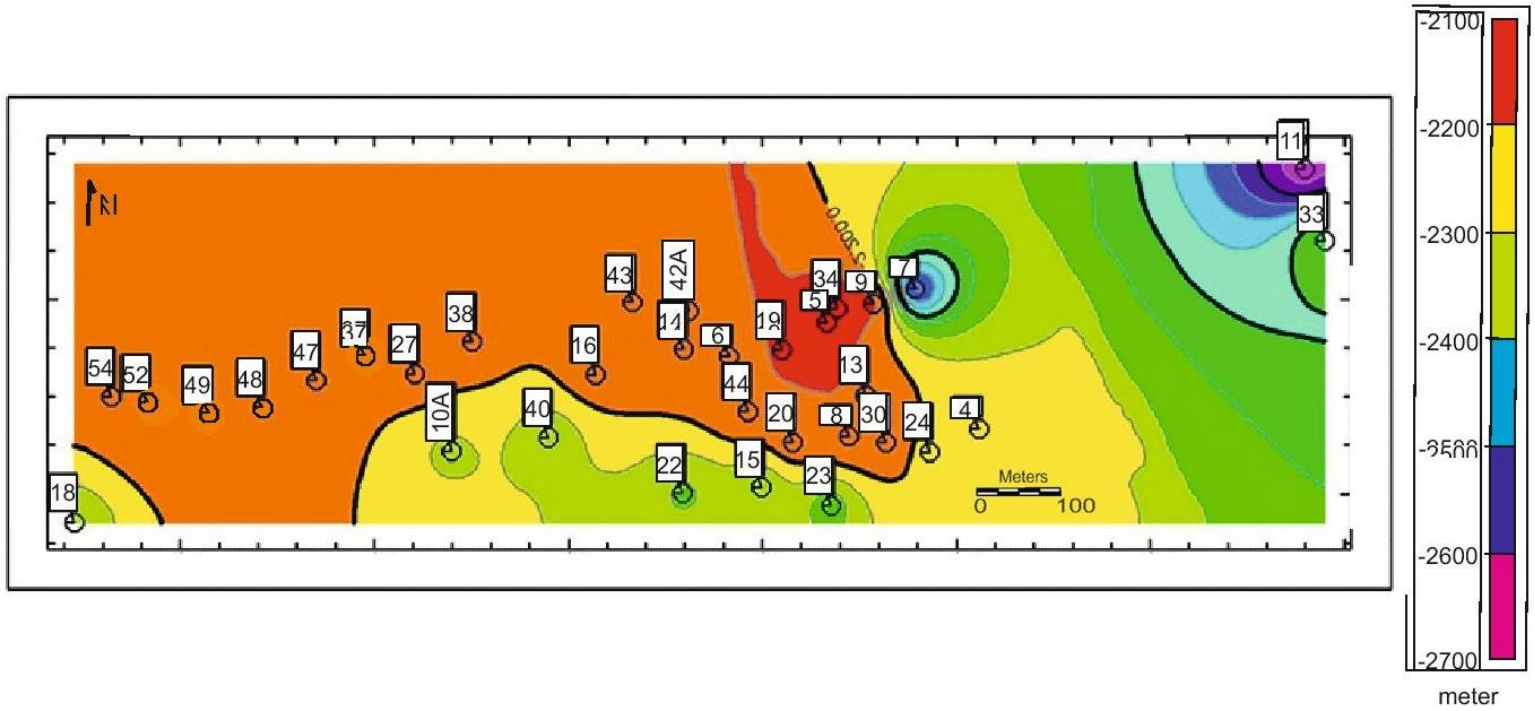

Figure 41: Structural contour map on the top of the Karababa Formation (scale: elevation-meter).

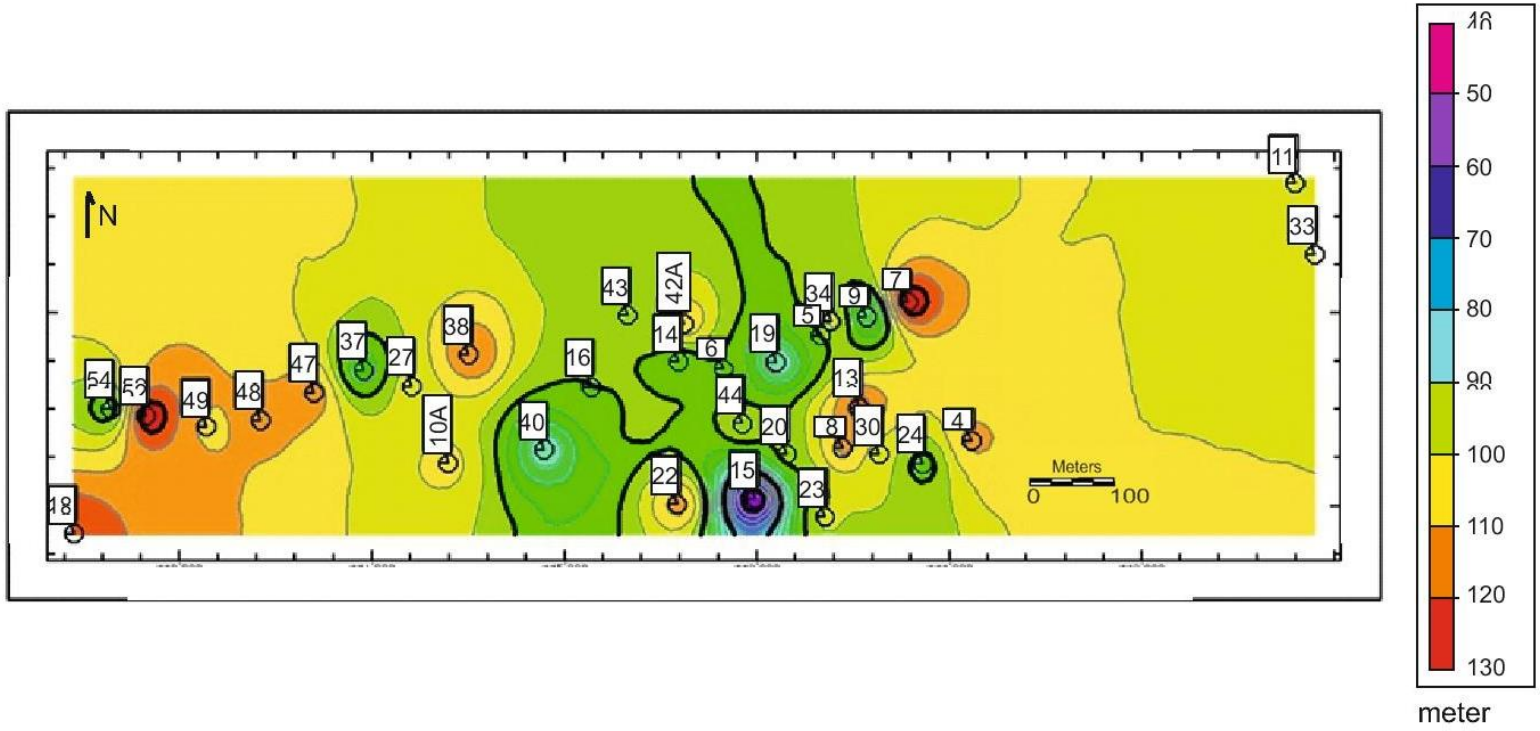

Figure 42: Isopach map of Karababa Formation at Cemberlitas oil field (scale: thickness-meter).

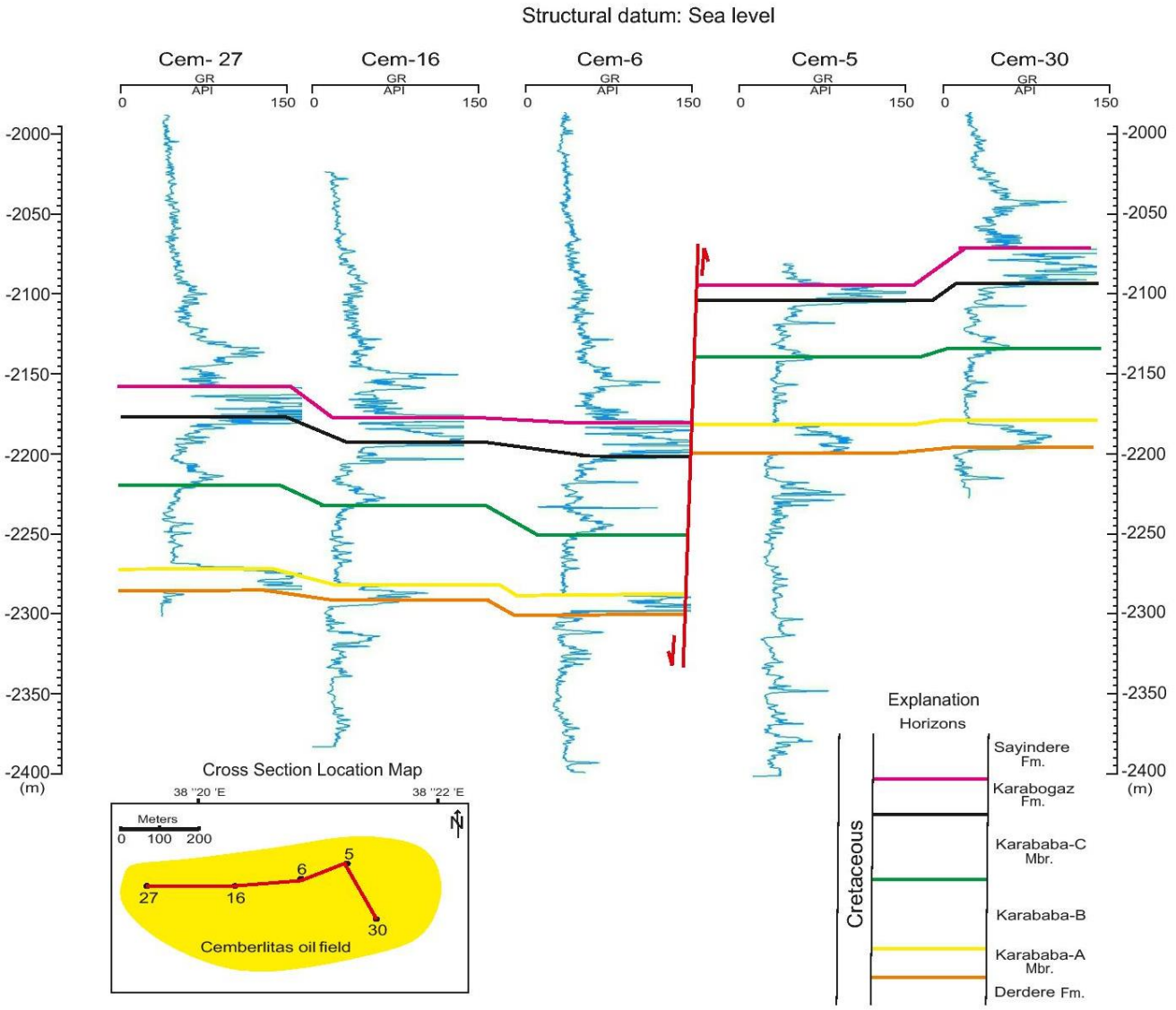

Figure 43: Structural cross section, Cemberlitas oil field, illustrating elevation changes in a west to east direction.

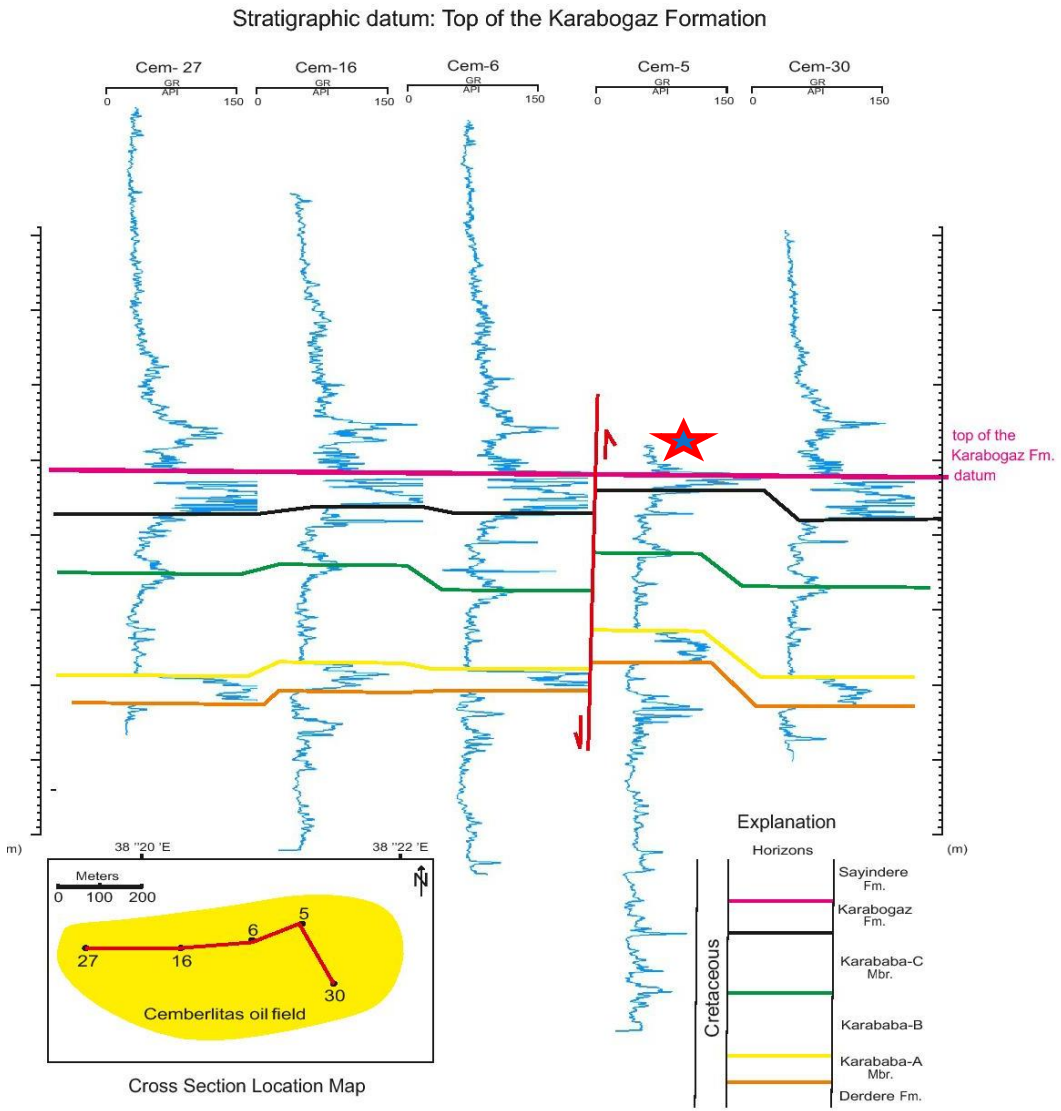

Figure 44: Stratigraphic cross section, Cemberlitas oil field, note total Karabogaz thickness at well permit # Cem5 where minimum.

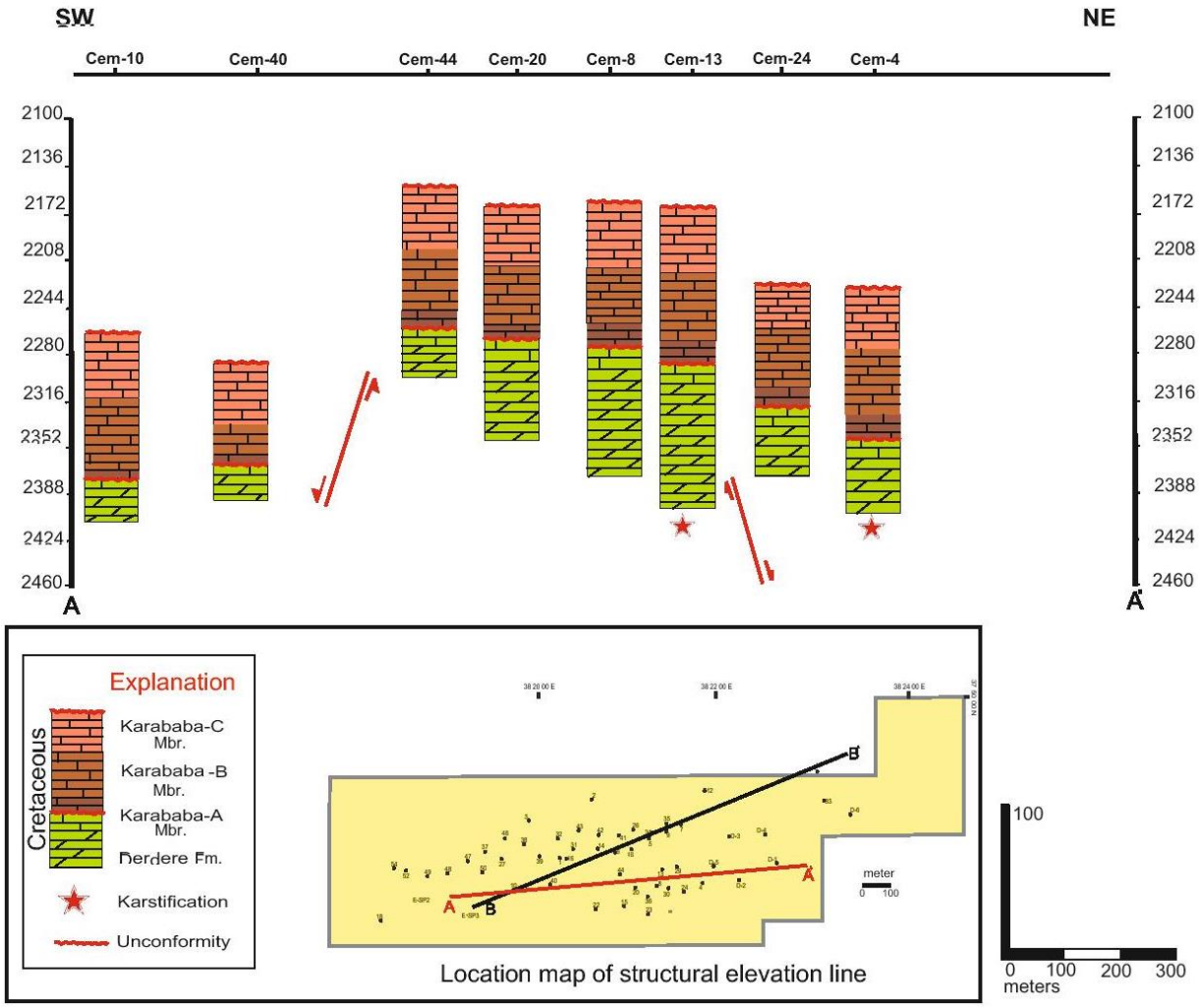

Figure 45: Diagram of the structural elevation of the Derdere and Karababa formations in the Cemberlitas oil field (EP2 line) (Structural datum-sea level).

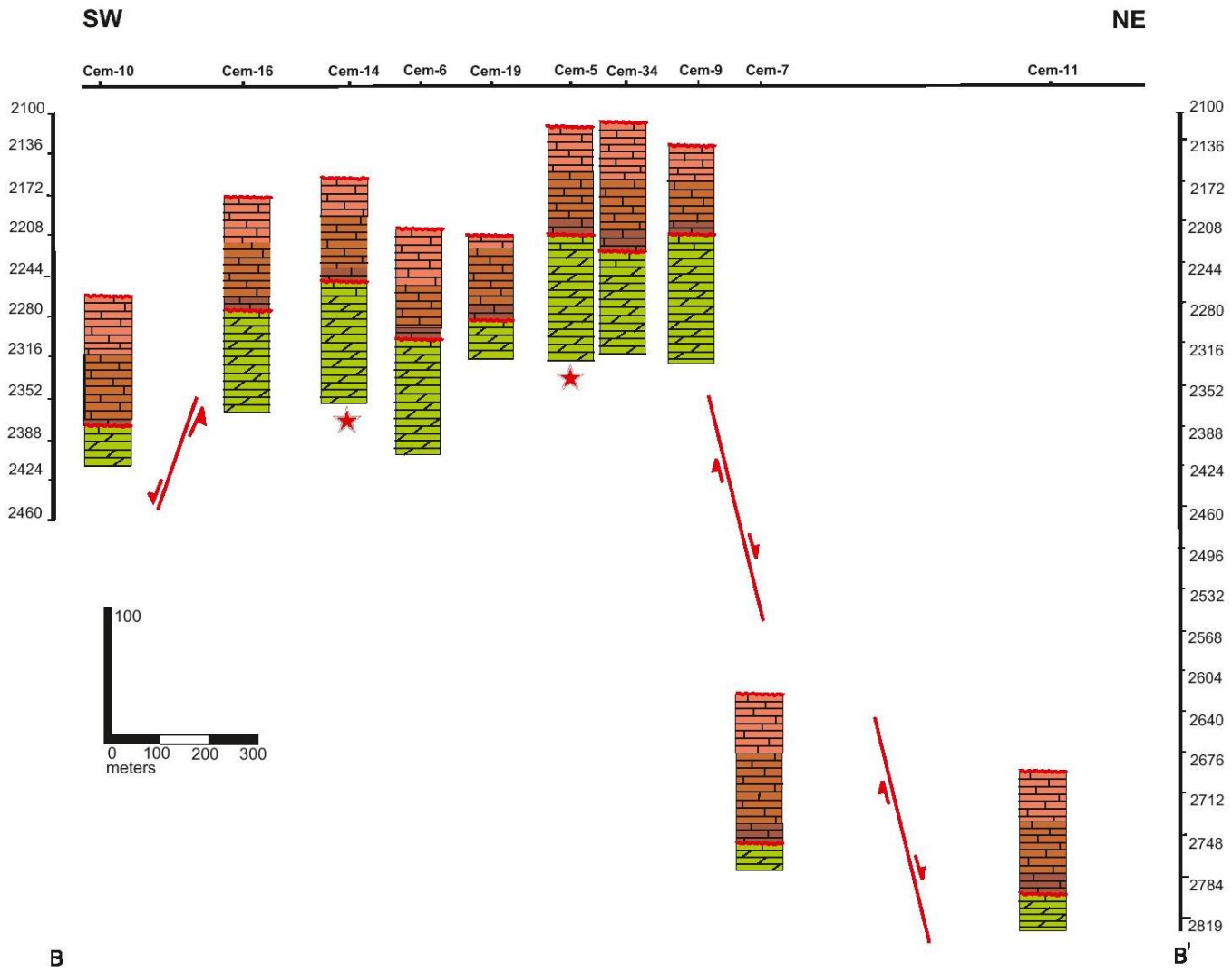

Figure 46: Diagram of the structural elevation of the Derdere and Karababa formations in the Cemberlitas oil field (EP3 line) (Structural datum-sea level).

Tectono- Karstification Model

Paleokarst breccia in the Cemberlitas oil field area appears to be mainly located in the upthrown side on extensional faults. The structural highs of these tilted blocks could have been temporarily emergent to cause karstification (Figure 47). Some of the analyzed karstic morphologies could correspond to large dissolution voids called flank margin caves (Wagner, 1985). These structures may have formed preferentially in the area of the discharging margin of a freshwater lens resulting from freshwater/sea water mixing or in relation to fracture systems (J.M. Molina et. al. 1999).

There are two lines of evidence for the interpretation above 1) presence of erosional surfaces that may have been created by normal faults and 2) a sea level rise that was preceded by a phase of emersion and karstification (Figures 47). In some places a prolonged phase of erosion in the pelagic realm, mainly current -related, is responsible for reducing sedimentation rate and causing erosion of the surface (Figure 47). The higher elevations of the normal faults were most likely affected by current activity strong enough to locally erode previous sediments, or to totally hinder sediment accumulation for longer time spans than in the lower parts of these fault blocks. Rapid block tilting on the fault blocks is envisaged as a major cause of the presence of non-deposition areas together with low-sedimentation areas. As a result, starved pelagic carbonate environments may have occurred during the deposition of the Karababa-A Member (Figure 47).

Many tectono-sedimentary models have been proposed to explain the effects of normal faulting and block rotation on carbonate depositional sequences (e.g. Bosence et al., 1998; Leeder and Gawthorpe 1987). Examples at the half-graben scale have been described in cases from the geological record (Bosence et al., 1998). These examples have largely confirmed the

tectono-sedimentary model of Leeder and Gawthorpe (1987) that footwall areas are often escarpment or accretionary platform margins with shelf margin buildups and footwall-derived redeposited facies, while hanging-wall dip-slopes develop margins or ramps evolving into rimmed shelf margins (Bosence et al., 1998).

The highest parts of the emerged blocks were preferentially karstified, with the degree of dissolution and karstification decreasing downward (Vera et al., 1988) (Figure 47). Whereas some blocks remained exposed until the late Cretaceous, others were exposed for only short periods of time and were relatively lightly karstified where prolonged exposure took place, extensive cavern development occurred. As a general rule, such palaeokarst systems were relatively localized, capping individual tilted blocks. Therefore there are considerable differences in karst development even in neighbuoring areas (Figure 47). The pelagic filling of the karstic cavities allows us to date the karstification process and to distinguish the different phases of karstification and filling (Figure 47). The analysis and precise dating of the sediments filling the cavities have allowed us to reconstruct the complex sedimentary history of every sector in the basin.

Tectonic and eustatic sea level fluctuations were the two main factors causing fault block emersion. Relative sea level changes, associated locally with fault block emersion, were followed by relative sea level highstands and the renewal of sedimentation. Detailed analysis of the paleokarst correlative paraconformity surfaces has provided great precision in the dating of the events controlling the genesis of all these features. There are other well described examples of paleokarst in the world. One of these examples is the long term karstification in the Turonian limestones of Israel (Buchbinder et al., 1983).

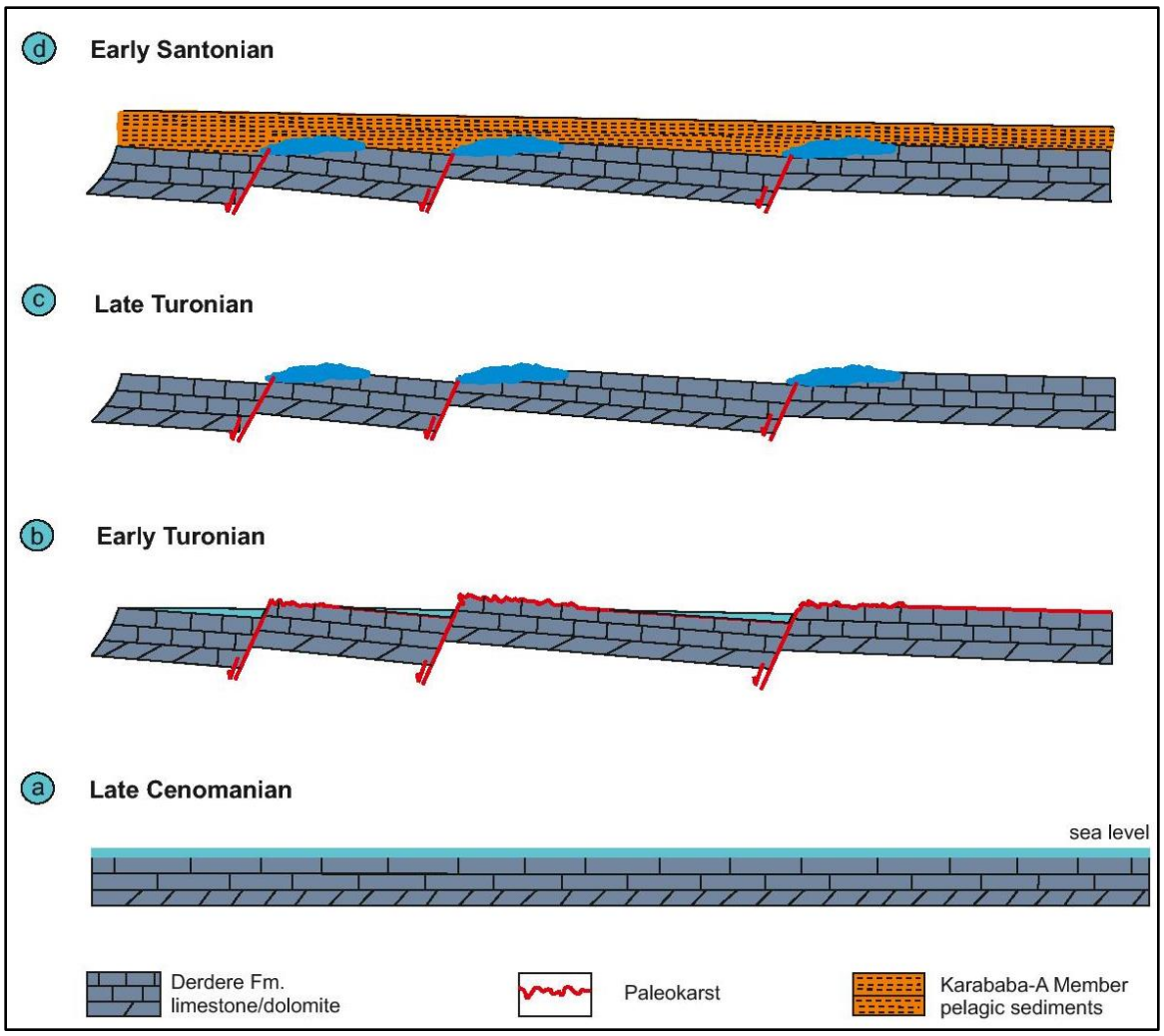

Figure 47: Evolution model of karstification on the Cemberlitas oil field.

5. DISCUSSION

5.1 Eustatic controls on deposition

Correlation of wells in the Cemberlitas area show that the Karababa Formation consists of a transgressive-regressive cycle (Figure 48). The transgressive parts of cycle are dominated by organic-rich carbonates while the regressive part consists of prograding units of bioclastic wackestone/packstones. The correlatability of this cycle over a wide area suggests that it is driven by regional relative changes of sea level rather than local effects (i.e. differential subsidence/uplift, sediment supply or climate).

The sea level continued to rise during the deposition of the Karababa Formation, causing a further relative deepening of the basin. This, together with the much shallower sill caused a much reduced circulation of the bottom waters. The resulting poorly oxygenated to anoxic bottom-water conditions allowed preservation of organic-rich material over a large part of the basin. At the same time, hardgrounds formed in the marginal areas (Cemberlitas area). A peak in source rock richness (peak in gamma-ray log, Figures 42 and 43) in the basal part of the Karababa Formation coincides with a period during which the source rock has a basin-wide distribution. This surface is overlain by a progradational, bioclastic, wacke/packstones sequence which progressively filled the basin. A decreasing rate of relative sea-level rise, or maybe a slight relative sea-level fall, enabled carbonate sedimentation at the basin margins to "catch-up" and supply enough material to built out. With this, water depths in the basin swallowed and bottom water circulation increased. At this stage anoxic to poorly oxygenated bottom waters

occurred only in the central, deepest, part of the basin. Moreover, the organic matter content of the organic-rich sediments shows a corresponding decrease.

Similar changes in relative sea level were also interpreted from outcrops of the platform facies of the Karababa Formation in the Hazro and Derik areas where a cycle of high and low energy can be recognized (Cater and Gillcrist, 1994). The occurrence of similar trends in relative sea-level changes is over wide areas and the absence of evidence for tectonic activity or climatic changes might indicate control by eustatic sea-level changes. The two eustatic sea-level cycles in the Karababa and Derdere formations are only minor cycles on the global sea-level curve and probably involve only a few meters to tens of meters of relative sea-level change (Figure 48).

A correlation of the SBs recognized in Cemberlitas with those from Haq et al. (1987), Hardenbol et al. (1998), Mancini and Puckett (2005), and Farouk and Faris (2012) is presented in Figure 48. The number of SBs correlates well with those from adjacent areas, especially in the Turonian and Santonian. However, different stratigraphic positions of the correlated sequences are most probably caused by limited biostratigraphic resolution and depend on the calibration of the biostratigraphic schemes used in the different studies. For practical reasons, identically named sequence boundaries are supplemented in the following discussions by listing their authors.

Correlation with Haq et al. (1987), Hardenbol et al. (1998);

The correlation with the SBs of Cemberlitas (Figure 48) shows Tu/Cem 1 boundary. Tu/Cem 1 apparently correlates with /Haq et al. (1987) and Hardenbol et al (1998) and represent a major sea-level fall. This may suggest that Tu/Cem 1 is equivalent to/Haq et al. (1987) and that the major sea level fall in late Turonian.

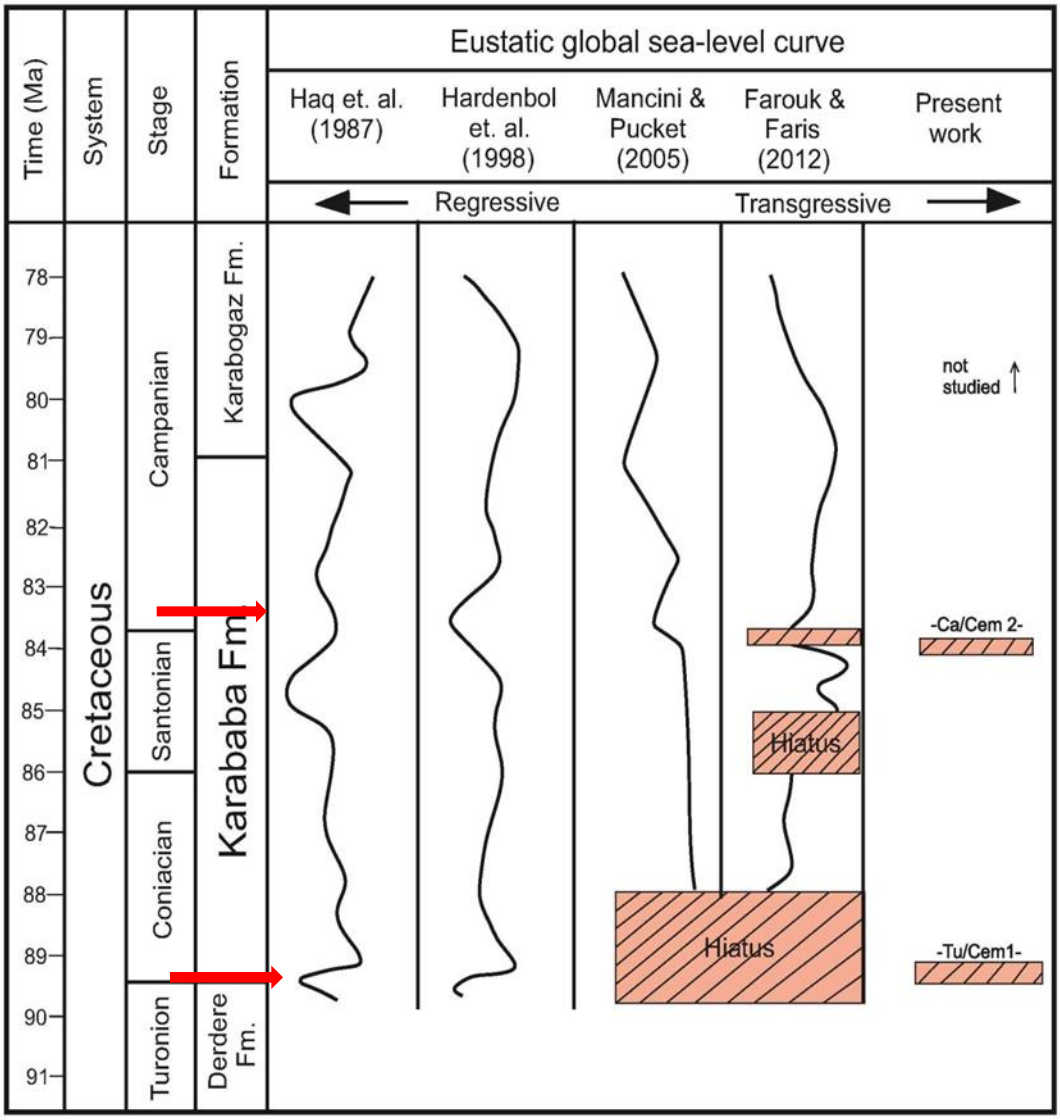

Figure 48: Relative sea-level curve during the Derdere-Karababa depositions in the Cemberlitas oil field area and its correlation with global sea-level curves.

Correlation with Mancini and Puckett (2005), Farouk and Faris (2012);

These authors reported some of the SBs described here. The Turonian/Coniacian sequence boundary (Tu/Co1) that unconformably separates the Derdere and Karababa formations which is most likely primarily denotes the effect of the major fall in eustatic sea level. This boundary was recognized as the end of the Turonian by (Haq et al., 1987; Hardenbol et al., 1998;

Mancini and Puckett 2005; Farouk and Faris 2012). However, the major hiatus associated with the TuCo1 boundary in the study area is more likely the result of period of subaerial exposure with karstification (Figure 48). The timing of event is shown in Figure 48. The timing of this event should be regarded as tentative because of the relatively poor biostratigraphic control on the age of the subsurface core sections. A hiatus across the Turonian/ Coniacian (T/C) boundary has been reported by (Celikdemir 1991). Although its precise biostratigraphic position cannot be confirmed in this study (Figure 48). The late Turonian shallowing event is recorded in the study area. In Cemberlitas, this gap is probably related to exposure on isolated highs which is probably related to local, tectonically induced depressions and structural highs.

The Karabogaz Formation rests disconformably on the Karababa Formation with a hiatus at the Santonian/Campanian stage boundary that denotes the Ca/Cem1 sequence boundary, easily recognized by its sharp nature. This regional sea-level rise can also be correlated to the global cycle chart of Hardenbol et al., 1998; Mancini and Puckett 2005; Farouk and Faris 2012.

6. SUMMARY AND CONCLUSIONS

Microfacies analysis during this study has led to the recognition of 8 microfacies. They are; (1) Fine crystalline dolomite, (2) Medium-coarse crystalline dolomite, (3) Bioclastic wackestone /packstone, (4) Lime mudstone, (5) Phosphatic-glauconitic planktonic wackestone, 6) Planktonic foraminiferous wackestone/packstone, (7) Dolomitic planktonic wackestone, and (8) Mollusk-echinoid wackestone/packstone. These microfacies suggest that the. Derdere Formation is a shallow marine lagoonal to shelf depositional environment and Karababa Formation indicates deposition in deep to shallow marine intra shelf depositional environment.

Variation in relative sea level led to the recognition of two-third order sequences in the subsurface section with sequence boundary SB1 and SB2 in the late Cretaceous Derdere and Karababa formations of the Mardin Group. The facies patterns clearly indicate relative sea level variations. The transgressive deposits display a predominance of deep subtidal facies, while highstand deposits show shallow subtidal facies. These boundaries are: late Turonian (SB1) and lower Campanian (SB2) in age. upper Karababa sequence shows transgressive (TST) and highstand (HST) and lower Derdere sequence shows highstand (HST) systems tracts and packages of facies.

Comparison of the sequence stratigraphic framework with the eustatic global sea level curves scheme reveals some different timing for the sequence boundaries. It is suggested here that the depositional history of the Derdere and Karababa formations was controlled by mainly global eustatic sea-level changes during the late Cretaceous.

The subaerial exposures are associated mainly with the regional Turonian unconformity. Following the deposition of the upper Derdere Formation a major sea level fall in the mid-Turonian exposed Cemberlitas area to the surface which resulted in regional Turonian unconformity. Profound changes due to karstification, took place at that time. These profound changes include development of solution widened fissures, collapse breccia, vugs and cave floor deposits. Changes due to karstification are limited to the upper few meters at the top of the formation.

Although structural control mechanism has not been recognized in deposition in Karababa and Derdere formations, late Cretaceous normal faulting due to flexural bending have effected the karstification and formation thicknesses.

REFERENCES

Aigner, T. and van Vliet, A., (1989), Hierarchy of depositional cycles in epeiric carbonate basin-fills: an example from Oman. 28th Int. Geol. Congr., Washington, D.C., Abstr., pp. 1-23-1-24.

Ala, M.A. and B.J. Moss (1979). Comparative Petroleum Geology of Southeast Turkey and Northeast Syria. Journal of Petroleum Geology, 1, 3-27.

Amthor, I.E. and Friedman, G.M., (1991). Dolomite-rock textures and secondary porosity development in Ellenburger Group carbonates (Lower Ordovician), west Texas and southern New Mexico: Sedimentology, v. 38, p. 343-362.

Amthor, I.E. and Friedman, G.M., (1992). Early to Late diagenetic dolomitization of platform carbonates: lower Ordovician Ellenburger group, Permian basin, West Texas J. Sediment Petro.62. 131-144.

Aydemir, A., Bahtiyar, I., Korpe, L. Soyhan, O., (2006). Petroleum generation potential of the Karabogaz Formation in Kahta Depression, Adıyaman, Southeastern Anatolia, TAPG Bulletin, 18-1, 1-15.

Ayres, M.G., Bilal, M., Jones, R.W., Slentz, L.W., Tartir, M. and Wilson, A.O., (1982), Hydrocarbon habitat in main producing areas, Saudi Arabia. Am. Assoc. Pet. Geol. Bull., 66(1): 1-9.

Bauer, J., Marzouk, A.M., Steuber, T., Kuss, J., (2001). Lithostratigraphy and biostratigraphy of the Cenomanian-Santonian strata of Sinai, Egypt. Cretaceous Research 22, 497-526.

Bottjer, D.J. and W.A. Bryant. (1980). Paleoenvironmental analysis of disconformity and condensed bed at contact of Austin and Taylor Groups (Upper Cretaceous), east, central and northeastern Texas. American Assoc. Petroleum Geol. Bull., v. 64, p. 679.

Bosence, D., Cross, N., Hardy, S., (1998). Architecture and depositional sequences of Tertiary fault-block carbonate platforms; an analysis from outcrop (Miocene, Gulf of Suez) and computer modeling. Mar. Pet. Geol. 15, 203–221.

Buchbinder, B., Magaritz, M., Buchbinder, L.G., (1983). Turonian to Neogene palaeokarst in Israel. Palaeogeogr. Palaeoclimatol. Palaeoecol. 43, 329–350.

Bachmann, M., and Kuss, J., (1998). The middle Cretaceous carbonate ramp of the northern Sinai: sequence stratigraphy and facies distribution. In: Wright, V.P., Burchette, T.P. (Eds.), Carbonate Ramps. Journal of the Geological Society, London, Special Publication 149, pp. 253-280.

Cater J.M.L., and Gillcrist, J.R, (1994). Karstic Reservoirs of the Mid-Cretaceous Mardin Group, SE Turkey: Tectonic and Eustatic Controls on their Genesis, Distribution and Preservation. Journal of Petroleum Geology, vol. 17(3), July 1994, pp. 253-278.

Catuneanu, O., (2002). Principles of Sequence Stratigraphy. Elsevier, New York, 386 p.

Celikdemir, E. M., Dulger, S., Gorur, N., Wagner, C., and Uygur, K. (1991). Stratigraphy, sedimentology, and hydrocarbon potential of Mardin Group, southeast Turkey. Special Publication of European Association of Petroleum Geologists, 1,439-454.

Clari, P.A., Dela Pierre, F., Martire, L., (1995). Discontinuities in carbonate successions: identification, interpretation and classification of some Italian examples. Sediment Geol. 100, 97– 121.

Cordey, W. G., and Demirmen, F. (1971). The Mardin Formation in southeast Turkey. Proceeding of I. Petroleum Congress of Turkey, 51-71.

Çoruh, T., Yakar, H. and Ediger, V.Ş., (1997). Güneydoğu Anadolu Bölgesi otokton istifin biostratigrafi atlası, T.P.A.O. Araştırma Merkezi Grubu Başkanlığı, Eğitim Yayınları No: 30, 510s.

Demirel, I. H., Yurtsever, T. S., and Guneri S., (2001). Petroleum systems of the Adıyaman Region, Southeastern Anatolia, Turkey, Marine and Petroleum Geology, 18, 391-410.

Dinçer, A., (1991), Güneydoğu Anadolu otokton stratigrafi birimleri, Güneydoğu Anadolu Stratigrafi Grubu, TPAO Report No: 2828.

Dockal, J. A., (1988). Thermodynamic and Kinetic Description of Dolomitization of Calcite and Calcitization of Dolomite 'Dedolomitization'. Carbonate and Evaporites, Vol. 3, No. 2, p. 125-141.

Dunham, R.J., (1962). Classification of carbonate rocks according to depositional texture. American Association of Petroleum Geologist, Memoir 1, 108–121.

Duran, O., and Alaygut, D. (1992). Porosity and permeability controlling mechanisms in the reservoir rocks around Adiyaman. Proc. of 9th Petroleum Congress of Turkey (pp. 390-406).

Einsele, G. (2000). Sedimentary basins: Evolution, Facies, and Sediment budget (second Edition). Springers, Berlin.

Flügel, E., (1982). Microfacies Analysis of Limestone. Springer-Verlag, Berlin, 589 pp.

Flügel, E., (2004). Microfacies Analysis of Limestone: Analysis, Interpretation and Application. Springer-Verlag, Berlin. 976 p.

Friedman, G.M., Sanders, J.E., and Kopaska-Merkel, D.C.,(1992). Principles of sedimentary deposits: Stratigraphy and Sedimentology. Macmillan Publishing Co., New York, 717 p.

Gorur, N., Celikdemir, E., and Dulger, S. (1987). Sedimentology, facies, sedimentation environment\ and paleogeography of the Mardin Group carbonates in XIth and XIIth Petroleum Districts of Turkey. TPAO Exploration Group Report No. 2321 unpublished.

Gorur, N., Celikdemir, E., & Dulger, S. (1991). Carbonate platforms developed on passive continental margins: Cretaceous Mardin Carbonates in southeast Anatolia as an example bull. Tech. Univ., Istanbul, 33,301-324.

Guven, A., Dincer, A., Tuna, M. E., Coruh, T., (1991). Güneydoğu Anadolu Kampaniyen – Paleosen otokton istifin stratigrafisi, T.P.A.O. Arama. Grubu Rap. No: 2828, 133p.

Hancock, J. M., and Kauffman, E. G. (1979). The great transgression of the Late Cretaceous. Journal of the Geological Society of London, 136, 175-186.

Haq, B.U., Hardenbol, J., and Vail, P.R., (1987). Chronology of fluctuating sea levels since the Triassic (250 million years ago to present). Science, 235, 1156–1167.

Haq, B.U., J. Hardenbol and P.R. Vail (1988). Mesozoic and Cenozoic chronostratigraphy and cycles of sea-level change. Society of Economic Paleontologists and Mineralogists, v. 42, p. 71-108.

Haq, B.U., (1991). Sequence stratigraphy, sea-level change, and significance for the deep sea, in D.I.M MacDonald, ed., Sedimentation, Tectonic and Eustacy: Sea-Level Changes at Active Margins: International Association of Sedimentologists Special Publication, no. 12, p. 3-39.

Harries, J.P. and Kauffman E. G., (1990). Pattern of survival and recovery following the Cenomanian-Turonian (Late Cretaceous) mass extinction in the Western Interior Basin, USA, in extinction events in Earth history, Springer-Verlag Berlin, pp. 277-298.

Hillgartner, H., (1998). Discontinuity surfaces on a shallow-marine carbonate platform (Berriasian, Valanginian, France and Switzerland). J. Sediment. Res. 68, 1093 – 1108.

Horstnik, F. (1971). The Late Cretaceous and Tertiary geological evolution of eastern Turkey. Proceedings of the 1st Petroleum Congress (pp.25-41).

Immenhauser, A., van der Kooij, B., van Vliet, A., Schlager, W., Scott, R.W., (2001). An ocean facing Aptian–Albian carbonate margin, Oman. Sedimentology 48, 1187–1207.

Loutit, T.S., Hardenbol, J., Vail, PR. and Baum, G.R., (1988). Condensed sections: the key to age determination and correlation of continental margin sequences. In Wilgus, C.K., Hastings, B.S., et al. (Eds.), Sea-Level Changes: An Integrated Approach. Spec. Publ.—Soc. Econ. Paleontol. Mineral., 42:183-213.

Lee, Y. I. and Friedman, G. M. (1987). Deep-Burial Dolomitization in the Lower Ordovicia Ellenburger Group Carbonates in West Texas and Southeastern New Mexico, Jour. Sedim. Petrol., 57, 544-557.

Leeder, M.R., Gawthorpe, R.L., (1987). Sedimentary models for extensional tilt-block=half-graben basins. In: Coward, M.P., Dewey, J.F, Hancock, P.L. (Eds.), Continental Extensional Tectonics. Geol. Soc. London Spec. Publ. 28, 139–152.

Logvinenko, N.V., (1982). Origin of glauconite in the recent bottom sediments of the oceans: Sedimentary Geology, v. 31, p. 43-48.

Luning S, Marzouk AM, Morsi AM, Kuss J (1998) Sequence stratigraphy of the Upper Cretaceous of central-east Sinai, Egypt. Cretac Res 19:153–196. doi:10.1006/cres.1997.0104.

Machel, H.G. and Anderson, J.H., (1989). Pervasive subsurface dolomitization of the Nisku Formation in central Alberta: Journal of Sedimentary Petrology, v. 59, p. 891- 911.

Perinçek, D., (1980). Sedimentation on the Arabian Shelf under the control of Tectonic Activity in Taurid Belt, Proceedings of the 1st Petroleum Congress, Turkey, 77-93.

Perincek, D., Günay, Y. & Kozlu, H., (1987). New observations about the strikeslip faults in East and Southeast Anatolia, Proceedings of The Seventh Turkish Petroleum Congress (Eds. Organization Committee of Turkish Association of Petroleum Geologists), 89–103.

Perincek, D., Duran, O., Bozdogan, N. and Coruh, T., (1991). Stratigraphy and paleogeographical evolution of the autochthonous sedimentary rocks in SE Turkey. Proceedings of Ozan Sungurlu Symposium 274–305.

Perincek, D., and Cemen, I., (1993).Late Cretaceous- Paleogene structural evolution of the structural highs of southeastern Anatolia; Proceedings of the Ozan Sungurlu International Symposium, p. 386 - 403.

Posamentier et al., H. W. Posamentier, G. P. Allen, D. P. James and M. Tesson, (1992).Forced regressions in a sequence stratigraphic framework: concepts, examples, and exploration significance, American Association of Petroleum Geologists Bulletin 76 (1992), pp. 1687–1709.

Rigo de Righi, M. R., & Cortesini, A. (1964). Gravity tectonics in foothills structure belt of Southeast Turkey. American Assoc. Petr. Geol. Bull., 48, 1915-1937.

Sarı, A. and Bahtiyar, I., (1999). Geochemical evaluation of the Besikli Oil Field, Kahta, Adıyaman, Turkey, Marine and Petroleum Geology 16, 151-164.

Sarg, J.F., (1988). Carbonate sequence stratigraphy. Sea-Level Changes: an Integrated Approach, Wilgus, C.K, Hastings, B.S, Kendall, C.G.St.C., Posamentier, H.W., Ross, C.A., Van Wagoner, J.C. (Eds.). Soc. Econ. Paleontol. Mineral. Spec. Publ. 42, 155±181

Schlager, W., (2005). Carbonate Sedimentology and Sequence Stratigraphy. SEPM (Society for Sedimentary Geology), Tulsa, Oklahoma, USA, 208 p.

Shaw, A. B.,(1964). Time in stratigraphy: New York, McGraw Hill, 352 p.

Sengor , A. M. C. & Yilmaz, Y. (1981). Tethyan evolution of Turkey: a plate tectonic approach. Tectonophysics 75, 181–241.

Slowakiewicz1, M., and Mikolajewski, Z., (2009). Sequence Stratigraphy of the Upper Permian Zechstein Main Dolomite Carbonates in Western Poland: A New Approach. Journal of Petroleum Geology, Vol. 32(3), July 2009, pp 215-234.

Sibley, D.F. and Gregg, J.M., (1987). Classification dolomite rock texture: Journal of Sedimentary Petrology, v. 57, p. 967-975.

Sibley, D.F., Gregg, J.M., Brown, R.G., and Laudon, P.R., (1993). Dolomite crystal size distribution, in Rezak, R., and Lavoie, D.L. (eds.), Carbonate Microfabrics: Springer-Verlag, New York, p. 195-204.

Sungurlu, O., (1974), VI. Bölge kuzeyinin jeolojisi ve petrol imkanları, Okay and Deltoz (Eds.), Türkiye Ikinci Petrol Kongresi, Tebliğler, 85-107.

Tardu, T., (1991). A sequence stratigraphic approach to the Mardin Group. Ozan Sungurlu Symposium Proceedings; Tectonics and Hydrocarbon potential of Anatolia and Surrounding Regions. November. Ankara Turkey.

Temple, P. G., and Perry, L. J., (1962). Geology and oil occurrence, South East Turkey. AAPG, 46,1596-1612.

Tuna, D. (1973). VI. Bölge litostratigrafi birimleri adlamasının açıklayıcı raporu: TPAO. Report no:813, 131 pages.

Vail, P.R., R.M. Mitchum, Jr., R.G. Todd, J.M. Widmier, S. Thompson, III, J.B. Sangree, J.N. Bubb, and W.G. Hatlelid, (1977). Seismic stratigraphy and global changes in sea level, in C.E. Payton, ed., and Seismic stratigraphy—applications to hydrocarbon exploration: American Association of Petroleum Geologists Memoir 26, p. 49-205.

Vail, P.R., Audemard, F., Bowman, S.A., Eisner, P.N., and Perez-Cruz, C., (1991). The stratigraphic signatures of tectonics, eustacy and sedimentology - an overview, in G. Einsele, W. Ricken, and A. Seilacher, eds., Cycles and Events in Stratigraphy. Springer-Verlag, Berlin, p. 617-659.

Vahrenkamp, V. C., and Swart, P. K., and Rutz, J. (1991). Episodic dolomitization of Late Cenozoic carbonates in the Bahamas: evidence from strontium isotopes, J. Sedim. Petrol. 61, 1002-1014.

Van Buchem, F.S.P., P. Razin, P.W. Homewood, J.M. Philip, G.P. Platel, J. Roger, R. Eschaed, G.M.J. Desaubliaux, T. Boisseau, J.-P. Leduc, R. Labourdette and S. Cantaloube (1996). High Resolution Sequence Stratigraphy of the Natih Formation (CenomanianTuronian) in Northern Oman: Distribution of Source Rocks and Reservoir Facies. GeoArabia Vol.1, No.1: p. 65-91.

Van Buchem et al. (2010). Barremian - Lower Albian sequence-stratigraphy of southwest Iran (Gadvan, Dariyan and Kazhdumi formations) and its comparison with Oman, Qatar and the United Arab Emirates. GeoArabia Special Publication 4, v. 2, pp. 503-548 (46 pages)

Van Wagoner, J.C., Posamentier, H.W., Mitchum, R.M., Vail, P.R., Sarg, J.F., Loutit, T.S., Hardenbol, J., (1988). An overview of the fundamentals of sequence stratigraphy and key definitions. In: Wilgus, C.K., Hastings, B.S., Kendall, C., Posamentier, H.W., Ross, C.A., Van Wagoner, J.C. (Eds.), Sea-level Changes e an Integrated Approach. SEPM (Society for sedimentary Geology) Special Publication, vol 42, pp. 39e45.

Vera, J.A., Ruiz-Ortiz, P.A., Garcı´a-Hena´ndez, M., Molina, J.M., (1988). Paleokarst and related sediments in the Jurassic of the Subbetic Zone, Southern Spain. In: James N.P., Choquette, P.W. (Eds.), Paleokarst. Springer, New York, pp. 364–384.

Wagner, C., and Pehlivanli, M. (1985). Karst geological interpretation of the Mardin carbonates in the Cemberlitas field. A plot. TPAO report 2051.

Wagner, C., Soylu, C., and Pehlivanli, M. (1986).Oil habitat of the Adiyaman area, southeast Turkey. A joint geological geochemical study. TPAO Report No. 2139 (unpublished).

Wagner, C., and Pehlivanli, M. (1987). Geological control in the distribution of source rocks and reservoirs in upper Cretaceous Carbonates of Southeast Turkey. TPAO.

Wilson, J. L., (1975). Carbonate facies in geologic history, Springer- Verlag, New York, Heidelberg, Berlin, 471p.

Yılmaz, Y., (1993). New evidence and model on the evolution of the southeast Anatolian orogen. Geological Society of America Bulletin 1993; 105, no. 2; 251-271.

Yildizel, Z., E. (2008). Depositional Stacking patterns and cycles of Garzan Formation in the Garzan-Gemlik oil field an approach to cycle to log correlation. PhD Thesis.

Zenger,D.H.,(1983),Burial dolomite in the Lost Burro Formation (Devonian), east-central California, and the significance of late diagenetic dolomitization. Geology, v. 11, p. 519-522.

Zenger, D.H. and Dunham, J.R, (1988). Dolomitization of Siluro-Devonian limestones in a deep core (5350 meters), southeastern New Mexico: in V. Shukla and P.A Baker, eds., Sedimentology and Geochemistry of Dolostones. Society of Economic Paleontology and Mineralogy Special Publication, v. 43, p. 161-173.

APPENDIX

Wells in the study area

Table 2: Thickness and the formations at their total depths of the wells in the study area.

Cem-54	Depth	Thickness
Mardin Group	-2193	152
Karababa Fm.	-2193	95
Kar-C	-2193	27
Kar-B	-2220	50
Kar-A	-2270	18
Derdere Fm.	-2288	57
Total depth	-2345	

Cem-42	Depth	Thickness
Mardin Group	-2167	212
Karababa Fm	-2167	118
Kar-C	-2167	50
Kar-B	-2217	52
Kar-A	-2269	16
Derdere Fm	-2285	94
Total depth	-2379	

Cem-52	Depth	Thickness
Mardin Group	-2141	162
Karababa Fm.	-2141	131
Kar-C	-2141	52
Kar-B	-2193	55
Kar-A	-2248	24
Derdere Fm.	-2272	31
Total depth	-2303	

Cem-40	Depth	Thickness
Mardin Group	-2284	109
Karababa Fm	-2284	81
Kar-C	-2284	48
Kar-B	-2332	22
Kar-A	-2354	11
Derdere Fm	-2365	28
Total depth	-2393	

Cem-47	Depth	Thickness
Mardin Group	-2177	132
Karababa Fm	-2177	119
Kar-C	-2177	62
Kar-B	-2239	45
Kar-A	-2284	12
Derdere Fm	-2296	13
Total depth	-2309	

Cem-37	Depth	Thickness
Mardin Group	-2206	128
Karababa Fm	-2206	89
Kar-C	-2206	46
Kar-B	-2252	37
Kar-A	-2289	6
Derdere Fm	-2295	39
Total depth	-2334	

Cem-34	Depth	Thickness
Mardin Group	-2100	202
Karababa Fm	-2100	111
Kar-C	-2100	50
Kar-B	-2150	43
Kar-A	-2193	18
Derdere Fm	-2211	91
Total depth	-2302	

Cem-30	Depth	Thickness
Mardin Group	-2158	145
Karababa Fm	-2158	107
Kar-C	-2158	47
Kar-B	-2205	46
Kar-A	-2251	14
Derdere Fm	-2265	38
Total depth	-2303	

Cem-27	Depth	Thickness
Mardin Group	-2176	124
Karababa Fm	-2176	108
Kar-C	-2176	44
Kar-B	-2220	54
Kar-A	-2274	10
Derdere fm	-2284	16
Total depth	-2300	

Cem-20	Depth	Thickness
Mardin Group	-2165	181
Karababa Fm	-2165	104
Kar-C	-2165	45
Kar-B	-2210	47
Kar-A	-2257	12
Derdere Fm	-2269	77
Total depth	-2346	

Cem-22	Depth	Thickness
Mardin Group	-2311	139
Karababa Fm	-2311	119
Kar-C	-2311	40
Kar-B	-2351	56
Kar-A	-2407	23
Derdere Fm	-2430	20
Total depth	-2450	

Cem-19	Depth	Thickness
Mardin Group	-2142	170
Karababa Fm	-2142	77
Kar-C	-2142	12
Kar-B	-2154	49
Kar-A	-2203	16
Derdere Fm	-2219	93
Total depth	-2312	

Cem-18	Depth	Thickness
Mardin Group	-2285	212
Karababa Fm	-2285	125
Kar-C	-2285	54
Kar-B	-2339	55
Kar-A	-2394	16
Derdere Fm	-2410	87
Total depth	-2497	

Cem-14	Depth	Thickness
Mardin Group	-2152	267
Karababa Fm	-2152	94
Kar-C	-2152	34
Kar-B	-2186	46
Kar-A	-2232	14
Derdere Fm	-2246	107
Sabunsuyu Fm	-2353	66
Total depth	-2419	

Cem-13	Depth	Thickness
Mardin Group	-2162	248
Karababa Fm	-2162	125
Kar-C	-2162	53
Kar-B	-2215	55
Kar-A	-2270	17
Derdere Fm	-2287	112
Total depth	-2399	

Cem-9	Depth	Thickness
Mardin Group	-2123	223
Karababa Fm	-2123	79
Kar-C	-2123	31
Kar-B	-2154	36
Kar-A	-2190	12
Derdere Fm	-2202	112
Total depth	-2314	

Cem-11	Depth	Thickness
Mardin Group	-2680	139
Karababa Fm	-2680	107
Kar-C	-2680	43
Kar-B	-2723	47
Kar-A	-2770	17
Derdere Fm	-2787	32
Total depth	-2819	

Cem-8	Depth	Thickness
Mardin Group	-2151	220
Karababa Fm	-2151	118
Kar-C	-2151	50
Kar-B	-2201	49
Kar-A	-2250	19
Derdere Fm	-2269	102
Total depth	-2371	

Cem-10	Depth	Thickness
Mardin Group	-2262	145
Karababa Fm	-2262	112
Kar-C	-2262	52
Kar-B	-2314	55
Kar-A	-2369	5
Derdere Fm	-2374	33
Total depth	-2407	

Cem-7	Depth	Thickness
Mardin Group	-2603	154
Karababa Fm	-2603	133
Kar-C	-2603	51
Kar-B	-2654	62
Kar-A	-2716	20
Derdere Fm	-2736	21
Total depth	-2757	

Cem-6	Depth	Thickness
Mardin Group	-2193	214
Karababa Fm	-2193	100
Kar-C	-2193	51
Kar-B	-2244	39
Kar-A	-2283	10
Derdere Fm	-2293	103
Sabunsuyu Fm	-2396	11
Total depth	-2407	

Cem-5	Depth	Thickness
Mardin Group	-2103	299
Karababa Fm	-2103	97
Kar-C	-2103	41
Kar-B	-2144	40
Kar-A	-2184	16
Derdere Fm	-2200	112
Sabunsuyu Fm	-2312	90
Total depth	-2402	

Cem-4	Depth	Thickness
Mardin Group	-2225	173
Karababa Fm	-2225	117
Kar-C	-2225	47
Kar-B	-2272	52
Kar-A	-2324	18
Derdere Fm	-2342	56
Total depth	-2398	